各種促進試験における表面保護材を塗布したモルタルの水分特性と美観変化に関する研究

STUDY ON MOISTURE CHARACTERISTIC AND AESTHETIC CHANGE OF SURFACE PROTECTIVE MATERIALS ON MORTAR UNDER VARIOUS ACCELERATED AGEING TESTS

各種促進試験における表面保護材を塗布したモルタルの水分特性と美観変化に関する研究

Feng Chen

Doctor of Philosophy

Division of Architecture, Civil and Environmental Engineering
MURORAN INSTITUTE OF TECHNOLOGY

TABLE OF CONTENTS

CHAPTER 1

INTRODUCTION

1.1 Background

Concrete is widely used for building constructions because it's convenient construction, low cost and easy usefulness of raw materials. Without the surface protective materials, architectural concrete is prone to be influenced by different factors during service. It may be damaged by UV radiation, lower temperature or cyclic wetting–drying. All those damages mentioned above will not only threaten the durability of architectural concrete structures but damage its shiny surface and defile its beauty (Holmes et al., 2014; Freedman et al., 1999; López et al., 2016; Chang, 2020).

Tile finishes have been commonly used in the external walls of buildings since the 1970s because it is an extremely durable, aesthetic, and water-resistant that is perfect for exterior walls. It is used commonly in high-rise buildings in Japan. However, because of the earthquake and weather factors, including temperature, humidity, wind, sunshine, and air pressure (Simpson et al., 1970), the delamination of the exterior wall tiles has caused many casualties and injuries in the past decade. In addition, it requires repair and reinforcement every 1 0 years, and it is very difficult to maintain and inspect the outer walls of high-rise buildings, which require manual labor and use the ropes or baskets (The Amended of Building Standard Law, 2008). This results in large costs due to increased maintenance, extensive replacements of the specific building products and any possible consequential building damages. To avoid this, the solution is to apply building products which have properly documented adequate and satisfactory long-term durability.

Both the aesthetic appearance and durability of concrete facades may be enhanced by coatings. Because the surface treatment has the advantages like the easy construction, relatively cheap and lower industrial waste when repair, and so on. In recent years, the European standard EN 1504 defines three types of surface treatments (NF EN 1504, 2005): silane and siloxane-based (water-repellent) coatings, silicate-based (pore blockers, also known as water glass) impregnations and coatings that create a continuous protective layer along the concrete surface. The first type of coating created a hydrophobic layer on the exposed concrete surface. The impregnation reaction product can clog the pores partially or filling the capillary pores. In the first type of impregnation, the active ingredient product creates a thin hydrophobic layer on the pores, while in the second type, the reaction product

can clog the pores and strengthen the concrete surface. However, even if the main purpose of the coating would be aesthetic the effects on durability must also be considered as they may not always be positive. Coatings act like barriers against moisture and aerial gases. They retard the flow of liquid moisture and gases through the surface of concrete in both directions. Especially the following phenomena depend on the permeability properties of coatings: capillary uptake of rainwater into concrete and evaporation of pore water from concrete to outside air.

The moisture state within the material, which is intimately related to the exposed environment, is typically determined by all degradation elements of concrete structures, which are dependent on the surface water repellent treatment. (Wang et al., 2020; Baltazar et al., 2014; Weisheit et al., 2016; Tian et al., 2020). As a result, a thorough understanding of the water repellency of surface impregnation for cement-based materials in various exposure situations is critical. It has important practical significance for the construction of engineering. When examining the impacts of coating materials on the durability of concrete, the influence of moisture content on the coating materials is particularly essential. Coatings usually slow down both the wetting and drying processes. It's often difficult to foresee the total impact of changing weather conditions. The situation is made even more problematic by the breakdown of coatings, which changes the permeability properties. As a result, final coating evaluation is a difficult operation that can only be accomplished by vast knowledge or precise moisture physical calculations paired with material tests. The internal frost damage of concrete is directly influenced by the moisture content of the concrete. Frost damage can be avoided if the moisture content of concrete is kept below the critical level. As a result, by reducing or delaying water uptake into concrete, coatings are thought to improve concrete resistance to frost damage. However, when a coating permeability is increased by deterioration, the coating protective characteristics may deteriorate with time. Because there is generally a thermal moisture movement through the wall, completely impermeable coatings cannot be employed in facades. Furthermore, an impermeable coating may prove to be extremely fragile over time, since minor flaws in the coating may produce a significant local rise in moisture content, jeopardizing the coatings adherence and concrete frost resistance. Weather conditions, concrete qualities, structural features, the protective impact of other structures, and coating

properties all play a role in the degradation of concrete facades.

On the other hand, because concrete wall buildings are exposed to the elements for 365 days, additional attention is required to keep the concrete clean and free of pollution. External factors such as wind, rainwater, static electricity, and ultraviolet rays cause pollution on the exterior of buildings, which starts with physical, electronic, chemical, and biological contact factors and is exacerbated by external factors such as wind, rainwater, static electricity, and ultraviolet rays (Shim, 2001). One of the most typical pollution phenomena noticed on the exterior of buildings is staining. Due to rains and wind, dust settles primarily on horizontal and sloping surfaces, leaving stains. Surface tension is the characteristic between rainwater and material. Surface tension is a sort of interfacial tension that is designed to shrink and take up the smallest feasible amount of space. In other words, surface tension exists between rainfall and outside materials, which attracts impurities and contaminates the exterior walls. The fixture becomes hydrophilic as the angle and rainfall surface tension decrease. Higher angle and rainwater surface tension make the fixture hydrophobic, whereas lower surface tension makes it hydrophilic. The outer material is less polluted the closer it is to the hydrophobic. The aesthetic degradation has generally been less researched in studies than the chemical and physical impact of pollutants on building fabric.

Therefore, it is necessary to explore the long-term durability and aesthetic of surface protection materials in the progress under a variety of service conditions (under harsh environmental and pollution conditions, etc.) by selecting materials that are appropriate, durable or have protection to reduce damage from external deteriorating environments.

1.2 Purpose and significance of the study

Based on the above background introduction, this study was conducted to determine the water and stain resistance of different surface protection materials by exposing materials with different water to ash ratios to various environmental and loading conditions simulating actual use conditions, mainly to investigate the effect of fluorine resins, silicate based and silane-based surface treatment agents on the permeability and anti-soiling of mortar. The main research objectives are as follows.

（1）Exploring the effects of coating film deterioration on fluorine resins, silicates and silane-based surface protective materials under warm water immersion.

（2）Exploration of the suitability of cementitious materials coated with fluorine resins, silicates and silane-based surface protective materials in humidity and cool-heat exposure environment.

（3）Assessment of the sensitivity of mortars to heat, UV radiation and water after weathering With coated of fluorine resins, silicate based and silane-based surface protective materials.

The application of concrete surface protective materials improves the durability of the structure, extends the life of the concrete structure and reduces its maintenance costs. And reduce the maintenance costs. The research significance of this thesis is mainly in two points.

（1）This thesis will clarify the effects and mechanisms of fluorine resin, silicate and silane surface protective materials on the durability of mortar and provide a theoretical basis for their application.

（2）This thesis uses the fluorine resin, sodium silicate and silane as surface protective materials to investigate their effects on the aesthetic properties of mortar and to provide a theoretical basis for their application in engineering practice.

1.3 Research aims and thesis organization

This thesis uses the three types of surface protective materials to evaluation the water resistance of mortars by the water absorption and moisture permeability test methods. The aesthetic properties of the surface protective materials were also assessed by appearance observation, color difference, gloss, roughness and contact angle, and was also assessed the anti-soiling assessed by coating method to pollutant and simulated raindrops method to pollutant.

This thesis is organized into seven chapters. The organization of this thesis and brief introduction of each chapter are given as follows:

Chapter 1 covers research background, the purpose and significance of the research, the research methodology and content and the literature review.

Chapter 2 materials and experimental methods.

Chapter 3 investigates the effect of humidity and cool-heat cycling exposure on the water absorption, moisture permeability and aesthetic properties of concrete samples coated with different surface coatings.

Chapter 4 examines the resistance to coating film deterioration of concrete samples coated with different surface treatments after warm water immersion.

Chapter 5 the degradation suffered by different surface treatments when exposed to UV radiation was studied was analyzed by visual observation of the change in appearance, gloss, color change and water permeability and anti-soiling.

Chapter 6 Get the applicability of surface protective materials is derived from a comparative analysis and discussion of the appearance change and durability for fluorine resin, sodium silicate and silane in different exposure environments. Furthermore, obtained the best anti-soiling effect of surface protective material, which can provide a valuable information for the surface protective material used the buildings.

Chapter 7 shows the thesis conclusion and further research work in the future.

The following is this thesis structure:

Chapter 1 Introduction
Previous research, problem definition, research objective, thesis organization

↓

Chapter 2 Materials and experimental methods
Including the properties of the materials, the equipment, experimental methods, and the experimental ratios

↓

Chapter 3 Evaluation of surface characterizations and water resistance of surface coatings after humidity and cool-heat cycling	**Chapter 4 Influence of surface protective material on appearance change and moisture properties after immersion in warm water**	**Chapter 5 Investigation on aesthetic and water permeability of surface protective material under accelerated weathering**

• Changes in brightness, roughness, contact angle on mortar
• Changes in anti-soiling Properties
• Influence of water resistance

↓

Chapter 6 Discusses the anti-soiling major influence factors of surface protective materials after three aging environments
• Influence of different accelerated aging
• Influence of different surface treatment

↓

Chapter 7 Conclusions
Summary and future work

1.4 Previous research

Surface protective materials have been the subject of extensive research over the last several decades, and the mechanisms are relatively well understood. Nonetheless, there are certain inconsistencies or competing hypotheses for describing the aesthetic and durability of surface protective materials behavior, which will be highlighted in the following paragraphs.

1.4.1 Types of surface protective materials

To date, the surface treatments can be divided in three different types, in accordance with European Standard EN 1504-2, illustrated in Fig.1.1: (i) hydrophobic impregnations that produce a water repellent surface generally with no pore filling effect; (ii) impregnations, which reduce the surface porosity by filling totally or partially the concrete pores; and (iii) coatings that produce a continuous protective layer along the concrete surface (Janz et al., 2004; EN 1504-2, 2001). The different action exerted by three different types of surface treatments against water (in the form of a drop) is depicted in the scheme in Figure1.2: while concrete shows a hydrophilic and absorbing behavior (untreated concrete), the coating makes a hydrophobic physical barrier (coating), the impregnation impedes water ingress by playing a hydrophobic interaction (impregnation), and the pore blockage hinders water absorption without resulting in a hydrophobic effect (pore blockage).
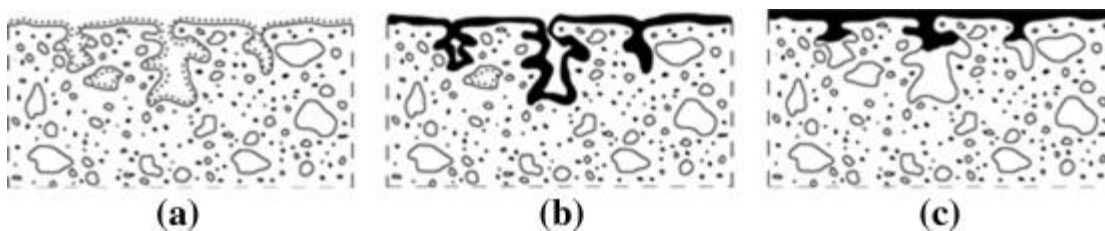

Fig. 1.1 Surface treatments classification: (a) hydrophobic impregnations, (b) impregnations, (c) coatings (adapted from (EN 1504-2, 2001; Wang et al., 2016; Kagi et al., 1995; Basheer et al., 1997))
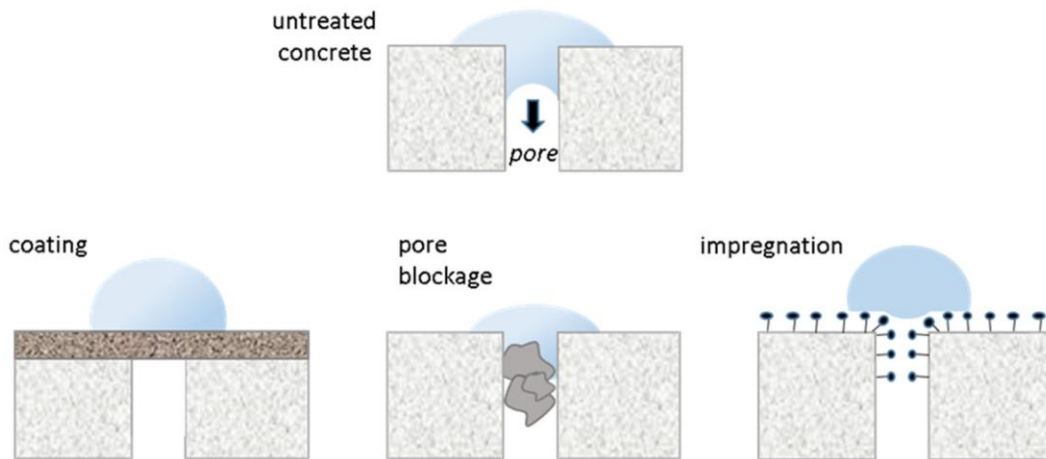
Fig. 1.2 Scheme depicting the different roles of the surface treatment towards water drop ingress and contact angle. Only coating and impregnation (pore liner) result in a hydrophobic effect (Mundo et al., 2020).

1.4.1.1 Hydrophobic Impregnation (Silane-based)

Hydrophobic impregnations work by raising the contact angle (the surface is termed hydrophobic when the contact angle is larger than 90° without affecting water vapor transit inside the cementitious matrix. The most typical hydrophobic impregnation uses silanes or siloxanes, which are tiny molecules (in the range of 1–7 nm) that may easily penetrate concrete pores and reduce surface tension. The attributes of the impregnating agent are determined by the properties of the alkyl group: the higher the molecular weight of the alkali group, the higher the degree of hydrophobicity of the treatment (Justnes, 2008).

Silane is a chemical compound with the formula SiH4 that is called after methane (CH_4). In a similar way to carbon-based organic molecules, a variety of functional organic groups can replace the hydrogen and establish covalent connections with silicon. It is usual to quote silanes with the general formula RSi (OR')$_3$ in the field of hydrophobizing agents, where R is a long or bulky alkyl group and R' is a relatively short alkyl group. Like ethyl since it should be hydrolysed by the hydroxides from the cement in order for it to coordinate to calcium (just like the -COO- group in fatty acid salts) and the R group poke out from the surface and is responsible for the hydrophobizing action.

There are two phases in the chemical interaction between the alkyl alkoxysilane molecule and the concrete silicate structure: hydrolysis and condensation. During hydrolysis, when moisture is provided to the silane molecules, unstable silanol molecules are formed. When moisture is added to the silane molecules during

hydrolysis, unstable silanol molecules develop. The unstable silanol molecules interact with the accessible hydroxyl groups of the silicate structure of the concrete during condensation, resulting in some cross-linking. As a result, the silicone's inorganic portion, which provides the water-repellent property, will orient itself, generating a water-repellent molecular brush. The key aspect of this reaction is that it occurs with the hydroxyl groups of the substructure, allowing for direct bonding with the concrete. The concrete alkalinity functions as a catalyst in this reaction. The reactions of mechanisms for hydrolysis and polymerization of silane in cement-based materials applied in this study are shown in Fig.1.3.
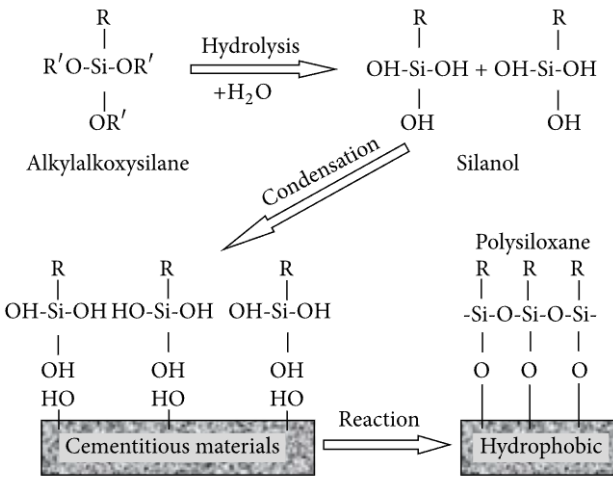
Fig. 1.3 Mechanisms for hydrolysis and polymerization of silane in cement-based materials.

The water repellency of surface impregnation of cement-based materials has been studied extensively (Medeiros et al., 2008; Dai et al., 2010; Fukui et al., 2017; Al-Kheetan et al., 2019), demonstrating that the waterproof impact of the hydrophobic surface impregnation treatment employing silane is to some extent important. Dai et al. (2010) investigated the long-term effectiveness of surface impregnation agents in improving the durability of marine reinforced concrete structures, as well as the impact of fractures on the water repellency of concrete surface impregnation. Al-Kheetan et al. (2010) used a scanning electron microscope (SEM) to image concrete pavement with various chemistries, as well as contact angle and water absorption tests, in order to assess the moisture behavior of concrete treated with hydrophobic surface impregnant. In general, prior

investigations have shown that hydrophobic impregnation can significantly reduce internal humidity and limit capillary water absorption (Medeiros et al., 2008; Al-Kheetan et al., 2019). Furthermore, it has been discovered that the exposure environment has a considerable impact on the penetration depth of surface impregnated silane into concrete (Medeiros et al., 2008; Wanget al., 2020). In fact, due to the aging of silane-based products, coatings and surface treatments may cause some adverse effects such as color change and component alterations, which should be avoided while restoring cultural objects (Anwaret al., 2020; Dai et al., 2010; Vipulanandan et al., 2011). Moreover, Medeiros et al. (2008, 2009) revealed that silane and siloxane are effective at preventing water penetration when the water pressure is less than 12,000 Pa. Hydrophobic surface treatments should only be applied when the water exposure conditions are fully understood, according to the findings. Moreover, Polder et al. (1996) investigated the high-temperature resilience of hydrophobic surface treatments such as silane and siloxane. The water absorption rate of the treated concrete increased considerably after half an hour of storage in a 160 °C chamber, according to the findings. After ultraviolet aging, Levi et al. (1996) discovered that the protection of silane, silicone, and fluorinated polymer on concrete water absorption fell by 50%. In laboratory accelerated freeze–thaw testing, some research have revealed that silane-treated concrete deteriorates faster than untreated concrete (Perenchio, 1988). Others have noted that this is not the case in genuine constructions (Pigeon et al., 1985; Vesikari et al., 1983). The hydrophobic effect of the pore liners may be overcome by the high-pressure water flow created during freezing and thawing, and these treatments may not provide the protection promised. As a result, determining the freeze–thaw endurance of surface-treated concretes is critical. surface-treated concrete's long-term durability. Although there has already been a lot of research done on the durability of concrete that hasn't been treated and concrete that has been treated with various hydrophobic agents Leung et al., 2008; Jia et al., 2016), from what is above stated so far, surprisingly few studies have been focused on the influence of exposure environments and pollution resistance on surface impregnation of cement-based materials.

1.4.1.2 Impregnations (silicate-based)

Impregnating coatings (i.e., pore-blocking treatments) are able to through capillary suction into concrete, this silicate compound reacts with calcium hydroxide and eventually forms insoluble CSH gel ($Ca–SiO_2$) which makes concrete denser (Kasselouri et al., 2001; Franzoni et al., 2013; Thompson et al., 1997; Pigino et al., 2012) and improve the impermeability of buildings (Ibrahim et al., 1999; Moon et al., 2007). The reactions of sodium silicate ($Na_2O–SiO_2$) type of impregnation are written in (1.1) (Franzoni et al., 2013; Dai et al., 2010):

$$Na_2SiO_3 + yH_2O + xCa (OH)_2 \qquad (1.1)$$
$$\rightarrow xCa \cdot SiO_2 \cdot yH_2O + 2NaOH$$

The fact that most commercial therapies are based on silicates (such as lithium silicate, sodium silicate, and calcium silicate) has piqued the interest of both academia and industry for the following reasons: They react with portlandite in the cement matrix to generate inorganic calcium-silicate hydrate (C–S–H gel) (Franzoni et al., 2013; Thompson et al., 1997; Pigino et al., 2012) and so avoid aging difficulties; surface treatments are more durable (Pigino et al., 2012), and the waterproofing effect is practically permanent (Thompson et al., 1997). They are waterborne and so environmentally beneficial (Baltazar et al., 2014; Franzoni et al., 2013; Kagi et al., 1995; Higgins et al., 1985). According to some findings (Dai et al., 2010), sodium silicate barely penetrates the concrete substrate and is poor at preventing water and chloride penetration. Furthermore, because of the increased alkali concentration, waterglass may increase the chance of an alkali–silica interaction. Others claimed it was effective at avoiding water adsorption and preventing carbonation (Franzoni et al., 2013). Kagi observed that post-treatment with cationic surfactants (alkylquaternary ammonium ions) increased its efficacy greatly (Dai et al., 2008), (Baltazar et al., 2014; Thompson et al., 1997; Pigino et al., 2012; Franzoni et al., 2013) the particular methods through which they improve concrete performance are still unclear. Because SiO2 precipitates in the pores, sodium silicates are excellent and efficient sealers, according to one viewpoint (McGettigan et al., 1992). Another possibility is that the silicates react with excess calcium hydroxide at the concrete surface to form calcium–silicate hydrates, which are relatively intractable. The silicates generate an expansive gel similar to that formed during alkali silicate reactions to fill the concrete spaces by swelling, according to a third viewpoint

(Thompson et al., 1997). Clearly, no common conclusion has been reached about the waterproofing mechanism of sodium silicate-based concrete sealers (Baltazaret al., 2014; Franzoni et al., 2013; Thompson et al., 1997; Pigino et al., 2012). Accordingly, exploring the exact mechanisms by which sodium silicate-based concrete sealers improve the water impermeability and pollution resistance of concrete structures is of great significance.

1.4.1.3 Coatings (Fluor-resin-based)

Surface coatings are defined as continuous films that operate as a physical barrier to prevent aggressive chemicals from penetrating concrete elements.

The basic components of a fluoropolymer are carbon and fluorine; it is primarily a fluorinated carbon chain polymer (Perepelkin, 2004), which provides it the capacity to withstand chemical attacks and repel water (hydrophobicity). The inclusion of fluorine groups in the polymer allows it to have a low surface energy, which reduces friction and adhesion while also enhancing the polymer's hydrophobicity (Li et al., 2002; Brady et al., 2000; Passaglia et al., 1994), respectively. Fluorinated polymers are highly beneficial as protective coatings because of these qualities, and they have been utilized for antifouling and anti-soiling applications. Fluorinated polymers are also resistant to degradation in outdoor applications because the C-F bond is particularly robust in the presence of visible and UV light (Scheerder et al., 2005).

Temperature and ultraviolet light had a significant impact on the efficacy of surface treatments, according to research. The protection of fluorinated polymer on concrete water absorption fell by 50% following UV aging, according to Levi et al. (2002); polymer-modified cementitious coatings have a high ultraviolet light resistance, allowing them to be used in direct sunlight.

1.4.2 Durability of concrete

Durability of concrete plays a critical role in controlling its serviceability. Water has a major role in the decomposition of concrete constructions (Barbucci et al., 1997; Delucchi et al., 1997; Franzoni et al., 2013). Therefore, many surface protection treatments for concrete have been used in recent years to prevent water penetration into concrete structures, hence extending the durability of new concrete structures (Baltazar et al., 2014). The interaction between water and materials, as well as the dynamic behavior of water on the surface or inside the materials, are always part of the hydrophobicity assessment and test techniques for materials. Water absorption and impermeability, which are based on water migration and transport modes such as capillary adsorption, diffusion driven by concentration, and infiltration driven by pressure, can be used to assess the hydrophobicity of cement-based materials in general (Basheer et al., 1997; Attanayake et al., 2006).

1.4.2.1 Water Absorption

Since water is essential for many forms of deterioration of concrete, a strong resistance to water penetration is a key criterion for surface treatments (Mehta et al., 2006; Attanayake et al., 2006). Surface treatments that minimize water absorption by 75% should be accepted, according to NCHRP Report 244 (Pfeifer et al., 1981). The German Committee for Reinforced Concrete specified that following treatment, there should be a maximum water absorption of 2.5 percent by mass and a reduction in water absorption of at least 50% of the untreated concrete, however the rationale for this is unclear (Pfeifer et al., 1981). Many surface coatings can minimize the amount of water that gets into the treated matrix. Epoxy coatings, silane with an acrylic topcoat, methyl methacrylate, and alkyl alkoxysilane are the best treatments for water permeability (Pigino et al., 2012). Medeiros et al. Pigino et al. (2008, 2009) demonstrated that silane and siloxane have a good capability of inhibiting water penetration as long as the water pressure was lower than 12,000 Pa. According to the findings, hydrophobic surface treatments should only be applied when the water exposure conditions are fully understood. Modified cementitious mortar coatings, on the other hand, have a slightly higher resistance to water penetration than the other treatments; however, they are highly recommended in the protection of structures in constant contact with water because, unlike other treatments, they have a greater resistance to leaching (Weisheit et al.,

2006; Franzoni et al., 2014). Inorganic surface treatments exhibited good resistance to water infiltration, according to Jia et al. (2016) investigation. Pretreatment with sodium fluosilicate improved the effect of sodium silicate, and magnesium fluosilicate had a similar effect to sodium silicate. Magnesium fluosilicate and sodium fluosilicate both show promise for use in the field.

1.4.2.2 Moisture permeability

Because concrete is a porous substance, it includes a certain amount of water that can either evaporate or remain inside depending on the climatic circumstances. As a result, the moisture content inside building works might be quite high if they are exposed to rainy weather or are not protected from moisture increase, or very low if the walls are in good shape.

Water is the most important factor in the formation of events like freeze/thaw cycles, which cause degradation. As a result, once water has infiltrated, it must be removed immediately and easily. Protective concrete coatings must consequently have a high-water vapor transmission rate to allow the concrete to dry without difficulties such as adhesion loss and subsequent coating detachment. As a result, waterproofing coatings can help to slow down the deterioration of concrete.

1.4.3 Aesthetic characteristic of surface protective material

The practically ability of a surface coating is protective the surface no change the appearance of a substrate is one of its most important characteristics. Surface coatings have been employed in construction buildings. Surface coating capacity to provide a variety of surface finishes, from flat to high gloss, as well as color, roughness, and contact angle effects, allows for a wide range of aesthetic appearances. Surface coatings, whether intended to highlight specific architectural components or to provide the appearance of natural stone concrete, are critical to a structure's overall aesthetics.

This section will discuss the important appearance qualities, specifically color, gloss, roughness, contact angle, and the specification and control of these qualities.

1.4.3.1 Color and Light

The color retention capabilities of a coating system are crucial in terms of aesthetics. Variations in the appearance parameters of color (particularly hue, lightness, and chroma) can cause a drastic change in the perception of a structure.

Hundreds of interfaces exist between coatings and cement materials in a coated film. Refraction happens at each of these interfaces when light is cast onto the surface, returning light to the observer's eyes. The refraction that happens between particles returns white light to the observer, allowing two incompatible transparent resins to look white or hazy. Specific wavelengths of light are absorbed by the pigments in the coating system, resulting in color variations visible by the observer. The remaining wavelengths are returned to the observer's eye, giving the appearance of a given hue. The primary transmitted wavelengths that establish its basic hue dominate the resulting color. Undertones of various wavelengths will alter this color, resulting in a unique tint. White is the color seen when no wavelengths are absorbed, and black is the color seen when there is no light at all.

Adopted by the "Commission International de l'Eclairage" CIE) in 1976, the CIELAB Uniform Color Space is a mathematical representation of color within a three-dimensional rectangular

coordinate system. The range of lightness (Black=0 and White=100), red to green (Green = -a and Red = +a), and blue to yellow (Blue=-b and Yellow=+b) are represented by three opponent axes L*, a*, and b* respectively.

1.4.3.2 Gloss

Gloss is the ability of a surface to reflect more light in directions close to the spectator than in others. The final level of gloss will be determined by the homogeneity of the coated surface. The level of gloss imparted by a coating is mostly governed by the binder and pigment ratios used in its formulation. The film's surface will generate a more regular reflection and hence a higher gloss finish as the quantity of binder material increases. In contrast, when the binder content is low, pigment granules are exposed, roughening the surface and resulting in a matte appearance. The gloss of a coating film is controlled by the ratio of the refraction indexes of both ingredients, in addition to the binder and pigment ratio.

The factors that influence surface sheen have been found to affect the performance and look of coatings. Because matte finishes have less binder, they are more vulnerable to mechanical damage than high gloss finishes. High gloss paints are also less stain resistant due to their flat surfaces. Strong gloss paints, despite their high resistance to mechanical damage, show defects more readily and cannot be restored locally without causing a significant change in gloss. It is because of this characteristic that matte finishes are so appealing.

1.4.3.3 Roughness

Roughness is a broad term that can convey a variety of information depending on the level of investigation: in civil engineering, the millimetric scale is commonly used to distinguish the various surface treatments. Surface "roughness" has two primary effects: mechanical interlocking and contact angle modification. The first is related to" surface waving," while the second is more influenced by "micro-roughness" (Czarnecki et al., 2003; Garbacz et al., 2006): micro-roughness can impact thermodynamic properties of surfaces by changing contact angle: an

increase in roughness usually results in greater liquid spreading on the solid surface. Wenzel's coefficient is used to calculate this effect. Surface roughness can be used to describe the topography of the concrete substrate prior to the application of a repair in the field of concrete patch repairs (Shen et al., 2019). The interface bond between the concrete substrate and the repair material is critical to the overall success and long-term durability of a concrete patch repair.

The amplitude and height distribution – parameters according to current standards – are the principle of roughness testing (ISO, NF). We first determine the sampling length used to perform the filtration process and obtain both roughness and waviness when considering a measured profile of a surface, as shown in Fig.1.4. This standard length is referred to as the cut-off length (x axis). The y axis usually denotes the profile's height. RI parameters, which are specified as follows, are determined locally on each cut-off or sampling length in all circumstances.

It is the mean departure of the profile from the reference line, Ra parameter: arithmetic mean deviation (Fig.1.2).

Thus, if Y(x) is the profile measured from the reference mean line and L is the length of the profile being assessed, then Ra is defined by (1.6)

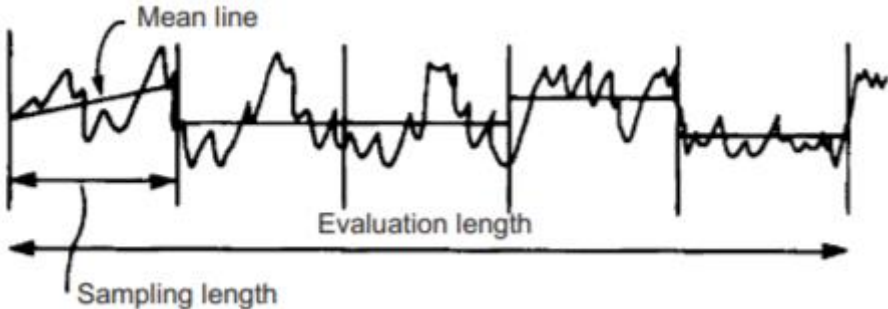$$R_a = \frac{1}{L} \int_0^L |Y(x)| \, dx \tag{1.2}$$

Fig. 1.4 Definition of the cut-off length

Which can be approximated by (1.3)

$$R_a \approx \frac{1}{n} \sum_{i=1}^{n} |Yi| \tag{1.3}$$

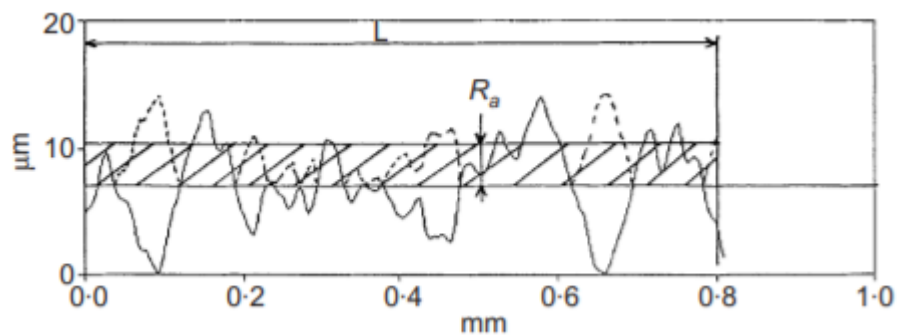Where n is the number of data effectively measured by the apparatus.

Fig. 1.5 Ra parameter average

1.4.3.4 Contact angle

Physical roughness and chemical heterogeneity can easily alter surface wettability, which is primarily determined by the chemical composition and microscopic geometry of the material surface. The contact angle (CA) is a measurement of a water droplet's wetting condition on a solid surface. The wetting state might be hydrophilic ($\theta > 90°$) or hydrophobic ($\theta < 90°$). Wetting states can be classified as superhydrophilic ($\theta < 10°$) or superhydrophobic ($> 150°$ and slide angle, $SA < 10°$) (Lin et al., 2014). With the assumption that the solid surface is glazed, chemically homogeneous, and undissolved, the CA can be determined using Young's equation (Young et al., 1995). However, in most realistic cases, solid surfaces are inevitably coarse and chemically heterogeneous. On coarse surfaces, hydrophobic wetting states commonly manifest in two forms, as shown in Fig.1.6b and 1.6c. Water has entirely permeated the rough grooves in the mode seen in Fig.1.6b, which is known as homogeneous wetting and characterized by the Wenzel model (Lin et al., 2014; Wenzel et al., 1936). When air is trapped between the water droplets and the surface as shown in Fig.1.6c, the mode is referred to as heterogeneous wetting, which is characterized by the Cassie model (Cassie et al., 1944). Surfaces described by the Wenzel model are typically 'sticky' in the sense that water droplets adhere better than a flat counterpart, whereas those described by the Cassie–Baxter model are typically 'slippery' in the sense that water droplets roll off more easily than a flat counterpart (Marmur et al., 2004; Zhang et al., 2013).
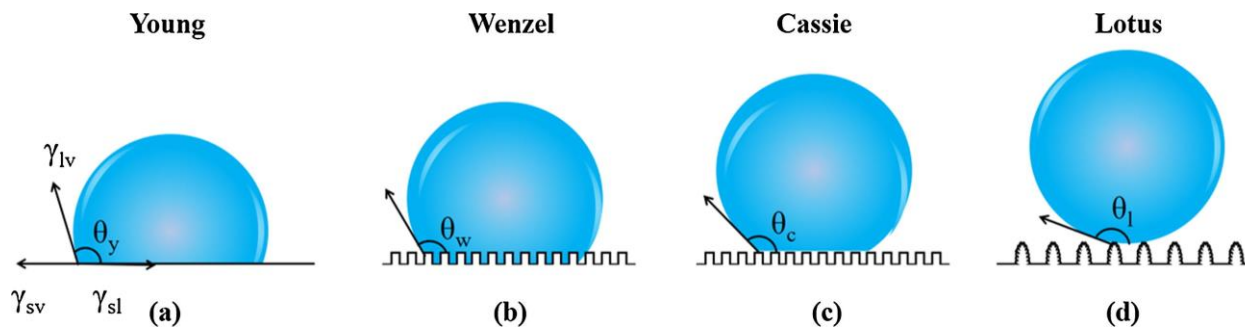
Fig. 1.6 (a) Liquid droplet on a smooth surface. (b) Liquid droplet in the Wenzel state. (c) Liquid droplet in the Cassie state. (d) Lotus effect. (She et al., 2018)

Though the surface treatment is based on the creation of hydrophobic interactions between the porous surface and water, CA values for impregnation treated concrete are scarcely reported in the literature. Franzoni et al. (2013) observed a remarkably low value (62°) for an ethyl silicate impregnated concrete, where the untreated material attained 30°. Furthermore, the organic-coated cement mortar used in the investigation by Karthick et al. (2018) reached 162.3°, significantly higher than the 45.5° of the reference concrete specimens.

1.4.4 Accelerated weathering

1.4.4.1 Humidity and cool-heat cycling

The cyclic absorption and desorption of water affects most coatings. Liquid permeation into the coating can produce swelling in some materials, and when the liquid evaporates, the coating shrinks due to the loss of moisture. The cyclical straining of the system is caused by recurrent stages of liquid permeation and evaporation. If the inner layer coating materials are at different points in the cycle than the top surface, the coating system may be subjected to additional stress. Surface stress cracking, as well as cracking and peeling of the entire coating system, can occur as a result of these periodic moisture fluctuations.

On the other hand, the high-pressure water movement created during freezing and thawing, may overwhelm the hydrophobic effect of the pore liners, resulting in inadequate protection from these treatments. This leads to the importance of assessing the freeze–thaw durability of surface treated concretes.

1.4.4.2 Warm water immersion

The significance of moisture in the degradation of costing is often overlooked based on the assumption that structures are only subjected to moisture by rain, splashing, or immersion. Water in a natural environment is caused by rain, melting snow and ice, or dew (high relative humidity). When water on the surface is absorbed by or flows through the coating, several types of deterioration can occur. The creation of an osmotic cell, which is induced by fluid passing through the coating and interacting with a water-soluble substance, is one type of deterioration. When concrete with a high salt content is covered, this can happen. The difference in solution concentration on either side of a semi-permeable membrane (coating) creates a spontaneous flow of liquid, which is known as osmosis, once water ponds on the surface of the coating. The flow of liquid through the membrane creates hydrostatic pressure, causing blistering and delaminating of the coating. Leaching has been studied by a number of academics as an inherent problem of concrete when immersed in water (Berne et al., 1998; Adenot et al., 1992; Li et al., 2008; Faucon et al., 1998). Maltais et al. (2004) studied the effects of the external environment on leaching and discovered that when immersed in deionized water, calcium hydroxide and C-S-H were leached,

however when immersed in sodium sulfate solution, ettringite and gypsum might be produced. The difference in leaching rates of cement pastes when immersed in different media was discovered by Kamali et al. (2016). They discovered that the overall amount of leaching in NH_4NO_3 solution after 19 days is 4–5 times greater than that in pure water after 114 days, and that this is true at both room temperature and high temperature (85 °C). Aside from the external environment, the microstructure of concrete has an impact on the leaching process. The water cement ratio (w/c) is the most essential factor in limiting leaching, according to Maltais et al. (2004). A smaller w/c results in a denser microstructure, which increases concrete's leaching resistance. The bigger the aggregate volume fraction is while w/c is held constant, the lower the leaching rate will be.

1.4.4.3 Xenon-arc light radiation

Accelerated weathering studies allow for a comparison of the performance characteristics of various coating systems under controlled exposure conditions. It's worth noting that no accelerated weathering test can completely replicate the genuine exposure environment for concrete structures. Accelerated weathering testing, on the other hand, if done correctly, can produce data that aid in the selection and installation of coating systems in a fraction of the time it takes for environment exposure studies.

Accelerated weathering (Wang et al., 2016; Wang et al., 2016; Wang et al., 2016) is a technique that uses laboratory equipment to simulate coating breakdown that occurs during actual outdoor exposure. Artificial weathering is sometimes referred to as accelerated weathering because at least one of the elements of weathering, primarily light, heat, and moisture, is either amplified or over a longer period of time than in natural exposure. Coating weather or degrade more quickly as a result of the increased exposure.

References:

N. Holmes, A. Browne, C. Montague, Acoustic properties of concrete panels with crumb rubber as a fine aggregate replacement, Constr. Build. Mater. 73 (2014), pp. 195-204

S. Freedman, Loadbearing architectural precast concrete wall panels, PCI J., 44 (5) (1999), pp. 92-115

Lopez, G. Guzman, A. Sari, Color stability in mortars and concretes. Part 2: Study on architectural concretes, Constr. Build. Mater. 123 (2016), pp. 253-284

Honglei Chang, Penggang Wang, Zuquan Jin, Gang Li, Pan Feng, Shoujie Ye, Jian Liu, Durability and Aesthetics of Architectural Concrete under Chloride Attack or Carbonation, Materials, 2020, 13(4), 839

J.W. Simpson, P.J. Horrobin, The weathering and performance of building materials, Department of Building, University of Manchester Institute of Science and Technology, UK (1970)

Ministry of land, Infrastructure, Transport and Tourism: 2008, https://www.mlit.go.jp/jutakukentiku/build/teikihoukoku/punflet.pdf

NF EN 1504, Products and Systems for the Protection and Repair of Concrete Structures, European Standard (2005)

P. Wang, Y. Wang, T. Zhao, C. Xiong, P. Xu, J. Zhou, et al., Effectiveness Protection Performance of an internal blending organic corrosion inhibitor for carbon steel in chloride contaminated simulated concrete pore solution, J Adv Concr Technol, 18 (2020), pp. 116-128

L. Baltazar, J. Santana, B. Lopes, M.P. Rodrigues, J.R., Correia Surface skin protection of concrete with silicate-based impregnations: influence of the substrate roughness and moisture, Constr. Build Mater, 70 (2014), pp. 191-200

S. Weisheit, S.H. Unterberger, T. Bader, R., Lackner Assessment of test methods for characterizing the hydrophobic nature of surface-treated high-performance concrete, Constr. Build Mater, 110 (2016), pp. 145-153

Y. Tian, P. Zhang, K. Zhao, Z. Du, T. Zhao Application of Ag/AgCl sensor for chloride monitoring of mortar under dry-wet cycles, Sens, 20 (2020), p. 1394

Shim, W. 2001. "Case of Building Pollution and Measures." Construction and Culture History 24–152.

Janz M., Byfors K., Johansson L. Annex F - surface treatments, Rehabcon Manual, Rehabcon IPS-2000-00063; 2004. 24p.

EN 1504-2-Products and Systems for the Protection and Repair of Concrete Structures-Definitions, Requirements, Quality Control and Evaluation of Conformity-Part 2: Surface Protection Systems for Concrete; ISO: Geneva, Switzerland, 2005.

D. Wang, P. Yang, P. Hou, L. Zhang, Z. Zhou, X. Cheng, Effect of SiO2 oligomers on water absorption of cementitious materials, Cem, Concr. Res, 87 (2016), pp. 22-30

D.A. Kagi, K.B. Ren, Reduction of water absorption in silicate treated concrete by post-treatment with cationic surfactants, Build. Environ, 30 (1995), pp. 237-243

P.A.M. Basheer, L. Basheer, D.J. Cleland, A.E. Long surface treatments for concrete: assessment methods and reported performance, Constr. Build. Mater, 11 (1997), pp. 413-429

Recent Advances in Hydrophobic and Icephobic Surface Treatments of Concrete, Rosa Di Mundo; Labianca, Claudia; Carbone, Giuseppe; Notarnicola, Michele. Coatings; Basel Vol. 10, Iss. 5, (2020): 449. DOI: 10.3390/coatings10050449

Harald Justnes, Low water permeability through hydrophobicity, SINTEF Building and Infrastructure, COIN Project report 1 - 2008

M. Medeiros, P. Helene, Efficacy of surface hydrophobic agents in reducing water and chloride ion penetration in concrete, Mater Struct, 41 (1) (2008), pp. 59-71

J.G. Dai, Y. Akira, F.H. Wittmann, H. Yokota, P. Zhang, Water repellent surface impregnation for extension of service life of reinforced concrete structures in marine environments: the role of cracks, Cem. Concr. Compos, 32 (2) (2010), pp. 101-109

K. Fukui, C. Iba, S. Hokoi, Moisture behavior inside building materials treated with silane water repellent, Energy Procedia, 132 (2017), pp. 735-740

P. Wang, Y. Wang, T. Zhao, C. Xiong, P. Xu, J. Zhou, et al., Effectiveness Protection Performance of an internal blending organic corrosion inhibitor for carbon steel in chloride contaminated simulated concrete pore solution, J Adv Concr. Technol, 18 (2020), pp. 116-128

M. Anwar, D.A. Emarah, Resistance of concrete containing ternary cementitious blends to chloride attack and carbonation, J Mater Res Technol, 9 (3) (2020), pp. 3198-3207

C. Vipulanandan, A. Parihar, M. Issac, Testing and modeling composite coatings with silanes for protecting reinforced concrete in saltwater environment, J Mater Civ Eng, 23 (12) (2011), pp. 1602-1608

Medeiros, M.; Helene, P. Efficacy of surface hydrophobic agents in reducing water and chloride ion penetration in concrete. Mater. Struct. Constr. 2008, 41, 59–71.

Medeiros, M.H.F.; Helene, P. Surface treatment of reinforced concrete in marine environment: Influence on chloride diffusion coefficient and capillary water absorption. Constr. Build. Mater. 2009, 23, 1476–1484.

Polder, R.B.; Borsje, H.; De Vries, H. Hydrophobic treatment of concrete against chloride penetration. Corros. Reinf. Concr. Constr. Proc. Fourth Int. Symp. 1996, 183.

Levi, M.; Ferro, C.; Regazzoli, D.; Dotelli, G.; Presti, A.L. Comparative evaluation method of polymer surface treatments applied on high performance concrete. J. Mater. Sci. 2002, 37, 4881–4888.

Perenchio WF. Curability of concrete treated with silanes, Concrete international; November 1988. p. 34–40.

M. Pigeon, J. Prevost, et al., Freeze–thaw durability versus freezing rate, ACI J (1985), pp. 684-692

Vesikari E. Prevention of frost-salt action on concrete by use of surface sealants, Nordic concrete research, No. 2; December 1983. p. 205–14.

C.K. Leung, H.G. Zhu, J.K. Kim, R.S. Woo, Use of polymer/organoclay nanocomposite surface treatment as water/ion barrier for concrete, J Mater Civ Eng, 20 (7) (2008), pp. 484-492

L. Jia, C. Shi, X. Pan, J. Zhang, L. Wu, Effects of inorganic surface treatment on water permeability of cement-based materials, Cem Concr Compos, 67 (2016), pp. 85-92

V. Kasselouri, N. Kouloumbi, and T. Thomopoulos, "Performance of silica fume-calcium hydroxide mixture as a repair material," Cement and Concrete Composites, vol. 23, no. 1, pp. 103–110, 2001.

E. Franzoni, B. Pigino, C., P. istolesiEthyl, silicate for surface protection of concrete: performance in comparison with other inorganic surface treatments, Cement Concrete Comp, 44 (2013), pp. 69-76

L. Thompson, M.R. Silsbee, P.M. Gill, B.E. Scheetz, Characterization of silicate sealers on concrete, Cement Concrete Res, 27 (1997), pp. 1561-1567

B. Pigino, A. Leemann, E. Franzoni, P. LuraEthyl, silicate for surface treatment of concrete – part II:

characteristics and performance, Cement Concrete Comp., 34 (2012), pp. 313-321

Ibrahim, M.; Al-Gahtani, A.S.; Maslehuddin, M.; Dakhil, F.H., Use of surface treatment materials to improve concrete durability. J. Mater. Civ. Eng. 1999, 11, 36–40.

Moon, H.Y.; Shin, D.G.; Choi, D.S., Evaluation of the durability of mortar and concrete applied with inorganic coating material and surface treatment system. Constr. Build. Mater. 2007, 21, 362–369.

R.C. Higgins, Waterproofing for Concrete, Reference and Guide, Sinak Corp. (1985)

J. Dai, Y. Akira, E. Kato, H. Yokota, Investigation of chloride ingress in cracked concrete treated with water repellent agents, 5th International Conference on Water Repellent Treatment of Building Materials, Aedificatio Publishers, Freiburg (2008), pp. 299-310

E. McGettigan, Silicon-based weatherproofing materials, Concr. Int., 14 (1992), pp. 52-56

Perepelkin, K.E, 2004. Fluoropolymer Fibres: Physicochemical nature and structural dependence of their unique properties. Fabrication, and Use. A Review. Fibre Chemistry, 36 (1), 43–58.

Li, X., et al., 2002. Semifluorinated aromatic side-group polystyrene-based block copolymers: bulk structure and surface orientation studies. Macromolecules, 35 (21), 8078–8087.

R.F. Brady, Clean hulls without poisons: devising and testing nontoxic marine coatings, J. Coat. Technol., 72 (900) (2000), pp. 45-56

E. Passaglia, M. Aglietto, F. Ciardelli, B. Mendez, 13 C NMR characterization of polymers from 2, 2, 2-trifluoroethyl methacrylate, Polym. J., 26 (10) (1994), p. 1118

J. Scheerder, N. Visscher, T. Nabuurs, and A.Overbeek, Novel, Water-Based Fluorinated Polymers With Excellent Antigraffiti Properties, JCT Research, Vol. 2, No. 8, October 2005

A. Barbucci, M. Delucchi, G. Cerisola, Organic coatings for concrete protection: liquid water and water vapour permeabilities, Prog Org Coat, 30 (1997), pp. 293-297

M. Delucchi, A. Barbucci, G. Cerisola, Study of the physico-chemical properties of organic coatings for concrete degradation control, Constr Build Mater, 11 (1997), pp. 365-371

P. Basheer, L. Basheer, D.J. Cleland, A.E. LongSurface treatments for concrete: assessmen tmethods and reported performance Constr. Build. Mater. 11 (7) (1997), pp. 413-429

U. Attanayake, X. Liang, S. Ng, H. Aktan Penetrating sealants for concrete bridge decks—selection procedureJ. Bridge Eng., 11 (5) (2006), pp. 533-540

P.K. Mehta, P.J. Monteiro, Concrete: Microstructure, Properties, and Materials, vol. 3, McGraw-Hill, New York (2006)

D.W. Pfeifer, M.J. Scali, Concrete sealers for protection of bridge structures. NCHRP report 244, Transport Research Board, National Research Council, 1981.

Franzoni, E.; Varum, H.; Natali, M.E.; Bignozzi, M.C.; Melo, J.; Rocha, L.; Pereira, E. Improvement of historic reinforced concrete/mortars by impregnation and electrochemical methods. Cem. Concr. Compos. 2014, 49, 50–58

L. Jia, C. Shi, X. Pan, J. Zhang, L. Wu, Effects of inorganic surface treatment on water permeability of cement-based materials, Cement Concr. Compos. 67 (2016), pp. 85-92

Czarnecki. L, Garbacz. A, Kostana. K, The Effect of Concrete Surface Roughnesson Adhesion in Industrial Floor Systems. Sth. Int. Colloq. - Industrial Floors, Esslingen, Germany, January 21-23; 2003: 168-174

A. Garbacz, L. Courard, K. Kostana, Characterization of concrete surface roughness and its relation to adhesion in repair systems, June 2006

Y. J. Shen, Y. Z. Wang, Y. Yang, Q. Sun, T. Luo, H. Zhang, Influence of surface roughness and hydrophilicity on bonding strength of concrete-rock interface, Construction and Building Materials, Volume 213, 20 July 2019, Pages 156-166

Y. Lin, J. He, Recent progress in antireflection and self-cleaning technology – from surface engineering to functional surfaces, Prog. Mater. Sci., 61 (8) (2014), pp. 94-143

T. Young, III. An essay on the cohesion of fluids, Philos. Trans. R. Soc. London, 1995, 65–87.

R.N. Wenzel, Resistance of solid surfaces to wetting by water, Ind. Eng. Chem., 28 (1936), pp. 988-994

A.B.D. Cassie, S. Baxter, Wettability of porous surfaces, Trans. Faraday Soc., 40 (1944), pp. 546-550

A. Marmur, The Lotus effect: superhydrophobicity and metastability, Langmuir, 20 (2004), pp. 3517-3519

X. Zhang, L. Wang, E. Leaven, Superhydrophobic surfaces for the reduction of bacterial adhesion, RSC Adv., 3 (30) (2013), pp. 12003-12020

W. She, X. H. Wang, C. W. Miao, Q. C. Zhang, Y. S. Zhang, J. X. Yang, J. X. Hong, Biomimetic superhydrophobic surface of concrete: Topographic and chemical modification assembly by direct spray, Construction and Building Materials, Volume 181, 30 August 2018, Pages 347-357

Karthick, S.; Park, D.-J.; Lee, Y.S.; Saraswathy, V.; Lee, H.-S.; Jang, H.-O.; Choi, H.-J. Development of water-repellent cement mortar using silane enriched with nanomaterials. Prog. Org. Coat. 2018, 125, 48-60.

U.R. Berner, Modeling the incongruent disolution of hydrated cement minerals. Radiochim. Acta. 1988; 44–45:387-393.

Adenot F., Buil M. Modeling of the corrosion of the cement paste by deionized water. Cem. Concr. Res. 1992; 22:489–496.

Li X.-Y., Fang K.-H. Research on leakage dissolution of hydraulic roller compacted concrete (RCC) J. Yangtze River Sci. Res. Inst. 2008;20:27–31.

Faucon P., Adnot F., Jacquinot J.F., Petit J.C., Cabrillac R., Jorda M. Long-term behaviour of cement pastes used for nuclear waste disposal: Review of physico-chemical mechanisms of water degradation. Cem. Concr. Res. 1998; 28:847–857.

Maltais Y., Samson E., Marchand J. Predicting the durability of Portland cement systems in aggressive environments—Laboratory validation. Cem. Concr. Res. 2004; 34:1579–1589

Kamali S., Moranville M., Leclercq S. Material and environmental parameter effects on the leaching of cement pastes: Experiments and modelling. Cem. Concr. Res. 2008; 38:575–585.

CHAPTER 2

MATERIALS AND EXPERIMENTAL METHODS

2.1 Overview

This chapter describes the conditions of the experiments, including the properties of the materials, the equipment, experimental methods, and the experimental ratios used in the experiments.

2.2 Experimental program

2.2.1 Materials

In this experiment, the materials are the white Portland cement with two types of mortar used in the experimental with w/c ratios of 0.45 and 0.55, as shown in Table 2.1. The cement with the specific gravity of 3.05 g/cm^3. The fine aggregates with the density of 2.65 g/cm^3 (crushed lime sand from Torigatayama, Kochi Prefecture, Japan).

Table 2.1 Mix proportions of mortar

W/C	Cement	Flow	Air content	Material content（kg/m^3）		
		（mm）	（%）	W	C	S
0.45	white Port-land cement	200	3.0	228	415	1606
0.55				228	508	1525

2.2.2 Mortar

Mortar mixtures were prepared in the laboratory 540 cubes with the dimensions of 150 mm × 150 mm × 20 mm were cast; 100 cubes with the dimensions of 70 mm × 130 mm × 10 mm were casted. 100 cubes with the dimensions of 300 mm × 300 mm × 20 mm were cast and according to the corresponding JIS (Japanese Industrial Standard) methods. After casting and initial curing for 24 hours in standard conditions, the specimens were removed from the molds and were cured in a controlled environment with a temperature of 20 °C and a relative humidity of 50 % for 28 days. There were two types of mortar were used in the experimental with water-cement ratios of 0.45 and 0.55.

2.2.3 Types of surface protective material

After 28 days of curing, a brush was used to coat the one-sided surfaces of the mortar specimens with each type of selected surface coating. The concrete coating was applied following the application process recommended by the suppliers exactly. Four concrete surface protective materials were used in this study. Table 2.2 listed the technical information of surface protective materials. Uncoated mortar specimens were also prepared as control. After the surface coating, all specimens were cured in the dry condition at a temperature of 20 °C and a relative humidity of 30 % for 14 days.

Table 2.2 Surface protective materials.

Types and Symbol	N Un-coated	A Silane1	B Silane2	C Fluor-resin	D Silicate
Coating procedure — First coating	—	— —	— —	water-based water-repellent	— —
Curing time	—	— —	— —	More than 16 hours	200 g/m² — —
Medium coating	—	— —	— —	Fluor-resin	— —
Curing time	—	— —	— —	More than 3 hours	100 g/m² — —
Top coating	—	Silane	Silane	Fluor-resin	Aqueous silicate
Curing time	—	More than 4 hours 200 g/m²	More than 6 hours 200 g/m²	More than 24 hours 100 g/m²	24 hours 250 g/m²

2.2.4 Accelerated weathering tests

2.2.4.1 Humidity and cool-heat cycling

To investigate the changes in the coating film when subjected to temperature changes after the coating has undergone wetting or soaking. Humidity and cool-heat cycling of the surface coating materials on samples was performed for 10 cycles, 20 cycles in three kind of constant temperature and humidity chamber according to Japanese standard: JIS K 5600-7-4, (1999). One cycle of humidity and cool-heat cycling is need 24 hours. The process is: put into$23\pm2℃$, (50 ± 5) %RH constant temperature and humidity water tank at 18 hours, and $-20\pm2℃$Constant temperature and humidity chamber3 hours, last one $50\pm1℃$, 95%RH constant temperature and humidity chamber3 hours. Table 2.3 listed the technical information about the humidity and cool-heat cycling test procedure

Table 2.3. The method of accelerated aging test

①	②	③
Immersion	Low temperature	High temperature
$23\pm2℃$, 95%RH	$-20\pm2℃$	$50\pm1℃$, (50 ± 5) %RH
18 hours	3 hours	3 hours

2.2.4.2 Warm water immersion

The sample was placed in a container and water was poured into a constant temperature heater at 40°C and immersed in 14 and 28 days in warm water at 40°C to promote the occurrence of swelling. The test was carried out according to the method of JIS K5600-6-2. In order to avoid absorbing water from other surface to act on the surface coating material, the side of the specimens were sealed with aluminum tape before the warm water immersion. Two hundred ten specimens were used in this test with a size of $150 \times 150 \times 20$ mm^3.

2.2.4.3 Xenon-arc light radiation

To simulate the potentially damaging effect of long-term outdoor exposure, generally accelerated weathering test were performed. Accelerated weathering of the surface coating materials on samples was performed for 5000

hours in a xenon-arc light test chamber according to Japanese standard: JIS K 5600-7-7:2008 (ISO 11341:2004).

The wetting and drying time were 1 cycle (120 minutes), with the wetting time of 18 minutes and the drying

time of 102 minutes. Wetting condition: at temperature 38 ± 3 °C and relative humidity RH95% and the

irradiance of 60 W/m^2 (in the range of 300 nm～400 nm) and spray water on the surface. Drying condition: the

irradiance of 60 W/m^2 (in the range of 300 nm～400 nm), with the relative humidity RH of 50%, the black panel

temperature of 63 ± 2°C. The test specimens to evaluate each performance of coatings was carried out at different

weathering hours, after 0 hours (initial test), 2500 hours and 5000 hours, respectively. Table 2.4 listed the

technical information about the accelerated aging test procedure. One hundred specimens were used in this test

with a size of $130 \times 75 \times 10$ mm^3. Fifty mortar specimens were used for 2500 hours and fifty for 5000 hours

weathering, respectively.

Table 2.4 The method of accelerated aging test

	Hour	Temperature	Black panel temperature	Relative humidity	Illuminance
	min	℃	℃	%	［w/m^2］
Wetting	18	38	-	95	60
Drying	102	-	63±2	50(40-60)	60

2.3 Performance evaluation experimental method

2.3.1 Visual observation

The visual observation was carried out according to the "Evaluation of Degradation of Coatings - Designation

of the amount and size of defects and the intensity of uniform changes in appearance" defined in Japanese

Standard: JIS K 5600-8-1~6 (2014). The evaluation is carried out under the bright illumination that the defect or

appearance change can be confirmed. The indication of the degree of uniform changes in the coating surface,

such as hue changes (e.g., yellowing) and calcification of the coating film, as shown in Table 2.5. If there are no

other agreements between the receiving parties, the grade is indicated as an integer. Three specimens for each

treatment and three untreated specimens from each concrete were used for a total of thirty specimens tested.

Table 2.5 Displaying grade of the degree of change

Grade	Degree of change
0	No change (i.e., there is no change to be observed.)
1	Very small (i.e., barely observed change.)
2	A slight (i.e., a clearly observed change. ）
3	Medium (i.e., a very clearly observed change.)
4	Critical (i.e., substantial change. ）
5	Very marked change.

2.3.2 Color differences

Color differences based on the visual characteristics of the film− calculation of color differences according to Japanese standard: JIS K 5600-4-6 (1999) and the results were evaluated using the color difference ΔE^*ab between two colors using the CIELAB color difference formula that is the geometric distance between two colors in the (CIE 1976) $L^*a^*b^*$ color space. The ΔE formulas are shown below:

$$\Delta E^*ab = [(\Delta L^*)^2 + (\Delta a^*)^2 + (\Delta b^*)^2]^{1/2}$$

$$\Delta L^* = L^*_T - L^*_R$$

$$\Delta a^* = a^*_T - a^*_R$$

$$\Delta b^* = b^*_T - b^*_R$$

Where $L*$ is the lightness, $a*$ is the green/red color component, $b*$ is the yellow/blue color component, and ΔL^*, Δa^* and Δb^* indicate the differences in $L*$, $a*$ and $b*$ between two specimens.

Each specimen was measured at four points (75 mm diameter) within the specimens (mean value was used).

2.3.3 Gloss

JIS K 5600-4-7 (1999), the glossiness was measured by "HORIBA IG-340". The axis of geometrically condition incidence light is typically at three angles of incidence $20° \pm 0.5°$, $60° \pm 0.2°$, and $85° \pm 01°$. The axis of the receiver shall match within ± 0.1 with respect to the mirror image of the axis of incident light. A smooth surface of polished black glass or a mirror is placed at the sample position, so that the image of the light source is formed in the center of the viewing aperture of the receiver. The width of the irradiated part of the specimen shall be significantly larger than the surface structure to be estimated, so that an average over the whole surface is obtained. The generally accepted width value is 10 mm. The measurement point is the same as the color difference.

2.3.4 Roughness

JIS B 0601-2001, the surface roughness is evaluated by the average roughness Ra [μm] according to "Mitutoyo SJ-210". Measurement is performed by a roughness tester that meets the specifications of JIS B 0601-2001 "Geometric characteristic specifications (GPS) - surface properties of products: contour curve method - terms, definitions and surface properties parameters". In both the x and y directions, four points are measured from a point 37.5 mm away from the angle toward the center.

2.3.5 Contact angle

The static contact angle is a simple parameter to characterize the hydrophobicity of the surface-coated concrete. In order to evaluate the surface hydrophobic effect of the treatments, the static contact angle was measured at 10 different points of specimens treated on one face was measured with a Drop Master 300 (Kyowa Interface Science Co., Ltd. Japan). A water drop of known volume was released on the concrete external surface by a flat needle placed from a known distance, determining the contact angle for the water drop pick-up.

2.3.6 Anti-soiling test

The anti-soiling test method standards is devised in the previous report (JIS B 0601-2001). This research reproduced two methods, one method is the simulated raindrops method to pollutant (Fig. 2.2) that occurs on the lower wall surface of the window, so that rainwater containing accumulated dust flows down uniformly to the sample surface. Two method is coating method to pollutant (Fig. 2.1).

The model contaminated water is a carbon black (manufactured by FW 200: Orion Engineered Carbons) according to the method for pollution accelerated test for construction exterior wall materials by JSTM J 7602. And the reason of choice carbon black that is easily disperses in water and stands out black by itself.

One method is the carbon black liquid coating uniformly on the surface to pollutant. Using a brush, apply the carbon black liquid coating uniformly on the surface of the test sample, which is placed flat, until the coated surface is no longer visible. And the experiment detail is show in Fig. 2.1.

Method two is the simulated raindrops method to pollutant that occurs on the lower wall surface of the window, so that rainwater containing accumulated dust flows down to the sample surface. We designed an experimental device to simulate carbon black liquid. To imitate the traces left by raindrops, one streak stain was generated by dropping a 50 mL suspension onto a corrugated sheet at 2 drops/sec and letting it flow down from the corrugated sheet onto a test piece. After dropping, it was dried for 20 minutes. In order to verify the cleanability of the surface protective material, spray cleaning and ultrasonic cleaning, two cleaning methods with different strengths were used. In order to show the rain falling in the form of a curtain of water, simulate the rain washing the carbon black trace using a water spraying machine. Spraying water on the wave board, water was allowed to flow down from the corrugated sheet to the test sample and washing was performed for 2 minutes. Ultrasonic cleaner, which generates a frequency of 40 kHz, cleaning is stronger than spray cleaning method. After 1 minute cleaning, using the 300cc water to wash away the carbon black particles on the surface of the test specimens. And the experiment detail is show in Fig. 2.2.

| The carbon black liquid | Coating method to pollutant | ultrasonic cleaning machine |

Fig. 2.1 Coating method to pollutant

| The carbon black liquid | Simulated raindrops method to pollutant | the spray cleaning method | ultrasonic cleaning machine |

Fig. 2.2 Simulated raindrops method to pollutant
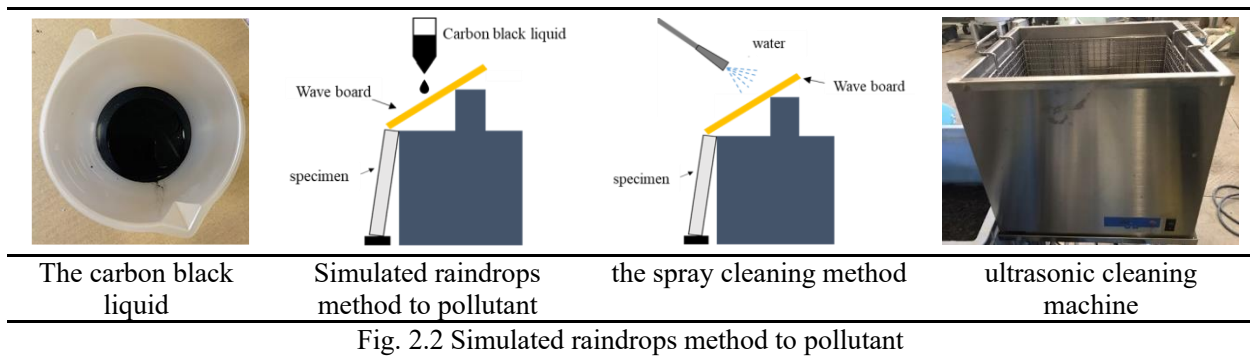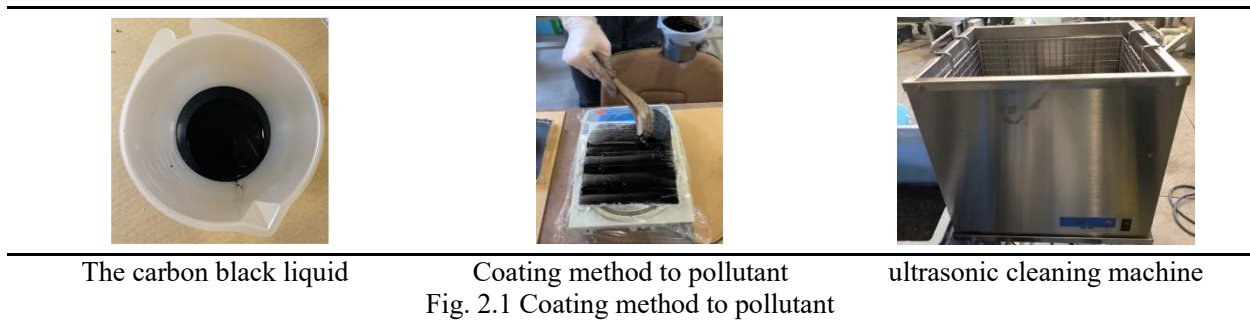
2.3.6.1 Visual observation

After dropping with the carbon black liquid, cleaning with a spray, and cleaning with ultrasonic waves, photographs were taken and the changes in appearance were visually observed.

2.3.6.2 ImageJ (Brightness, Pollution area fraction, Pollution average width)

Brightness is the degree of brightness of a color, where $L^* = 0$ represents black and $L^* = 100$ represents white. The brightness difference was calculated by measuring the brightness of the entire surface of the test piece before and after the anti-soiling test using the image processing software "ImageJ". The brightness difference, ΔL^*, was determined from the following formula: $\Delta L^* = | L^* - L0^* |$, where ΔL^* is brightness difference, L^* is average brightness after carbon black liquid dropping test, and $L0^*$ is average brightness before carbon black liquid dropping test. Pollution average width measured by the image processing software "ImageJ". The threshold value was set to 150 after binarizing. Measure the width within the length range of 15 cm from top to bottom.

2.3.7 Water absorption test

As water ingress into concrete is directly or indirectly responsible for all its degradation processes, the resistance after accelerated aging test of the treated and untreated specimens the radiation and water ingress is the destructive element for these materials.

The water absorption tests were conducted with NSK Specification "Permeable Water Absorbent Preventive Material" was determined using the Japan standards NSKS-04. The prepared composite specimens were dried in oven at 80 °C until the specimen mass remained constant, followed by submerging in water for 24 hours. The changes in the mass of the specimens could be used to evaluate the water absorption ratio was calculated by dividing the surface area (in cm^2) with the weight growth (in mg) of the sample. For each treatment, three specimens of each concrete were used, and three untreated specimens were retained.

2.3.8 Moisture permeability test

Moisture permeability is the resistance of a material to water vapor diffusion through a unit of surface area. The moisture permeability test was performed on the specimens treated on the surface and on the untreated ones for comparison according to Japan standard JSCE-K571-2005: specimens were weighed in surface-dry conditions after keeping immersed in water 3 days. After that the container is weighed to determine every day the amount of water that has exited the contain percentage after 7 days.

References

JIS K 5600-7-7:2008 (ISO 1134: 2004): Testing methods for paints−Part 7: Long-period performance of film−Section 7: Accelerated weathering and weathering to artificial radiation (Weathering to filtered xenon-arc radiation) (In Japan)

JIS K 5600-8-1~6:2014: Testing methods for paints-Part 8: Evaluation of degradation of coatings-designation of quantity and size of defects, and of intensity of uniform changes in appearance-section 1: general principles and rating schemes (In Japan)

JIS K 5600-4-6:1999: Testing methods for paints−Part 4: Visual characteristics of film−section 6: Colorimetry (Calculation of color differences) (In Japan)

JIS K 5600-4-7:1999Testing methods for paints−Part 4: Visual characteristics of film−section 7: Specular gloss, Japan (In Japan)

JIS B 0601-2001: Definitions and designation of rolling circle waviness (In Japan)

NSKS-004 penetration type water absorption prevention materials, Japan Building Coating Materials Association (In Japan)

JSCE-K571-2005: Test methods of surface penetrants for concrete structures (In Japan)

JIS K 5600-7-4,1999: Testing methods for paints−Part 7: Long-period performance of film−Section 4: Humidity and cool-heat cycling test (In Japan)

CHAPTER 3

EVALUATION OF SURFACE CHARACTERIZATIONS AND WATER RESISTANCE OF SURFACE COATINGS AFTER HUMIDITY AND COOL-HEAT

3.1 Overview

Concrete is widely used for building constructions because its easy construction, low cost and easy usefulness of raw materials (Marie et al., 2012). Freeze-thaw (F-T) damage in concrete constructions is a frequent materials-related discomfort that expresses itself in two ways (Fagerlund et al., 2004): Internal frost damage causes bulk cracking and loss of integrity, and (2) surface scaling causes the mortar component to enlarge and flake.

However, there is a shortage of data on evaluating surface change, associated moisture absorption, and anti-soiling at the same time. A lot of study has gone into finding effective ways to improve the freeze-thaw endurance of concrete structures and reduce the consequent economic losses. Concrete surface treatment is a low-cost method that has been generally praised for its effectiveness and cost savings (Scarfato et al., 2012; Vacchiano et al., 2008). Organic and inorganic surface treatments can be distinguished (Delucchi et al., 1997; Franzoni et al., 2013). Organic surface treatments have greater barrier qualities, but their service life is restricted by working circumstances, particularly in hot and humid environments (Jones et al., 1995; Vries et al., 1997; Kotnarowska et al., 1999; Al-Turaif et al., 2013). Inorganic surface treatments, on the other hand, have a longer service life; nevertheless, the application of inorganic treatments and their interactions with the concrete substrate are poorly understood. As a result, more research is required to fully understand the rising point.

Furthermore, various research (Basheer et al., 2006; Ibrahim et al., 1999; Sandrolini et al., 2012; Pigino et al., 2012) have explored and confirmed the benefit of silane-based pore liners on concrete durability. Mirza et al. (2011) examined the performance of numerous surface treatments in safeguarding concrete structures with w/c ratios of 0.55 and 0.70 at low temperatures, including 28 silanes, 13 siloxanes, 12 cement-based sealers, 2 epoxies resins, 2 acrylic resins, and 1 silicate. The best performance was provided by silane and siloxane family impregnations in that study, in which the surface protections were applied and cured for 14 days at a temperature of only 4 °C; silicates, as in previous studies, performed poorly in terms of water absorption and water vapor transmission capacity. Pigino et al. (2012) recently investigated the properties and performance of ethyl silicate for surface treatment of concrete with w/c ratios of 0.45 and 0.65. Both concrete showed a considerable reduction in capillary suction, chloride diffusion coefficient, and carbonation depth after treatment, showing that this form

of silicate has a lot of promise. We also investigated the changes in color and brightness provided by the concrete over time in this study, which could be important in some outdoor applications for aesthetic reasons.

In the previous studies it was observed that the water is a fundamental part of many forms of concrete degradation. The capacity of surface treatment materials to resist water penetration is an essential measure of their performance (Mehta et al., 2006). Surface treatments can successfully increase the longevity of concrete structures in coastal conditions by minimizing water absorption (Franzoni et al., 2013; Basheer et al., 1997; Delucchi et al., 1997; Hansson et al., 1998). Water absorption of coated cement mortars is substantially lower than that of uncoated samples, according to Almusallam et al. (2003), but performance of the same type of generic surface treatments varies greatly. As a result, any water repellent or moisture-resistant surface treatment should be thoroughly tested before being widely used. Surface treatments capacity to improve concrete freeze-thaw resistance is related to its ability to prevent water infiltration. Basher et al. (2006) indicated that the number of freeze-thaw cycles before initial cracking of silane-treated concrete doubled compared to uncoated samples. The effect of silane on the freeze-thaw resistance of concrete was affected by the initial moisture content of the concrete and water pressure (Basheer et al., 1997).

As previously stated, only a small number of studies have been undertaken to test alternative surface treatments for improved concrete freeze/thaw resistance (Basheer et al., 2006). However, no study has definitively shown whether the change in surface characterizations and water resistance, as well as the change in anti-soling that happens during freezing and thawing, are related.

To minimize time and money in durability investigations, accelerated test methods with acceleration factors of high temperature and/or sustained load were frequently utilized. Therefore, the objective of the current study is included several commercial products of surface treatment in the test program, including two concrete sealers, one coating, one impregnation, and two water repellents. To characterize the product effectiveness, the surface coated mortar was subjected to 20 wet/freeze/thaw (50℃ dry) cycles. To help interpret the difference in product performance, the surface-coated mortar specimens were tested for their water absorption, moisture permeability. To characterize the product surface change under deterioration, the appearance characteristics and dirt resistance

effectiveness of mortar coated by each product was tested. For all the laboratory tests, the untreated concrete was used as control.

3.2 Results and discussion

3.2.1 Influence of different surface protective materials on appearance characteristics

3.2.1.1 Visual observation

As shown in Fig.3.1 (w/c 0.45), Fig.3.2 (w/c 0.55), there were no change in the appearance of the coating, such as swelling, rusting or cracking, until 20 cycles of repeated heating and cooling. N, C and D are slightly deeper in color than the initial value of C0. The water-cement ratio of 0.55 followed the same trend as that observed for the 0.45 appearance.

0.45	N	A	B	C	D
C0					
C10					
C20					
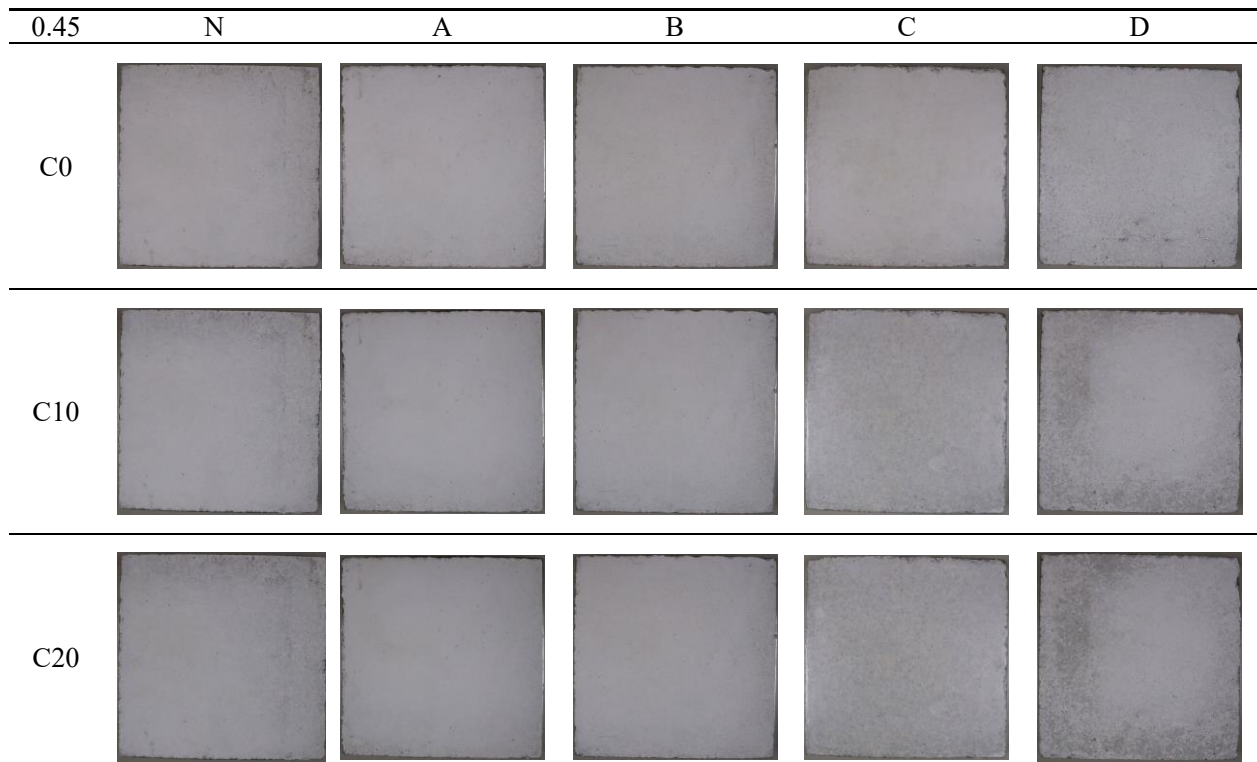
Fig. 3.1 Visual observation for each type of coating after humidity and cool-heat cycling ageing, w/c 0.45

0.55	N	A	B	C	D
C0					
C10					
C20					
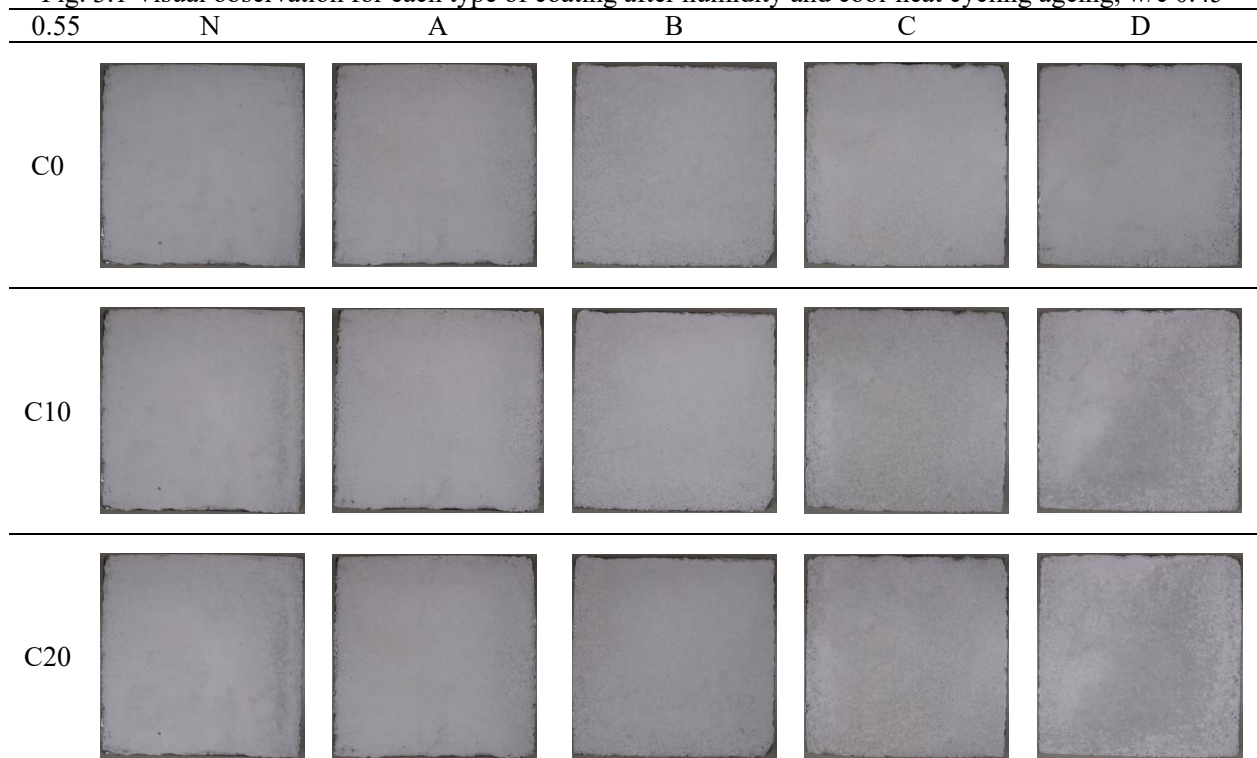
Fig. 3.2 Visual observation for each type of coating after humidity and cool-heat cycling ageing w/c 0.55

3.2.1.2 Brightness

Fig. 3.3 shows the results for the brightness of color difference. There was no change in the brightness of the specimens up to 20 cycles, except for C. On the other hand, the retention of lightness of all specimens was more than 98%. This result is consistent with Fig.3.1, Fig.3.2. The brightness of water-cement ratios 0.45 and 0.55 show a similar tendency.
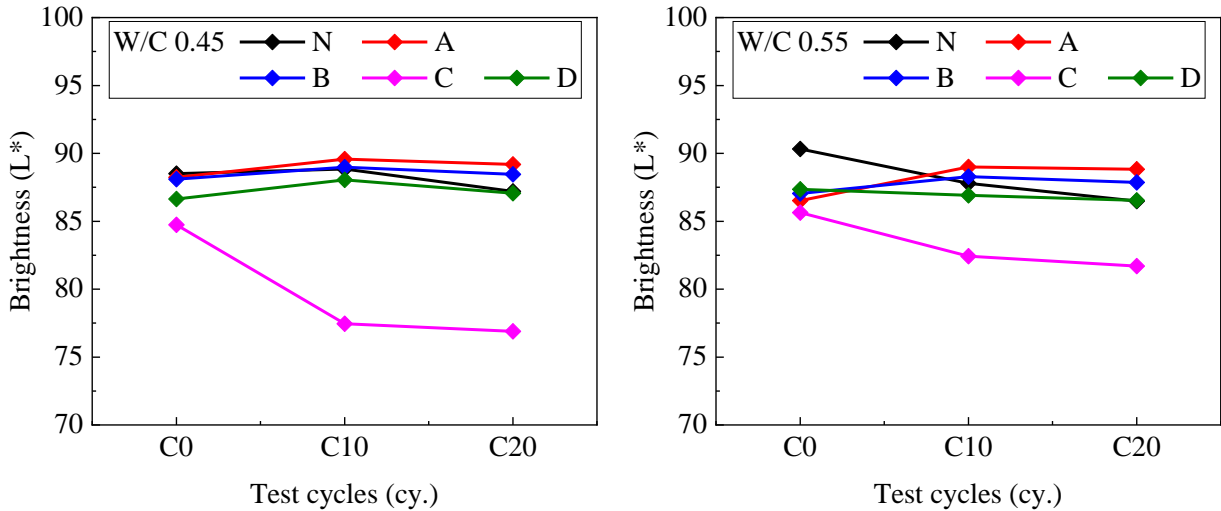
Fig. 3.3 Brightness for each type of coatings after humidity and cool-heat cycling ageing (0, 10 and 20 cycles)

3.2.1.3 Gloss

The loss of gloss metric was utilized to track the physical changes in the samples. In fact, as the body of the binder is removed, the surface of a pigmented film gradually roughens, resulting in a loss of shine. Gloss is measured by comparing the reflection of a visible beam of light from the surface to a standard black glass surface. The most frequent coating specification is to state the maximum period the coating will keep a gloss level greater than 50% of its original value (UNI EN. ISO 11341, 2004; UNI EN. ISO 11507, 2007; UNI AN ISO 2813, 1999). In Fig. 3.4 are reported the plot of loss of gloss versus time of aging determined for all the samples o after humidity and cool-heat cycling ageing (0, 10 and 20 cycles).

In the case of surface protective materials A, B and C, the tendency of gloss to be similar to that of no coating was observed, suggesting that there was little effect on glossiness after 20 cycles of repeated heating and cooling. For fluoropolymer C, the gloss level was higher. In other words, the gloss of the surface coating material became higher because of the coating film on the surface. In addition, the silicate type, which has the highest gloss among the surface coating materials, is a water-based material and is closer to the wet color than other types of coating materials.
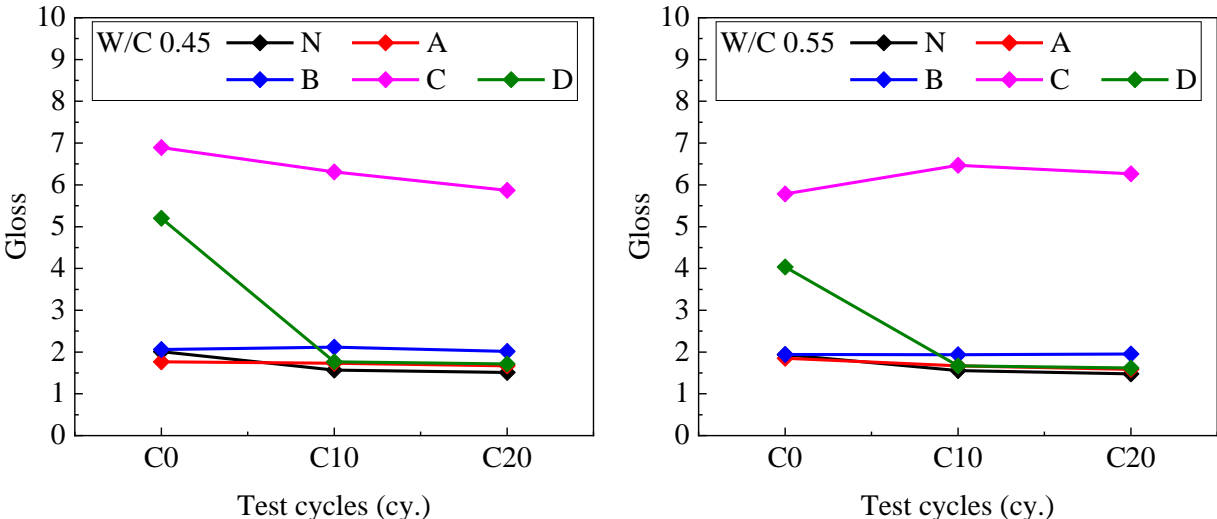
Fig. 3.4 Gloss for each type of coatings after humidity and cool-heat cycling ageing (0, 10 and 20 cycles)

3.2.1.4 Roughness

The result of surface roughness shown in Fig.3.5. Overall, the arithmetic means roughness increased slightly with the number of warm and cold cycles. After 20 cycles of water-cement ratio 0.45, the arithmetic mean roughness of silanes A and B and silicate D was greater than that of uncoated N. The water-cement ratio 0.55, the arithmetic mean roughness of silanes A, B and silicate D was similar to uncoated N. The arithmetic mean surface roughness of fluor-rein C has a small after humidity and cool-heat cycling espouse.
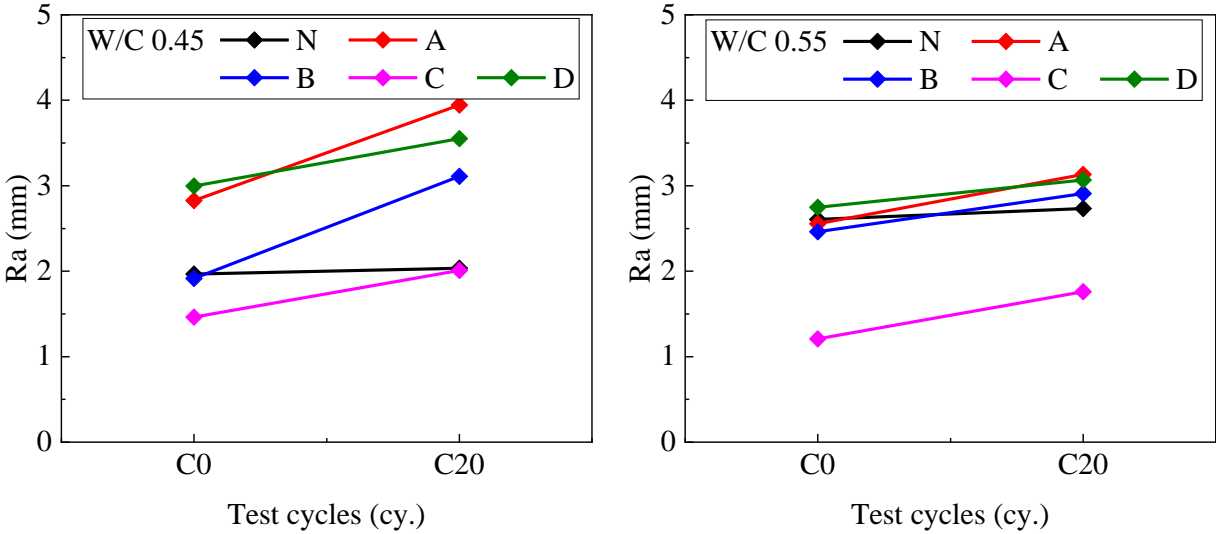
Fig. 3.5 Roughness for each type of coatings after humidity and cool-heat cycling ageing (0, 10 and 20 cycles)

3.2.1.5 Contact angle

The contact angle is an index of wettability. The larger of the contact angle, the more hydrophobic the material is the smaller of the contact angle, the more hydrophilic of the material is. The change in hydrophilicity over time was evaluated by measuring the water contact angle after each cycle. A contact angle of 90° to 150° is considered to be the standard value for a hydrophobic material.

The contact angle results are shown in Fig.3.6. The contact angles of the uncoated specimens ranged from 25.8° to 72.46°. When the silane surface impregnant was applied, the contact angle was higher for all the products than when it was not applied. Therefore, it can be said that the silane surface impregnant added a hydrophobic function to the concrete surface. In particular, the contact angle of silane system B ranged from 126.21° to 126.82°, a significant difference. The contact angle of fluor-rein C ranged from 84.72° to 95.51°, indicating that the hydrophobic function was added to the concrete surface.

The contact angle of silicate D ranged from 17° to 41.89°, which was lower than that of the uncoated material, and was about 40° to 80° smaller than that of the other surface protection materials, confirming its high hydrophilic effect.

After 20 cycles of hot and cold cycles, the contact angle of the surface protective material became larger. The reason of this tendency needs to be considered in the future.
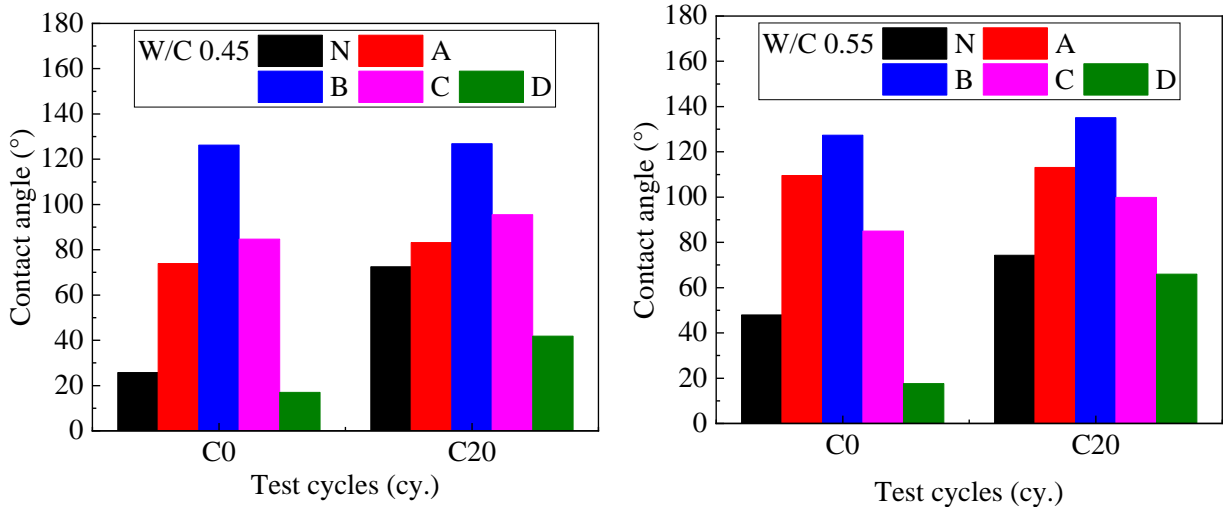
Fig. 3.6 Contact angle for each type of coatings after humidity and cool-heat cycling degradation (0, 10 and 20 cycles)

3.2.2 Effect of different surface protective materials on permeability

3.2.2.1 Water absorption

Fig. 3.7 shows the results of the water absorption test for mortar.

The water absorption of the uncoated specimens tended to decrease after 20 cycles of heating and cooling. This is due to the progress of hydration and densification near the surface layer. For mortar specimens, the water absorption was decreased coated four types of surface protective materials. A and B showed the least water absorption among all other coatings. Regarding concrete surface protective materials, silane A and B coatings would be the most suitable and compatible treatment to reducing water permeability of concrete.

On the other hand, the water absorption of the specimens coated with the surface protective materials was lower than that of the uncoated specimens for all the surface protective materials except for D. This indicates that the water absorption suppression effect was sufficiently demonstrated. The silicate D has higher water absorption same tendency to N. Because D has lower contact angle value (<90°) that indicates that is hydrophilicity of coating.
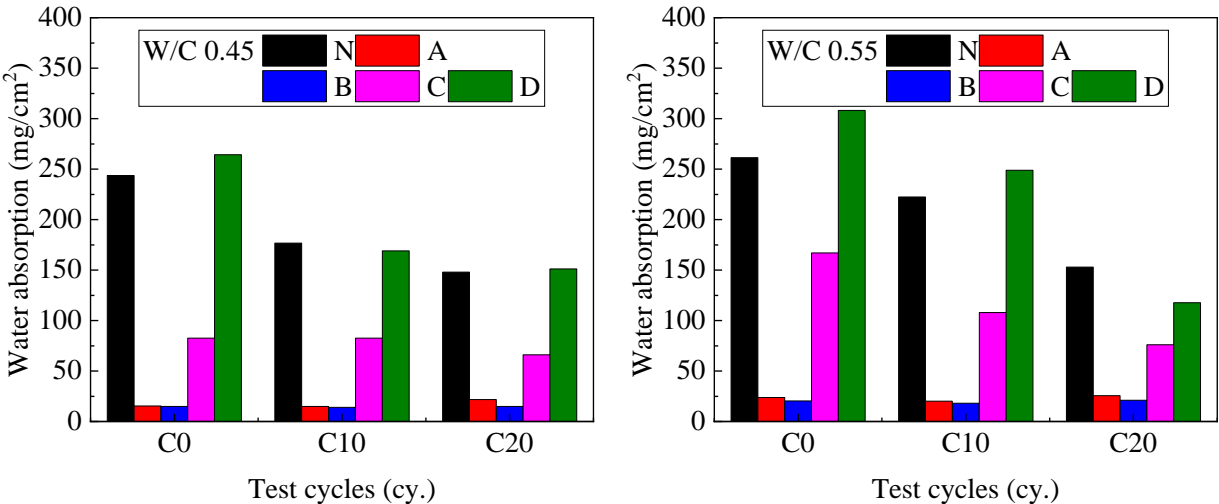
Fig. 3.7 Water absorption for each type of coatings after humidity and cool-heat cycling ageing (0, 10 and 20 cycles)

3.2.2.2 Moisture permeability

Fig. 3.8 shows the results of the moisture permeability test for mortar.

Regardless of the repeated cycles of heating and cooling and the water-cement ratio, the uncoated specimen N

and the silicate system D have relatively high moisture permeability. In contrast, silane-based A and B and fluor-

resin C coatings showed very lower permeability.

In concrete, more water than necessary for hydration is used as mixing water for the purpose of workability,

so that water dissipation due to drying continues after hardening. Therefore, if the surface of concrete is covered

with a finish coating material which has almost no water and moisture permeability, it may cause problems such

as blistering of the finish coating layer, excessive moisture permeability towards the inner wall and the

occurrence of mold. Therefore, it is desirable that the finishing material used for the surface finish of the exterior

wall of a building should ideally have low water permeability and moderate moisture permeability.
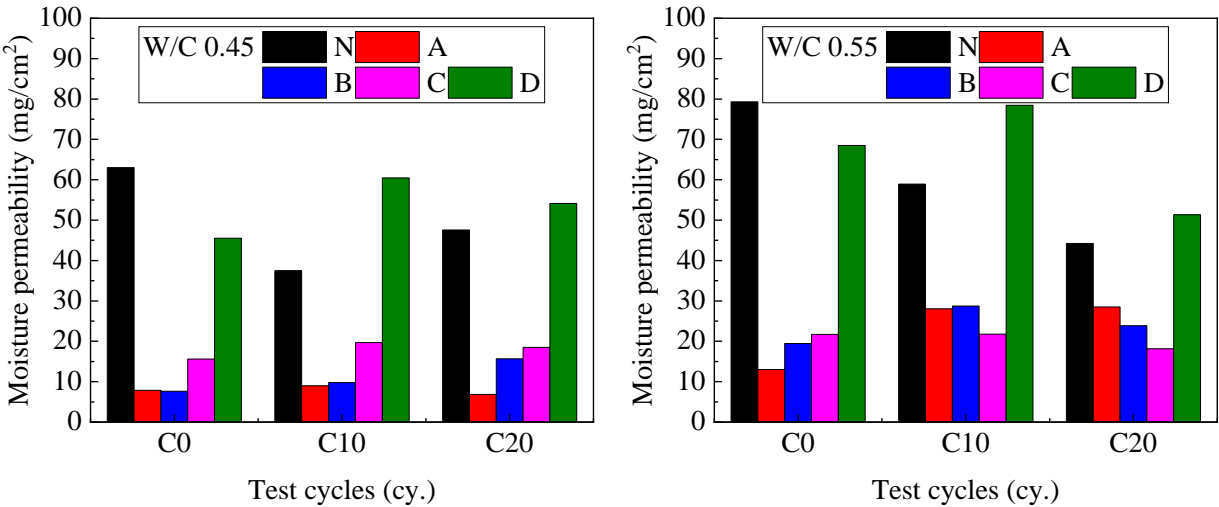
Fig. 3.8 Moisture permeability for each type of coatings after humidity and cool-heat cycling ageing (0, 10 and 20 cycles)

3.2.3 Effect of different surface protective materials on different methods of anti-soiling test

3.2.3.1 Coating method to pollutant

Visual observation

To further investigate the contaminants on and the destruction of the samples, take photographs of all the samples before and after carbon black coated and after cleaning by ultrasonic cleaning are shown in Fig. 3.9.

After soiling, N, A, C, D is similar, where carbon black liquid is spreading evenly on the surface. However, B coating has high hydrophobic surfaces, because the carbon black water is in the form of drops on the surface. After soiling, N, A, C, D is similar, there surfaces are almost covered by contaminants. However, B coating has high hydrophobic surfaces, because water is in the form of drops and readily rolls on the surface to carry the dust and dirt away. After cleaning, the majority of the contaminants are removed by ultrasonic cleaning. N, C, D, are soiled most seriously, and its surface is almost covered by contaminants, it is difficult to clean the contaminants, especially after 20 cycles ageing.

0.45	N0	N20	A0	A20	B0	B20	C0	C20	D0	D20
Pollution										
Ultrasonic cleaning										

0.55	N0	N20	A0	A20	B0	B20	C0	C20	D0	D20
Pollution										
Ultrasonic cleaning										
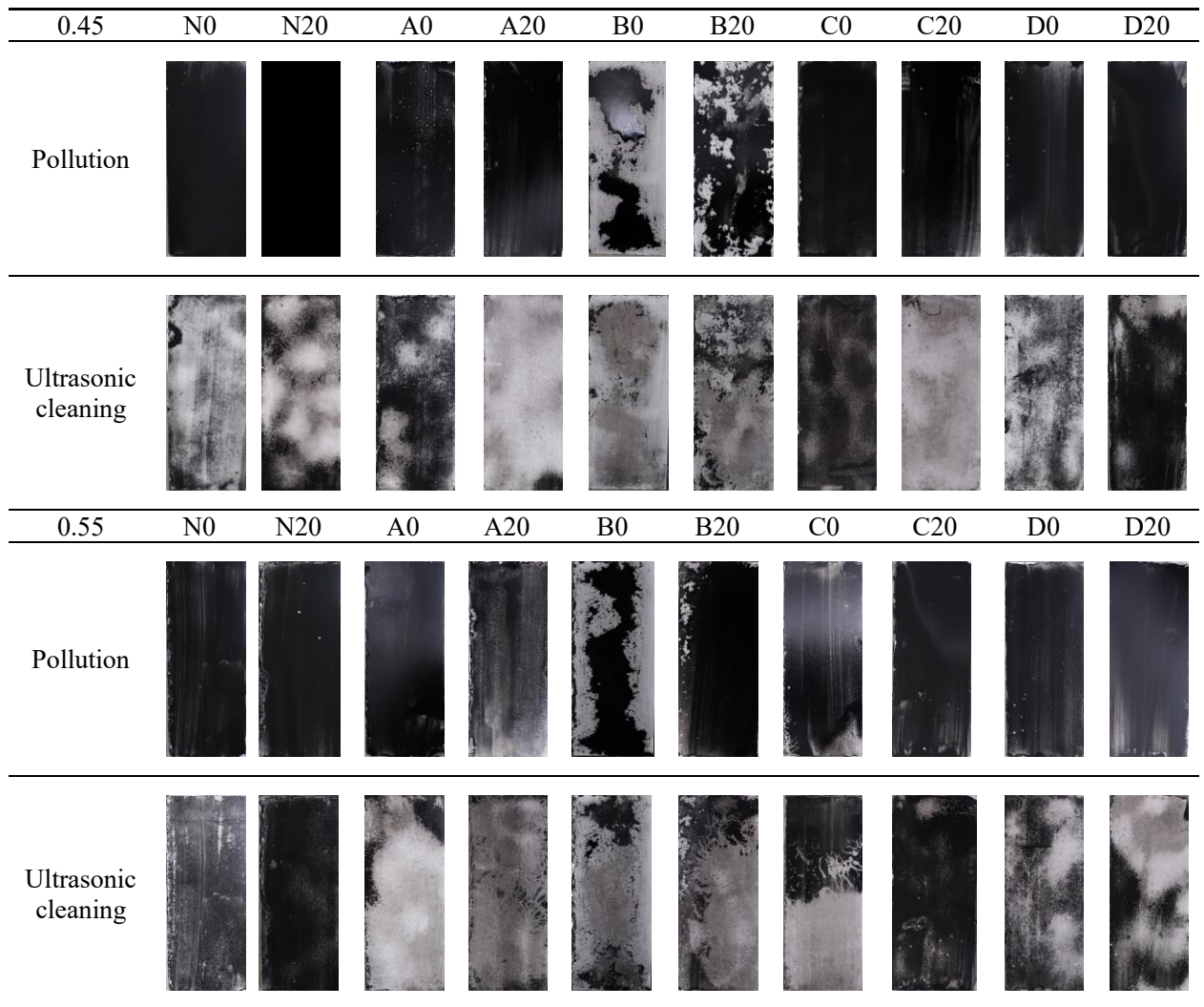
Fig. 3.9 visual observation for each type of coating after coating method to pollutant

Brightness

Fig.3.10 shows the brightness difference (ΔL*). Initial, at w/c 0.45, the brightness difference (ΔL*) of B and

D became smaller than N. At w/c 0.55, the brightness difference (ΔL*) was smaller than N. After 20 cycles

ageing, at w/c 0.45, the brightness difference (ΔL*) both A and C was smaller than N. The brightness difference

(ΔL*) both B and N has same tendency.
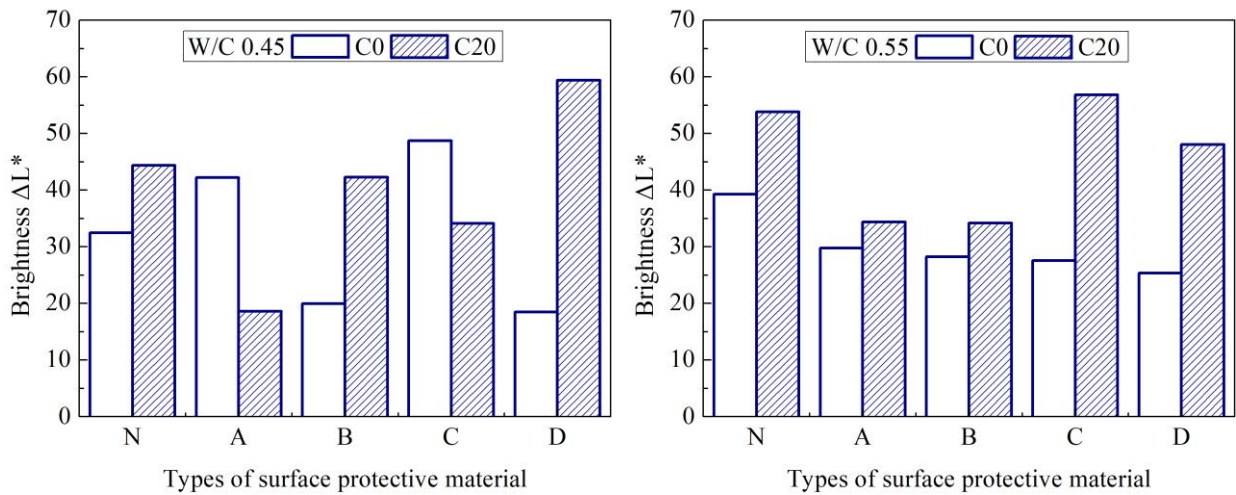
Fig. 3.10 Brightness difference for each type of coating after coating method to pollutant

Pollution area fraction

Fig.3.11 shows the pollution area fraction. At all levels, B was about 40~60% after contamination.

After 20 cycles ageing, after pollution, the pollution area fraction of B was lower than N and other coatings.

After ultrasonic cleaning, the pollution area fraction of A, B and C was lower than N.
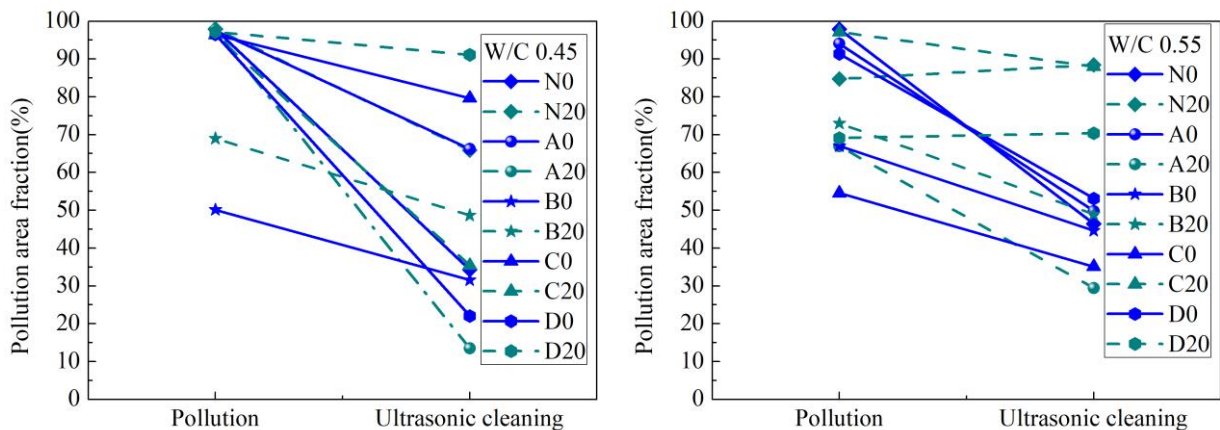
Fig. 3.11 Pollution area fraction for each type of coating after coating method to pollutant

3.2.3.2 Simulated raindrops method to pollutant

Fig.3.12, Fig.3.13 shows the results of visual observation. The initial (C0) test, both cement-water ratios 0.45 and 0.55, the flow liquid dropped on surface of silane A and B was fast during pollution, resulting the raindrops was thin and stains. The pollution raindrops line was fat on surface D coating. After cleaning, D coating was removed by ultrasonic cleaning, the brightness difference (ΔL^*) (Fig.3.14) and pollution average width (Fig.3.15) of which lowest even after cleaning. Because the contact angle of D coating is $17° < \theta < 41.89°$, indicating that the hydrophilic, the hydrophilic coating in a film wise manner and carries away dust particles as water running downslope to the bottom of the panel (Bahattab et al., 2016).

After C20, B coating was both cement-water ratios 0.45 and 0.55, the pollution raindrops liquid flowed faster and stain thinner. After clearing, all of the specimens the majority of the contaminants could not remove by spray cleaning and ultrasonic cleaning. Among the four types of surface protective materials, B coating are soiled most lightest, and its surface is little covered by contaminants. Both brightness difference (ΔL^*) and pollution average width was the smallest (Fig.3.14, Fig.3.15).
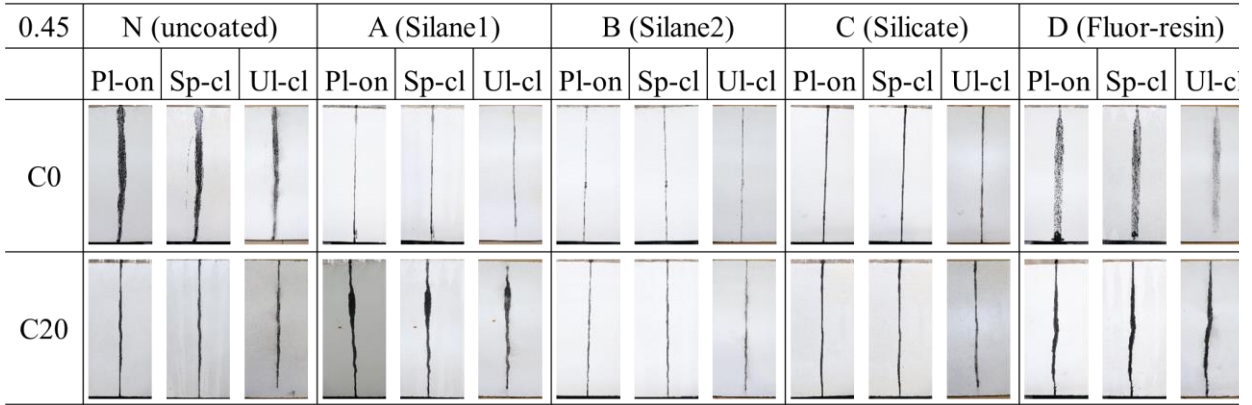
0.45	N (uncoated)			A (Silane1)			B (Silane2)			C (Silicate)			D (Fluor-resin)		
	Pl-on	Sp-cl	Ul-cl	Pl-on	Sp-cl	Ul-cl	Pl-on	Sp-cl	Ul-cl	Pl-on	Sp-cl	Ul-cl	Pl-on	Sp-cl	Ul-c
C0															
C20															

Fig. 3.12 Visual observation for each type of coating after simulated raindrops method to pollutant, w/c 0.45

0.55	N (uncoated)			A (Silane1)			B (Silane2)			C (Silicate)			D (Fluor-resin)		
	Pl-on	Sp-cl	Ul-cl	Pl-on	Sp-cl	Ul-cl	Pl-on	Sp-cl	Ul-cl	Pl-on	Sp-cl	Ul-cl	Pl-on	Sp-cl	Ul-c
C0															
C20															
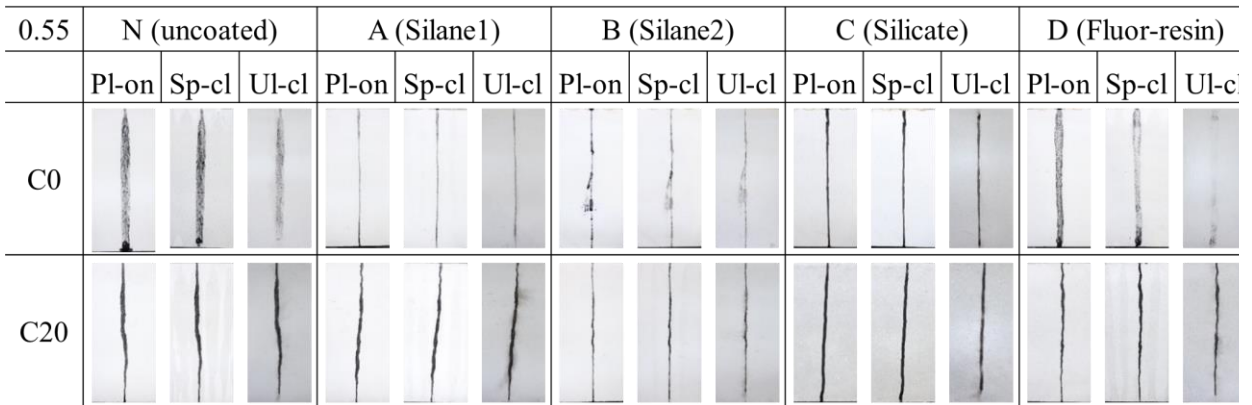
Fig. 3.12 Visual observation for each type of coating after simulated raindrops method to pollutant, w/c 0.55
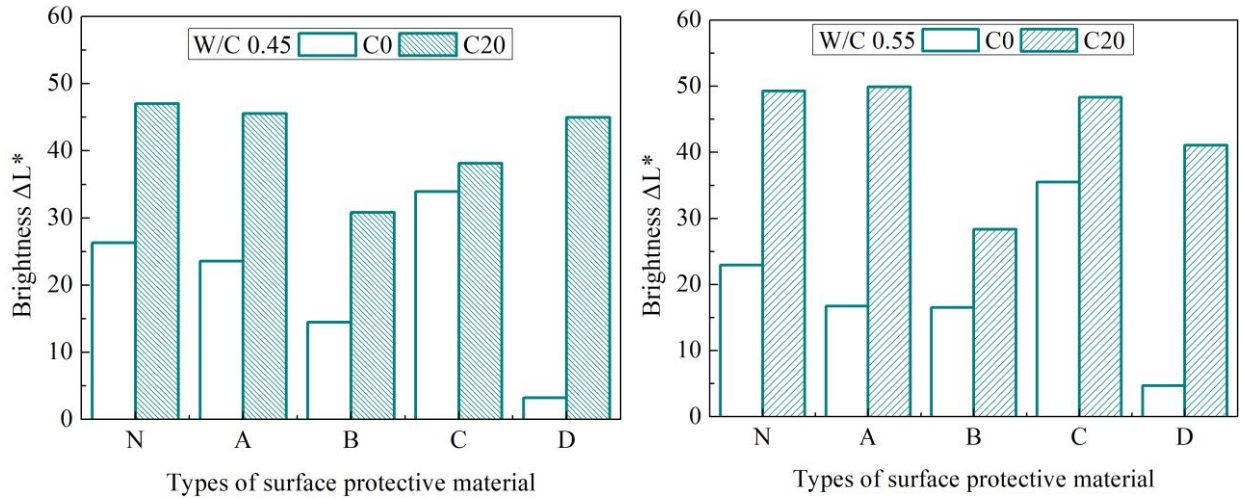
Fig. 3.13 Difference in lightness for each type of coating after simulated raindrops method to pollutant
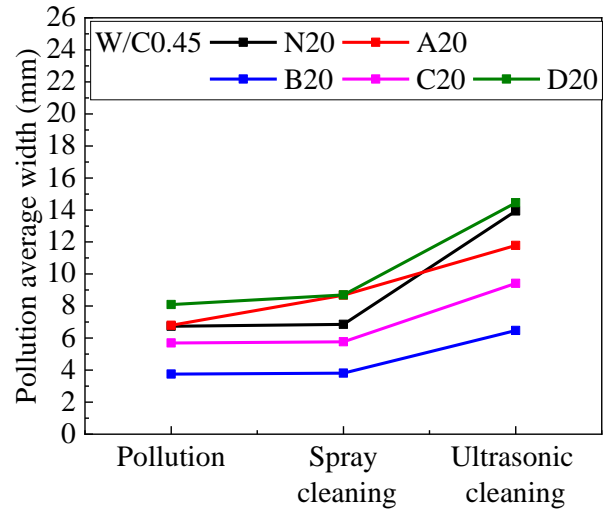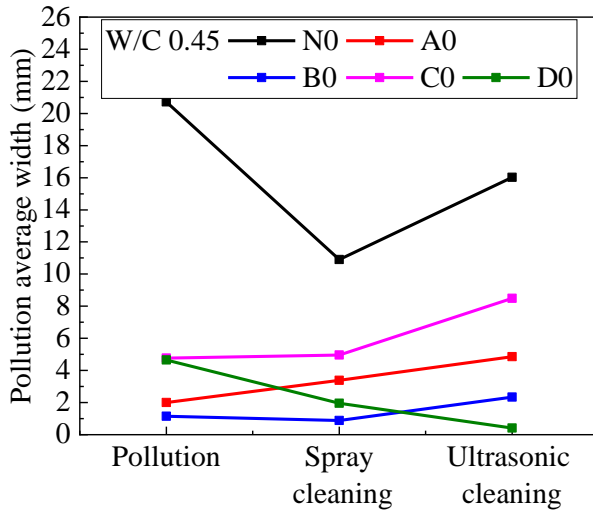
Fig. 3.14 Pollution average width for each type of coating after simulated raindrops method to pollutant, w/c 0.45
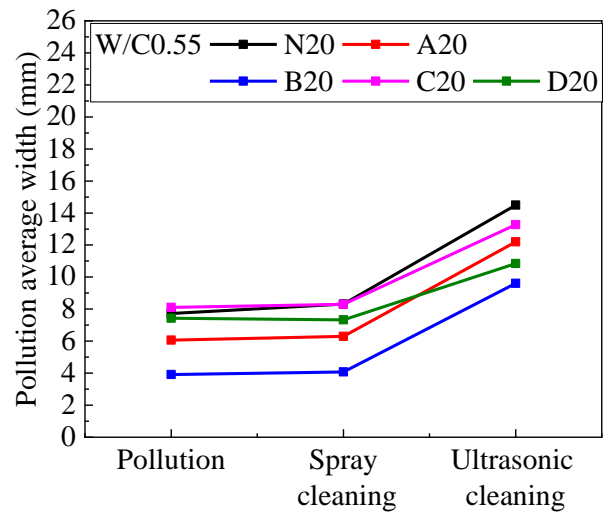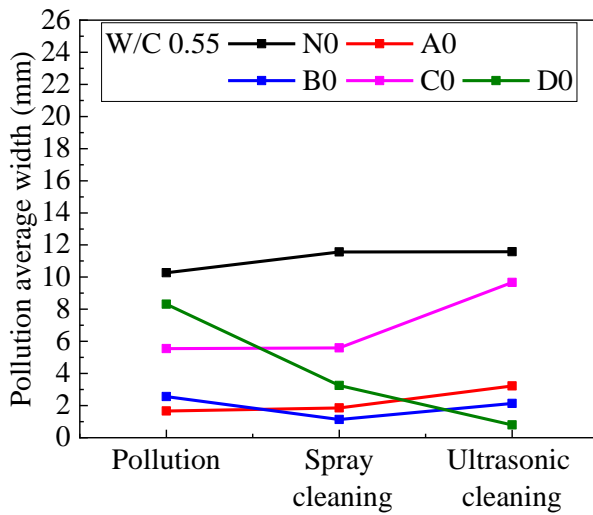
Fig. 3.15 Pollution average width for each type of coating after simulated raindrops method to pollutant, w/c 0.55

3.3 Conclusions

In this chapter, to characterize the product effectiveness, the surface coated mortar was subjected to 20 wet/freeze/thaw(50 °C dry) cycles of mortar samples made with w/c = 0.45 and 0.55, coated with different types of surface protective materials has been investigated in this study. To help interpret the difference in product performance, the surface-coated mortar specimens were tested for their water absorption, moisture permeability. To characterize the product surface change under deterioration, the appearance characteristics and dirt resistance effectiveness of mortar coated by each product was tested. On the other hand, use the coating method and simulated raindrops method to pollutant of anti-soiling test of comparative experiments were performed by humidity and cool-heat cycling for 20 cycles to systematically study the effects of anti-soiling performance of surface protective materials. The following conclusions can be drawn based on the experimental results.

Testing the four types surface protecive material in this study showed promising results in protecting concrete from water absorption. While A and B showed the least water absorption rate between all other coatings. Regarding concrete surface protective materials, silane A and B coatings would be the most suitable and compatible treatment to reducing water permeability of concrete.

Regarding aesthetic properties, the color, gloss and roughness have acceptable variations after exposure. For the coated samples A, B and D after 20 cycles of aging test, was still keep the brightness of 98% and this stands for a good resistance in term of discoloration. Also, for the C we had observed, after 20 cycles of aging, the brightness has a small decreased than others types

By coating method to pollutant, after the aging tests, expect N, C coating, A, B, D coatings practically maintained the same efficiency as at time zero. Among the four types of surface protective materials, hydrophobic C encountered the most serious soiling problems in both before and after aging tests, which was ascribed to it having the largest adhesion force between contaminants and the surface.

By the simulated raindrops method to pollutant, the either hydrophilic or hydrophobic N, D and A, B, C were compared. In terms of surface chemistry, the A and B with a hydrophilic surface showed a better soiling resistance than the hydrophobic ones.

References:

I. Marie, H. QuiasrawiClosed-loop recycling of recycled concrete aggregatesJ. Cleaner Prod., 37 (2012), pp. 243-248

G. Fagerlund, A Service Life Model for Internal Frost Damage in Concrete. Report TVBM-3119Lund Institute of Technology, Lund, Sweden (2004)

Paola Scarfato, Luciano Di Maio, Maria Letizia Fariello, et al., Preparation and evaluation of polymer/clay nanocomposite surface treatments for concrete durability enhancement, Cem. Concr. Compos. 34 (2012), pp. 297-305

C.D. Vacchiano, L. Incarnato, P. Scarfato, D. Acierno, Conservation of tuff-stone with polymeric resins, Construct. Build. Mater., 22 (2008), pp. 855-865

M. Delucchi, A. Barbucci, G. Cerisola, Study of the physical-chemical properties of organic coatings for concrete degradation control, Constr. Build. Mater., 11 (7) (1997), pp. 365-371

E. Franzoni, B. Pigino, C. Pistolesi, Ethyl silicate for surface protection of concrete: performance in comparison with other inorganic surface treatments, Cem. Concr. Compos., 44 (2013), pp. 69-76

M.R. Jones, R.K. Dhir, J.P. Gill, Concrete surface treatment: effect of exposure temperature on chloride diffusion resistance, Cem. Concr. Compos., 25 (1) (1995), pp. 197-208

I.J. De Vries, R.B. Polder, Hydrophobic treatment of concrete, Constr. Build. Mater., 11 (4) (1997), pp. 259-265

D. Kotnarowska, Influence of ultraviolet radiation and aggressive media on epoxy coating degradation, Prog. Org. Coat., 37 (3) (1999), pp. 149-159

H.A. Al-Turaif, Surface morphology and chemistry of epoxy-based coatings after exposure to ultraviolet radiation, Prog. Org. Coat., 76 (4) (2013), pp. 677-681

L. Basheer, D.J. ClelandFreeze-thaw resistance of concerts treated with pore linersConstr Build Mater, 20 (10) (2006), pp. 990-998

M. Ibrahim, A. Al-Gahtani, M. Maslehuddin, F. DakhilUse of surface treatment materials to improve concrete durabilityJ Mater Civ Eng, 11 (1) (1999), pp. 36-40

F. Sandrolini, E. Franzoni, B. PiginoEthyl silicate for surface treatment of concrete Part 1: Pozzolanic effect of ethyl silicateCem Concr Compos, 34 (3) (2012), pp. 306-312

B. Pigino, A. Leemann, E. Franzoni, P. LuraEthyl silicate for surface treatment of concrete Part II: Characteristics and performanceCem Concr Compos, 34 (3) (2012), pp. 313-321

J. Mirza, C. Abesque, M.A. BérubéEvaluation of surface sealers for concrete hydraulic structures exposed to low temperaturesMater Struct, 44 (1) (2011), pp. 5-12

B. Pigino, A. Leeman, E. Franzoni, P. LuraEthyl silicate for surface treatment of concrete – Part II: characteristics and performanceCement Concr Compos, 34 (2012), pp. 313-321

P.K. Mehta, P.J. Monteiro, Concrete: Microstructure, Properties, and Materials, vol. 3, McGraw-Hill, New York (2006)

E. Franzoni, B. Pigino, C. Pistolesi, Ethyl silicate for surface protection of concrete: performance in comparison with other inorganic surface treatments, Cem. Concr. Compos., 44 (2013), pp. 69-76

P. Basheer, L. Basheer, D.J. Cleland, A.E. Long, Surface treatments for concrete: assessment methods and

reported performance, Constr. Build. Mater., 11 (7) (1997), pp. 413-429

M. Delucchi, A. Barbucci, G. Cerisola, Study of the physico-chemical properties of organic coatings for concrete degradation control, Constr. Build. Mater., 11 (7) (1997), pp. 365-371

C.M. Hansson, L. Mammoliti, B.B. Hope, Corrosion inhibitors in concrete-part I: the principles, Cem. Concr. Res., 28 (12) (1998), pp. 1775-1781

A.A. Almusallam, F.M. Khan, S.U. Dulaijan, O. Al-Amoudi, Effectiveness of surface coatings in improving concrete durability, Cem. Concr. Compos., 25 (4) (2003), pp. 473-481

L. Basheer, D.J. Cleland, Freeze–thaw resistance of concretes treated with pore liners, Constr. Build. Mater., 20 (10) (2006), pp. 990-998

P. Basheer, L. Basheer, D.J. Cleland, A.E. Long, Surface treatments for concrete: assessment methods and reported performance, Constr. Build. Mater. 11 (7) (1997), pp. 413-429

L. Basheer, D.J. Cleland, Freeze-thaw resistance of concerts treated with pore liners, Constr Build Mater, 20 (10) (2006), pp. 990-998

UNI EN. ISO 11341, published 01-09-2004; Paints and varnishes – Artificial weathering and exposure to artificial radiation – Exposure to filtered xenon-arc radiation.

UNI EN. ISO 11507, published 18-10-2007, Paints and varnishes – Exposure of coatings to artificial weathering – Exposure to fluorescent UV lamps and water.

UNI AN ISO 2813:1999; Paints and varnishes – Determination of specular gloss of non-metallic paint film at 20°, 60° and 85°.

M.A. Bahattab, I.A. Alhomoudi, M.I. Alhussaini, M. Mirza, J. Hegmann, W. Glaubitt, P. LöbmannAnti-soiling surfaces for PV applications prepared by sol-gel processing: Comparison of laboratory testing and outdoor exposureSol. Energy Mater. Sol. Cells, 157 (2016), pp. 422-428

CHAPTER 4

INFLUENCE OF SURFACE PROTECTIVE MATERIAL ON APPEARANCE CHANGE

AND MOISTURE PROPERTIES AFTER IMMERSION IN WARM WATER

4.1 Overview

Water molecules not only be affected by the freeze-thaw cycle, but also affected by warm water immersion. In Chapter 3, the influence of freeze-thaw cycles on surface protective materials has been demonstrated, while the influence of hot and humid environment has not been clarified

Coating application on porous substrates such as formed concrete and concrete block can cause bubbling similar to that seen in coatings applied to carbon steel that are subjected to immersion service or prolonged exposure to high-moisture environments. In these cases, the concrete substrate inherent porosity traps trapped air or moisture. Air is present because it will inhabit any open space that is not under vacuum, and moisture enters the structure from the exterior or interior. Interior moisture can come from "vapor drive" (i.e., humidity and condensing moisture) from the interior of the structure, and exterior moisture often enters through the natural porosity of the concrete substrate and along cracks, fissures, or control joints. When a non-breathable coating is applied to porous substrates, air and moisture are often "locked" within the substrate. As a result, any condition (such as sunlight) that causes the air to warm and the moisture to vaporize causes the concrete to expand and increase its pressure. Bubbles are frequently formed due to increased pressure on the backside of the covering.

Moreover, Leaching is also the natural dissolution and diffusion of calcium ions in cement paste. It has been identified as one of the factors that contribute to durability issues and has been thoroughly researched. Leaching has been studied by a number of academics as an inherent problem of concrete when immersed in water (Faucon et al., 1998). Maltais et al. (2004) studied the effects of the external environment on leaching and discovered that when immersed in deionized water, calcium hydroxide and C-S-H were leached, however when immersed in sodium sulfate solution, ettringite and gypsum might be produced. The difference in leaching rates of cement pastes when immersed in different media was discovered by Kamali et al. (2008). They discovered that the overall amount of leaching in NH_4NO_3 solution after 19 days is 4–5 times greater than that in pure water after 114 days, and that this is true at both room temperature and high temperature (85 °C). Aside from the external environment, the microstructure of concrete has an impact on the leaching process. The water-to-cement ratio (w/c) is the most essential factor in limiting leaching, according to Maltais et al. (2004). A smaller w/c results in

a denser microstructure, which increases concrete's leaching resistance. The bigger the aggregate volume fraction is while w/c is held constant, the lower the leaching rate will be.

The hydration of cement in concrete, which occurs simultaneously with leaching, makes the microstructure of concrete denser and improves its impermeability water (Ma et al., 2013). Under immersion conditions, it is possible that the struggle between leaching and hydration determines the evolution of concrete qualities such as permeability. According to a recent study, hygrothermal exposure can produce matrix swelling, and if the matrix is exposed to an overly severe environment, such as 80 °C water, the matrix can lose weight and suffer mechanical property loss (Kamali et al., 1998). Although transport properties in general concrete have been investigated broadly, studies on transport properties of the surface layer of concrete can rarely be found in the literature (Liu et al., 2013). To fill this gap, a series of studies need to be conducted.

Therefore, in the objective of this study, mortar specimens were coated the surface protective materials to immerse in 40°C water, and the evolution of the surface permeability of concrete under such immersion conditions investigated. Mechanisms behind the influence of the immersion are revealed in light of appearance change and ant-soling experimental methods. The resulting data can be considered as the reference in a more extensive investigation (Kamali et al., 2008), and can provide a baseline for potential models of transport processes in concrete subjected to complex environment.

This paper focuses on the analysis of the changes in the aesthetic properties of the surfaces and the water permeability of four types of coatings under the warm water immersion and further outlines to obtain more information on the degradation of the protective properties of the exterior wall protective coatings. Observation of the appearance and water contact angle, color differences, roughness and water absorption, moisture permeability, evaluation of the aesthetics between coatings and concrete were examined in order to monitor age-related changes. To assess the protective performance of coating materials, the resistance to pollution was determined. The aim of this study is to develop relationships between coating deterioration and protection performance and also to show the influence of surface protection material on its physical and aesthetic deterioration.

4.2 Results and discussion

4.2.1 Surface characterization of coatings

The appearance of the surface covering material after 28 days of warm water immersion showed the Fig. 4.1, Fig. 4.2.

In the immersion test of water, a small swelling occurred on the fluorine resin-based C surface 1 to 2 weeks after immersion, and after 28 days, swelling occurred on most samples. No abnormalities were observed after 28 days when silane systems A, B and silicate D were applied. This is because in the case of the external deterioration factor for the fluor resin coating material, it is considered that the deterioration factor due to the penetration of water from the inside strongly works.

0.45	N	A	B	C	D
W0					
W14					
W28					
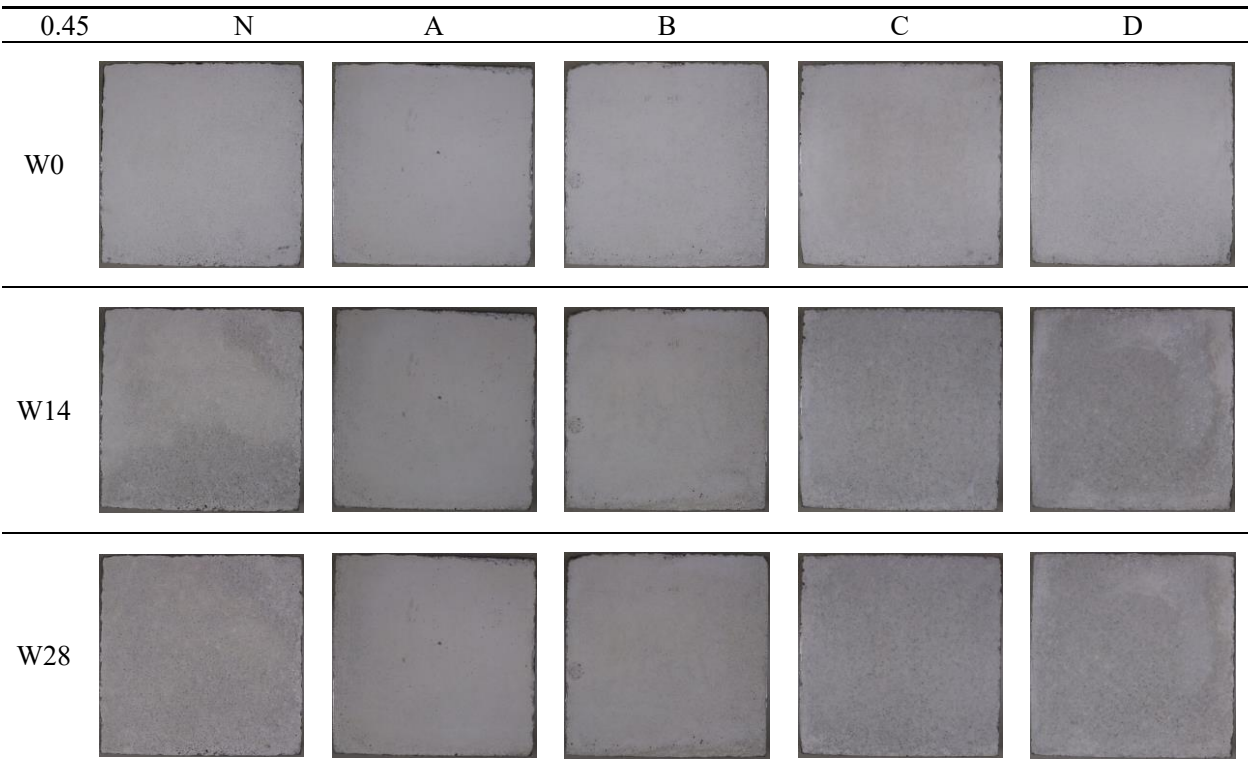
Fig. 4.1 Visual observation for each type of coating before and after immersion in warm water, w/c 0.45

0.55	N	A	B	C	D
W0					
W14					
W28					
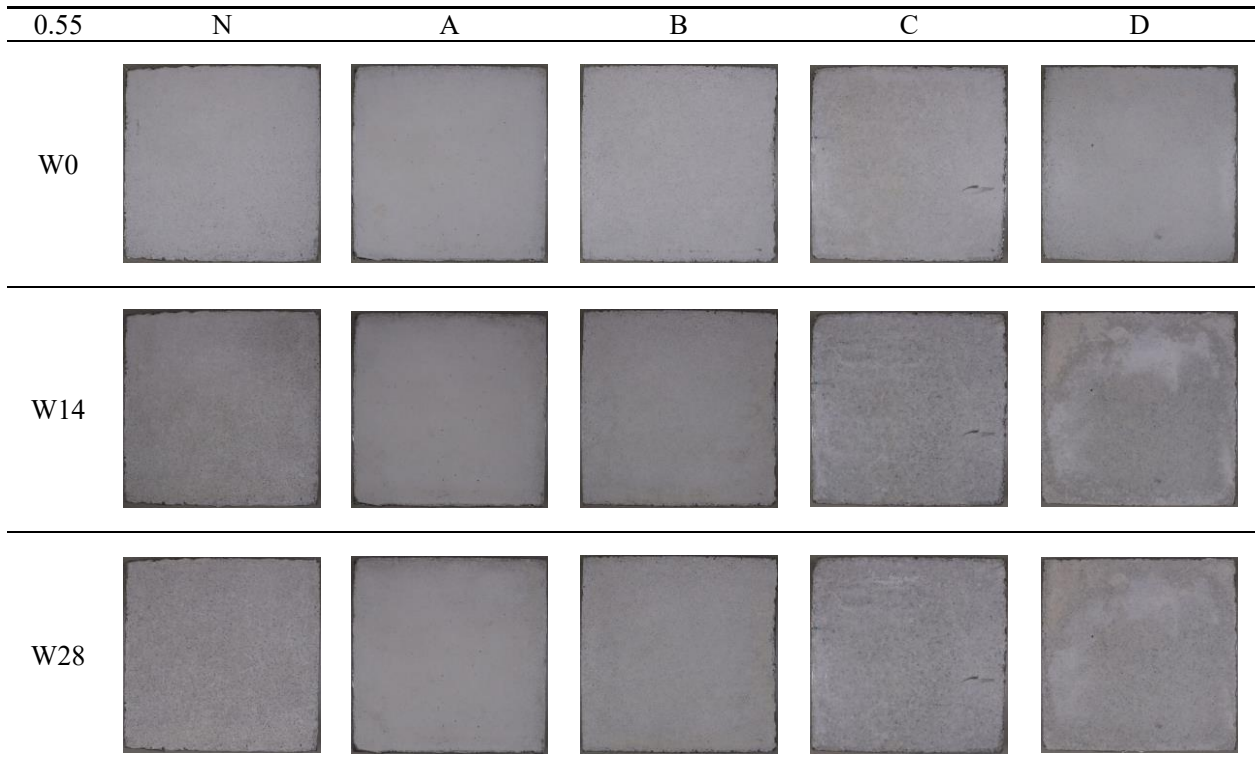
Fig. 4.2 Visual observation for each type of coating before and after immersion in warm water, w/c 0.55

Fig.4.3 shows the results for the brightness of color difference, indicating reduced brightness for all coated specimens after 28 days warm water immersion. The highest decrease in L∗ value was observed for the C coated. This suggests that this is probably because of its immersion of water, a small swelling occurred.
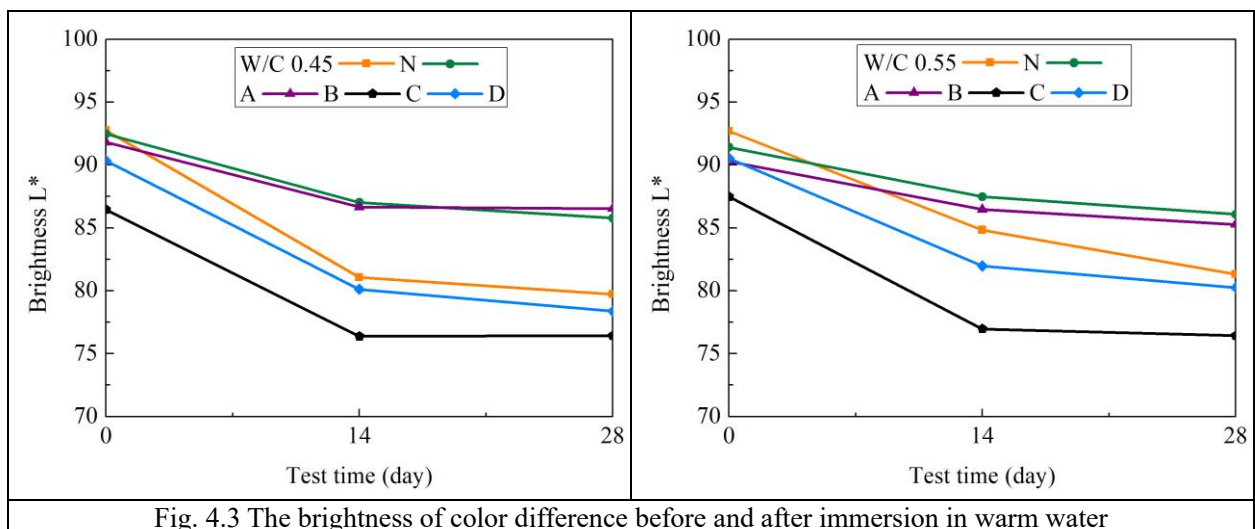
Fig. 4.3 The brightness of color difference before and after immersion in warm water

To further evaluate the morphological characteristics of the surface protective material before and after water immersion, the surface roughness values of each sample were obtained by calculating the arithmetic average of the absolute values of the height difference between the mean plane and each single point in the sample. The roughness values of the B, C and D samples were much higher than those of other samples, as shown in Fig. 4.4. One possible interpretation for this phenomenon is that silane B can form a framework structure inside of the mortar, which restricts the molecular mobility of the silane (Kim et al., 2017). This suggests that this is probably due to the hydrophilic nature. Moreover, the roughness values of C were found to increase after water immersion, which is thought be caused by the generation of bumps on the surface of the fluor-resin. According to previous studies, the hydrophobicity of silane and fluor-resin has a great impact on its moisture susceptibility (Singh et al., 2018).
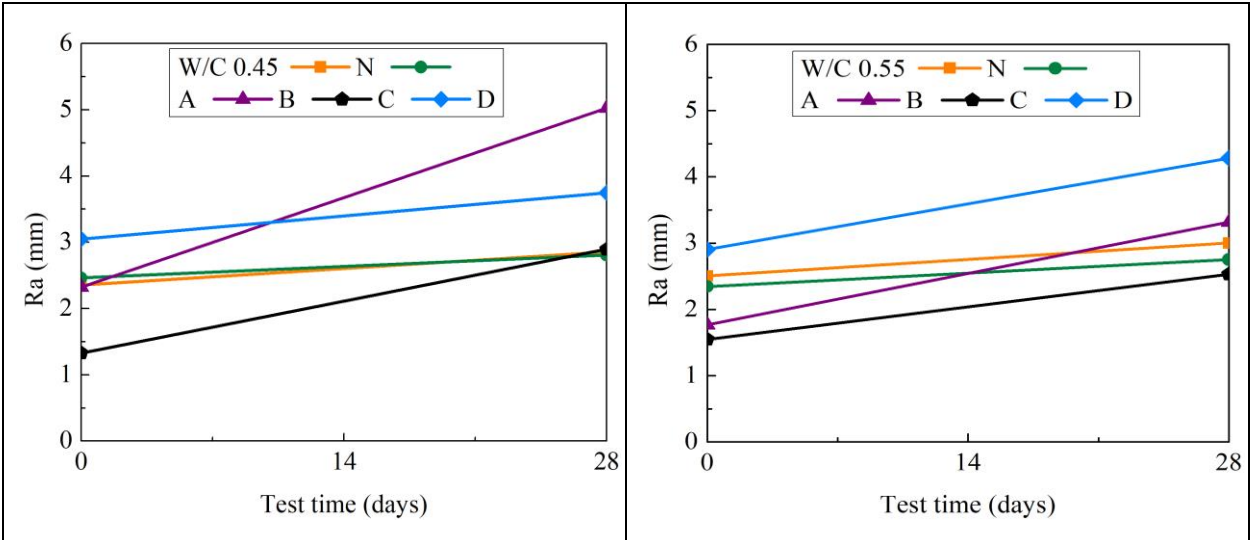
Fig. 4.4 Results for roughness of surface coating before and after immersion in warm water

Therefore, the contact angles were measured in this study, as shown in Fig.4.5. The wetting property of a surface is commonly characterized by measuring the water contact angle. Quantified using the value of contact angle which is greater than 90. The lower contact angle value (<90 °) indicates the hydrophilicity of coating.

These results show that after 28 days water immersion the silane B while the contact angle still remained at about 90 °. Silane B although higher contact angles are more stable in terms, but their roughness were increased when subjected to water immersion. N and D had lower contact angle value (<90 °) indicates that is hydrophilicity of coating.
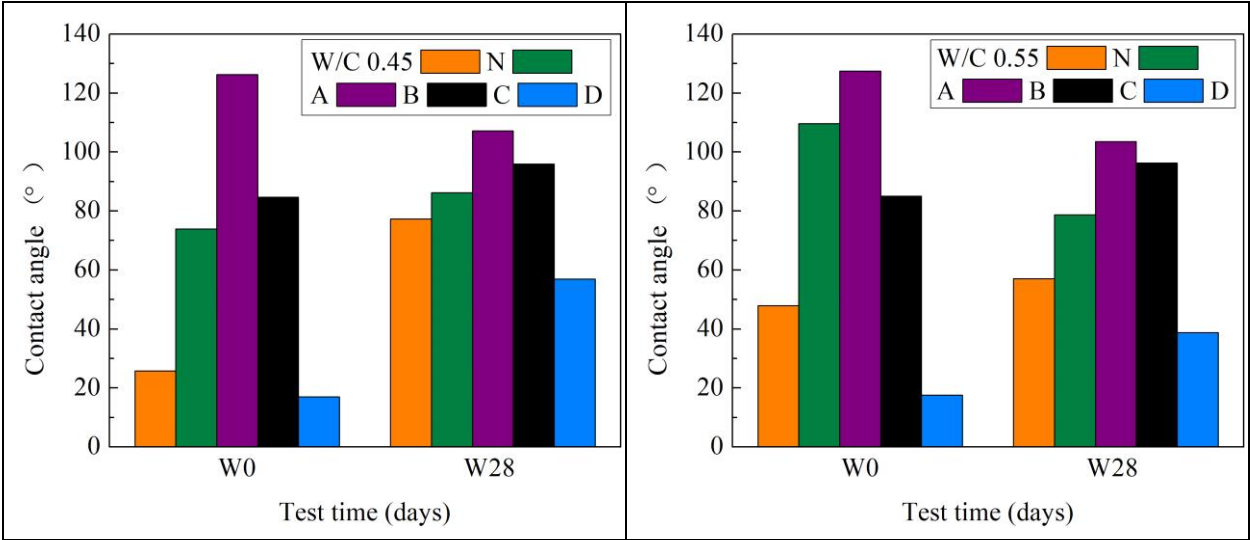
Fig. 4.5 Contact angle test before and after immersion in warm water

4.2.2 Water absorption result

Fig. 4.6 shows the results of the water absorption test for concrete. It can be seen that the uncoated sample (N) quickly absorbs water before water immersion. After about 28 days of water immersion, the water uptake decreased. Samples D coated with silicate pore blockers show a similar tendency. This suggests that this is probably due to the hydrophilic nature of the deposited material (Hager et al., 2010; Ranzoni et al., 2013) as the result of contact angle shown in Fig.4.5.Specimens coated with silane A with high penetration and silane B with high water repellency showed similar water absorption property and hardly any water absorption during the whole water immersion period, together with the contact angle results in Fig. 4.5, suggesting their hydrophobicity was still kept after water immersion because of its deep penetration. Some studies indicate that the residual effect of such coatings still gives better service life for treated concrete (Aguiar, et al., 2008; Christodoulou et al., 2013). Specimens C showed an increased water absorption after 28 days water immersion. In the immersion test of water, a small swelling occurred and there was a slight increased roughness and decreased the brightness (Fig.1, Fig.2).
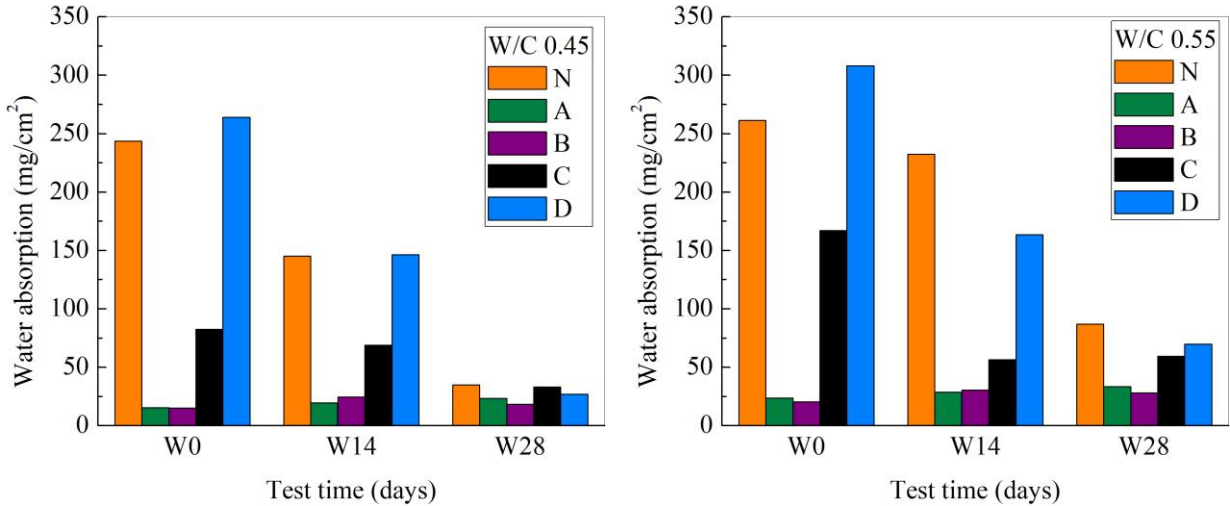
Fig. 4.6 Water absorption results change, before and after immersion in warm water

4.2.3 Moisture permeability result

The moisture barrier properties of the silane, silicate and fluor resin-based coating with mortar were studied using the moisture permeability test. The weight moisture permeability into water immersion time for mortar with and without coatings are shown in Fig.4.7. The mortar specimen with and without coating were fully saturated after immersing water 3 days before the moisture permeability testing in the constant temperature permeability represents the specimen moisture release and humidity room. Therefore, their weight moisture weighted at 7 days.

After 28 days water immersion, it is obvious that the presence of uncoated N and silicate D significantly reduced the moisture permeability of mortar. The penetration depth of silane in the concrete by the coating along with the excellent barrier characteristics of silane were mainly responsible for the reduced moisture permeability.
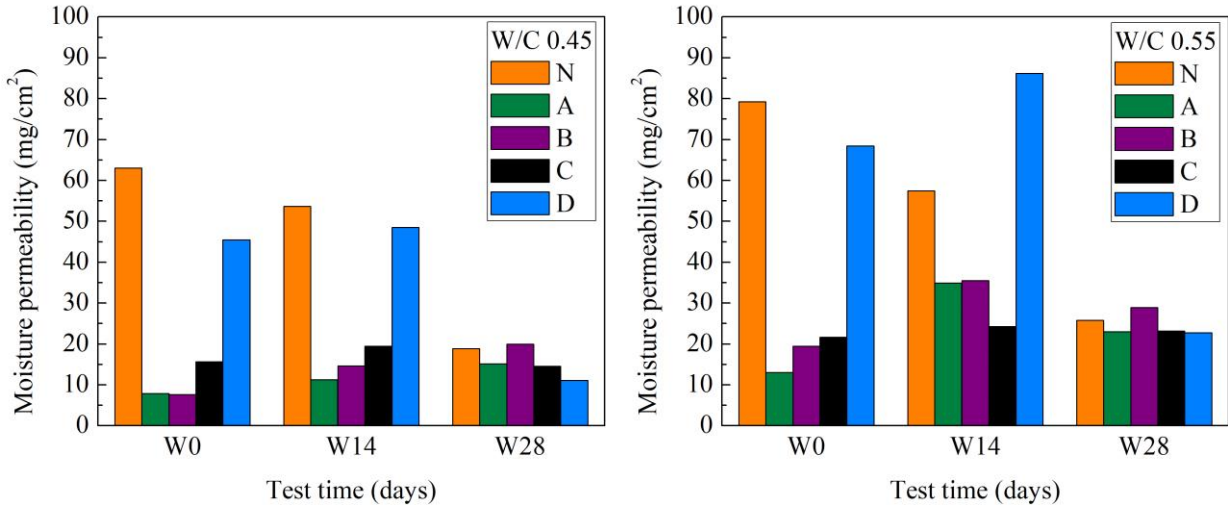
Fig. 4.7 Show the moisture permeability results before and after immersion in warm water

4.2.4 Anti-soiling test

4.2.4.1 Coating method to pollutant

Visual observation

The pollution resistance capability of the four types coating was checked by visual observation. Carbon black were coated on the specimens as shown in Fig. 4.8, Fig. 4.9. Specimen measurements exhibited changes pollution area fraction in initial (not water immersion) with decreased after ultrasonic cleaning, especially B and D. This means that the four types coating material has cleanability. And the silane B due to the water-repellent properties of the treated surface, spreading of carbon black water is inhibited, which results in the occurrence of the carbon black vestiges was less than other specimens. The most hydrophilicity coated specimen D was confirmed to be anti-fouling as the pollution area fraction was bit on its surface. This can be ascribed to the higher hydrophilicity of silicate-based, and to the actual onset of self-cleaning based on superhydrophilicity, which allows a better removal by water of the dirt accumulated onto the surface (Ganesh et al., 2011; Wang et al., 1997; Fujishima et al., 2006). However, surface coatings tend to degrade over time under warm water immersion. After cleaning, all coating specimens the carbon black pollution area fraction became widely the same as uncoated N specimens, except C. After cleaning, pollution area fraction was tested to observe possible cleanability of the four types of surface protective material. In all coating specimens the carbon black pollution area fraction became widely the same as uncoated N specimens, after 28 days warm water immersion, except C. Together with the result of brightness, roughness and the anti-soiling test of visual observation photograph had same tendency.

0.45	N0	N28	A0	A28	B0	B28	C0	C28	D0	D28
Pollution										
Ultrasonic cleaning										
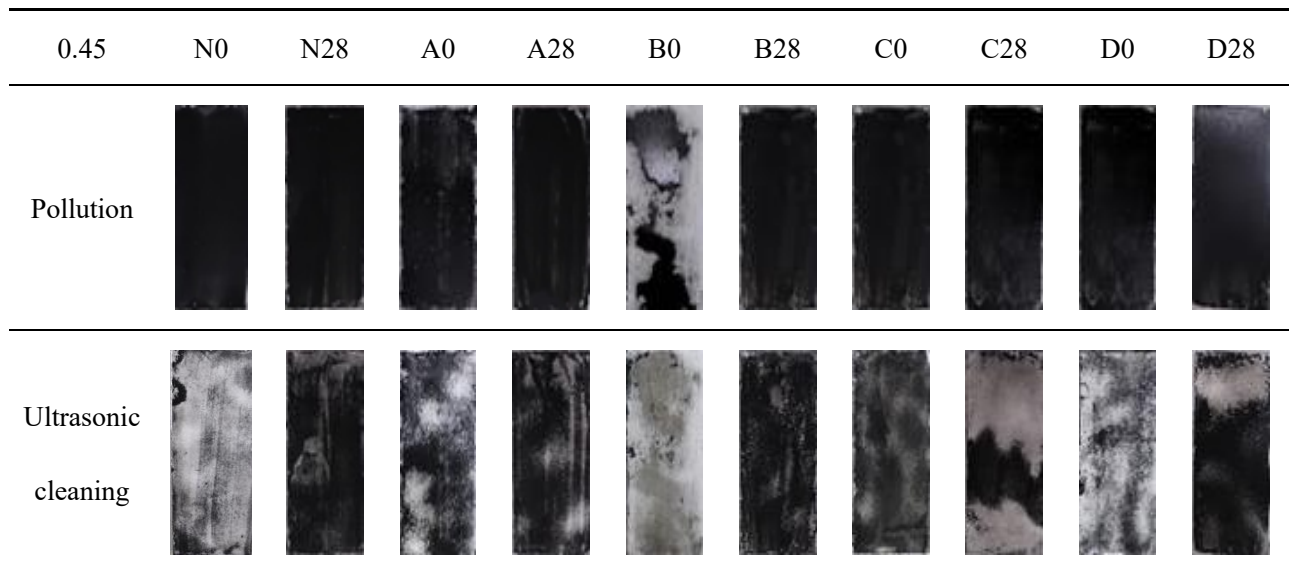
Fig. 4.8 The visual appearance of the uncoated and coated specimens after pollution and ultrasonic cleaning of anti-soiling test. w/c 0.45

0.55	N0	N28	A0	A28	B0	B28	C0	C28	D0	D28
Pollution										
Ultrasonic cleaning										
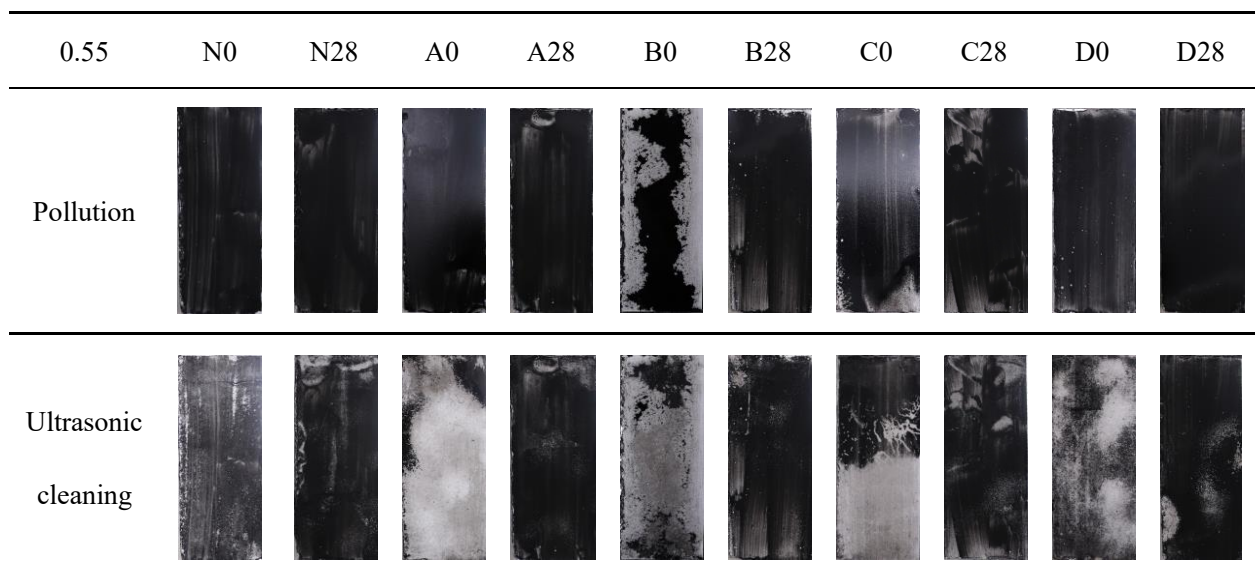
Fig. 4.9 The visual appearance of the uncoated and coated specimens after pollution and ultrasonic cleaning of anti-soiling test. w/c 0.55

Brightness

In Fig. 4.10, after 28 days warm water immersion all of the specimen measurements exhibited large changes brightness after water immersion, with increased ΔL*, except C. Together with the result of pollution area fraction and the anti-soiling test of visual observation photograph had same tendency.
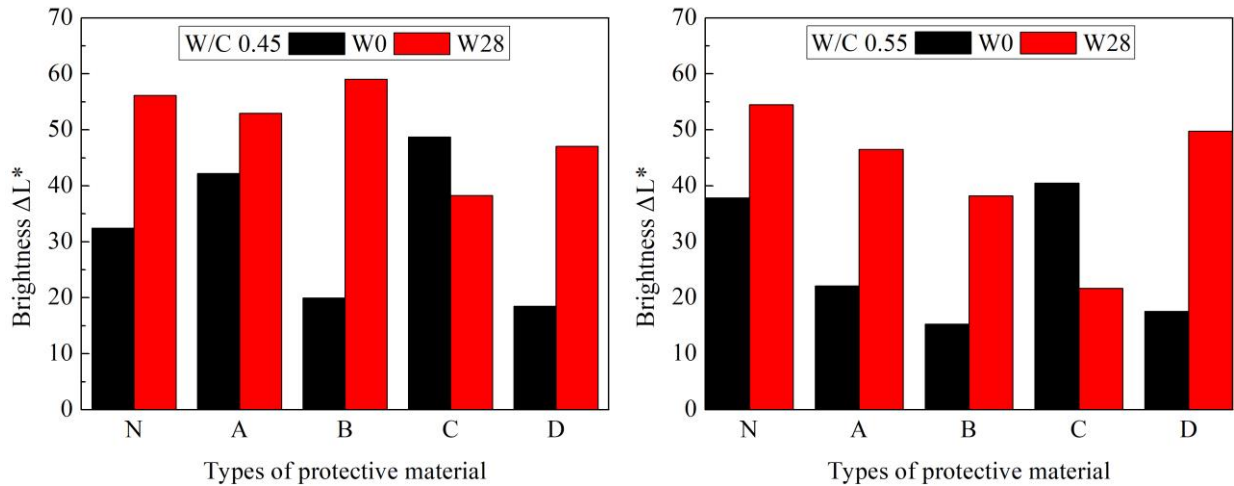
Fig. 4.10 Brightness difference results of anti-soiling test before and after immersion in warm water

Pollution area fraction

Fig. 4.11 shows the pollution area fraction. For W/C=44.9%, the pollution area fraction decreased significantly after ultrasonic cleaning. The appearance observation and brightness difference also changed in the same way. The reason for this is that C has a strong bonding force between atoms in the composition and is less affected by accelerated degradation effects.
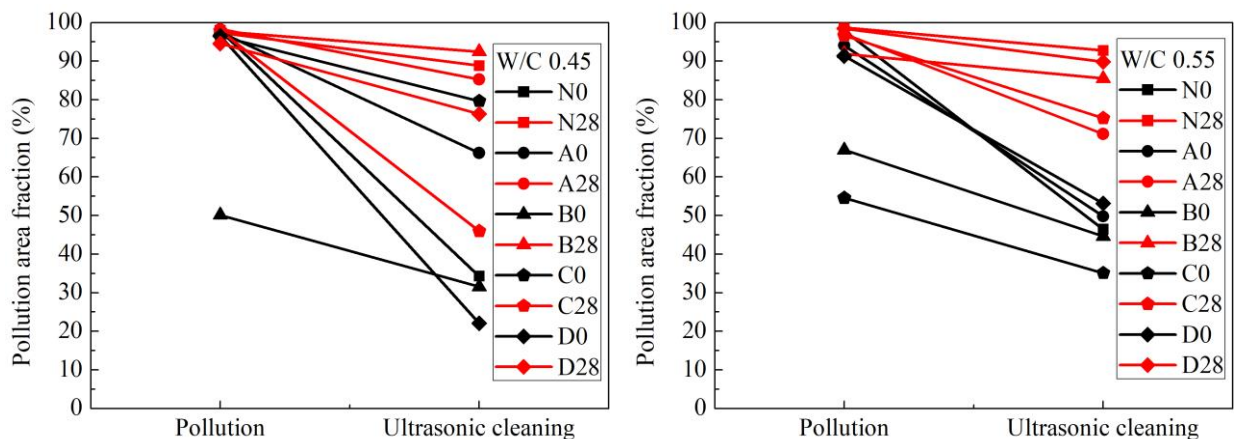
Fig. 4.11 The results of pollution area fraction

4.2.4.2 Simulated raindrops method to pollutant

Fig.4.12, Fig.4.13 shows the results of visual observation. Brightness difference (ΔL*) and pollution average width results was shown Fig.4.14, Fig.4.15, Fig.4.16.

The initial (W0) test, both cement-water ratios 0.45 and 0.55, the flow liquid dropped on surface of silane A and B was fast during pollution, resulting the raindrops was thin and stains. The pollution raindrops line was fat on surface D coating. After cleaning, D coating was removed by ultrasonic cleaning, the brightness difference (ΔL*) (Fig.4.14)and pollution average width (Fig.4.15) of which lowest even after cleaning.

After 28 days ageing, all the specimens became fatter of the pollution raindrops liquid line than W0. B coating was both cement-water ratios 0.45 and 0.55, the pollution raindrops liquid flowed is thinner than others. After clearing, all of the specimens the majority of the contaminants could not remove by spray cleaning and ultrasonic cleaning. Among the four types of surface protective materials, B coating and C coating are soiled lightest, both brightness difference (ΔL*) and pollution average width was the smallest (Fig.4.14, Fig.4.15, Fig.4.16).

0.45	N (uncoated)			A (Silane1)			B (Silane2)			C (Silicate)			D (Fluor-resin)		
	Pl-on	Sp-cl	Ul-cl	Pl-on	Sp-cl	Ul-cl	Pl-on	Sp-cl	Ul-cl	Pl-on	Sp-cl	Ul-cl	Pl-on	Sp-cl	Ul-c
W0															
W28															
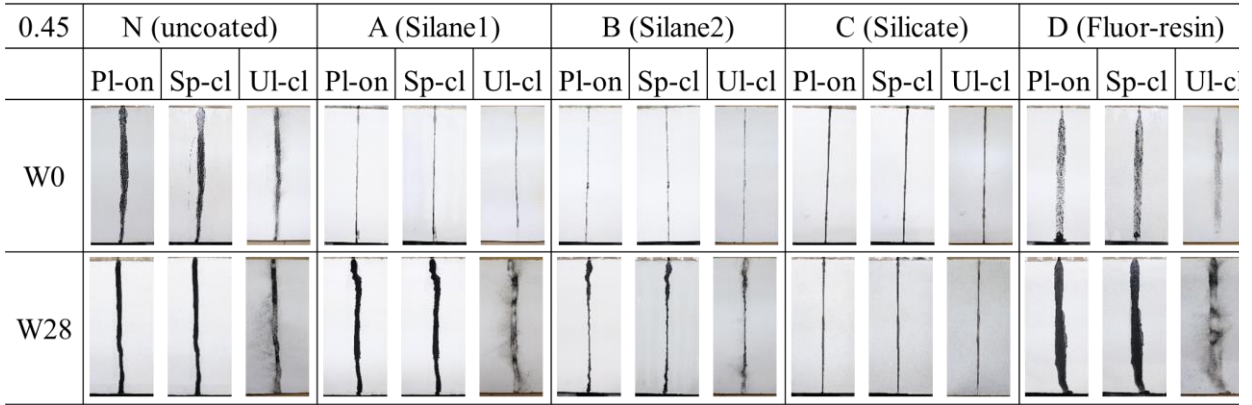
Fig. 4.12 show the results of visual observation. w/c 0.45

*Pl-on: Pollution, Sp-cl: spray cleaning, Ul-cl: ultrasonic cleaning

0.55	N (uncoated)			A (Silane1)			B (Silane2)			C (Silicate)			D (Fluor-resin)		
	Pl-on	Sp-cl	Ul-cl	Pl-on	Sp-cl	Ul-cl	Pl-on	Sp-cl	Ul-cl	Pl-on	Sp-cl	Ul-cl	Pl-on	Sp-cl	Ul-c
W0															
W28															
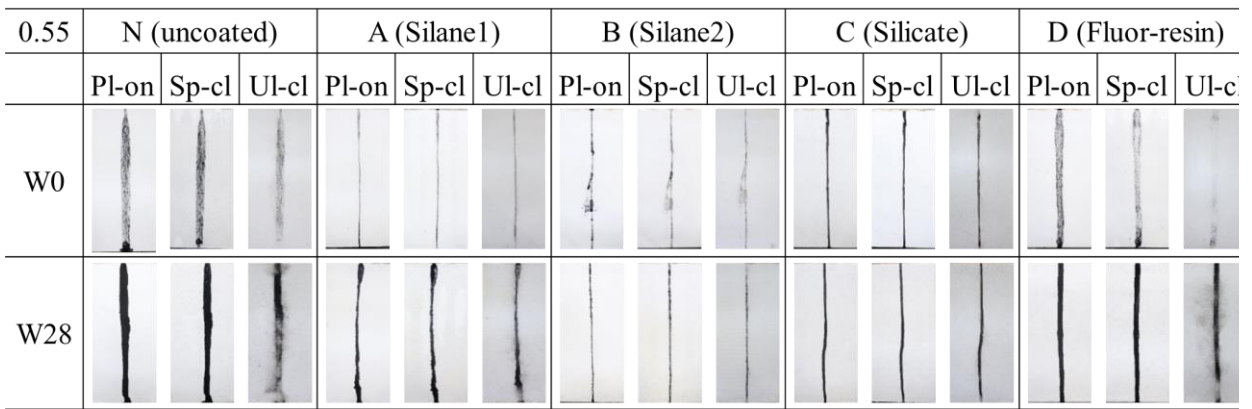
Fig. 4.13 show the results of visual observation. w/c 0.55
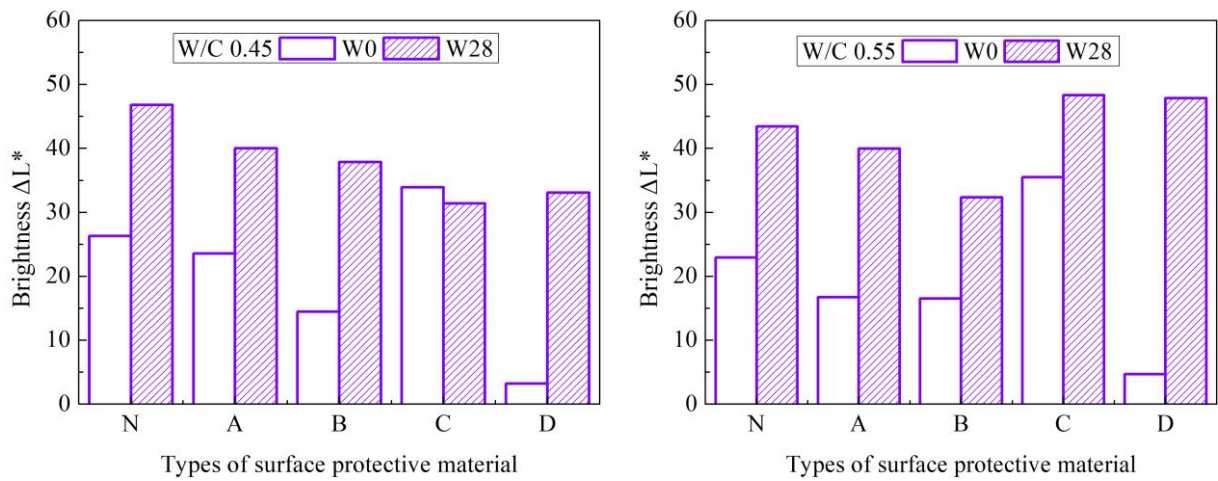
Fig. 4.14. Brightness difference measurement results of anti-soiling test after water immersion 28 days.
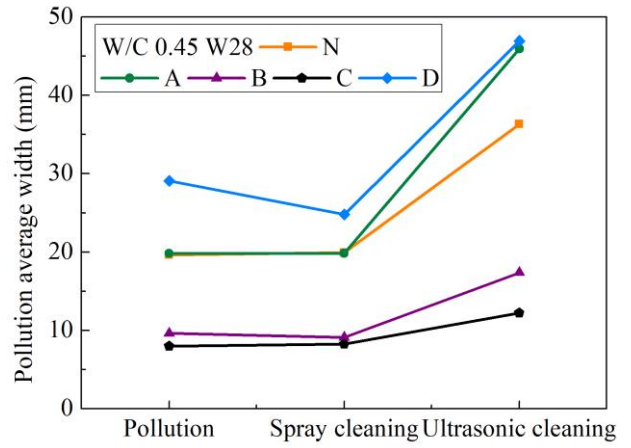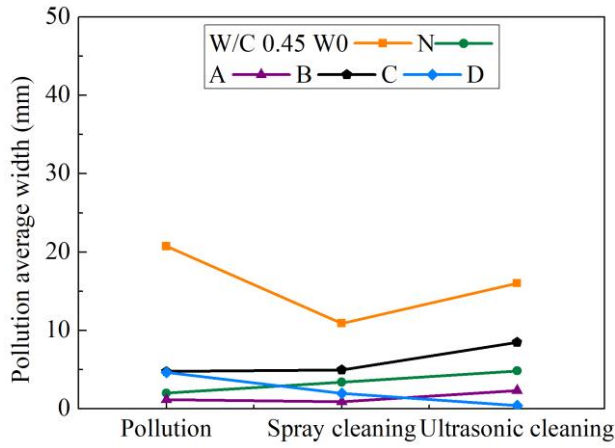
Fig. 4.15 Pollution average width for each type of coating after simulated raindrops method to pollutant, w/c 0.45
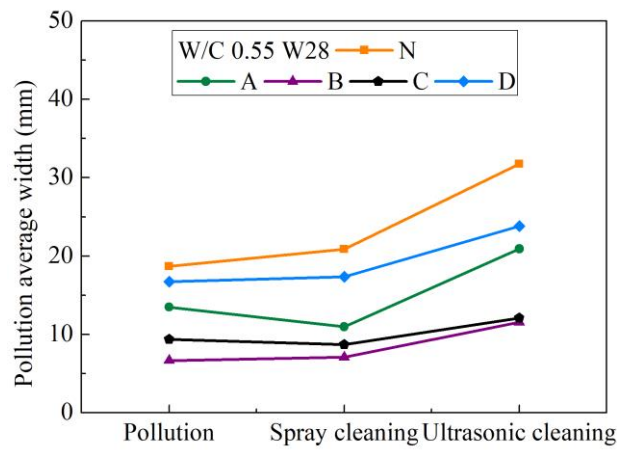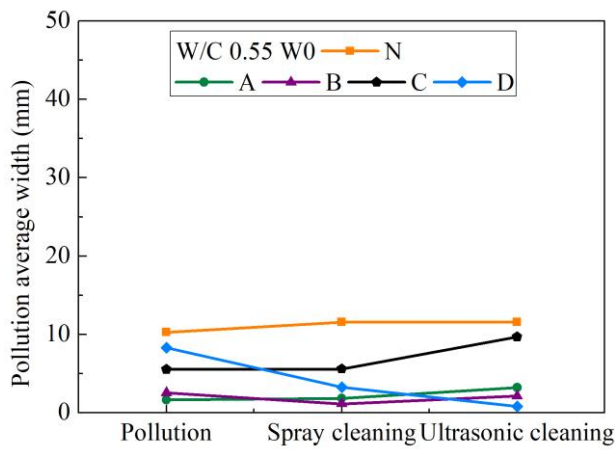
Fig. 4.16 Pollution average width for each type of coating after simulated raindrops method to pollutant, w/c 0.55

4.3 Conclusion

In this study, the impacts of water immersion on the aesthetic and water permeability of surface protective materials were evaluated. Based on the analysis and discussion of the laboratory test results, the following conclusions can be drawn:

The aesthetic properties could be changed by warm water immersion. After 28 days in warm water immersion, the color, gloss and roughness have changed on the surface of coated A, B, C, D. The small swelling occurred on the fluorine resin-based C surface. The least influence on aesthetics is the silane A and B.

The water resistance of the four coats was assessed, it was found that for mortar samples coated silane A and B and fluor resin C coating showed relatively higher effect of restrain water absorption compared to uncoated N and silicate D coating. Moreover, the longer of immersion in warm water, the moisture permeability becomes higher of silane A and B and fluor resin C.

After water immersion, the surface coating material silane B and fluor-resin C has the good stain-resistant.

References:

Berner U.R. Modeling the incongruent disolution of hydrated cement minerals. Radiochim. Acta. 1988; 44 - 45:387–393.

Faucon P., Adnot F., Jacquinot J.F., Petit J.C., Cabrillac R., Jorda M. Long-term behaviour of cement pastes used for nuclear waste disposal: Review of physico-chemical mechanisms of water degradation. Cem. Concr. Res. 1998; 28:847–857.

Maltais Y., Samson E., Marchand J. Predicting the durability of Portland cement systems in aggressive environments—Laboratory validation. Cem. Concr. Res. 2004; 34:1579–1589.

Kamali S., Moranville M., Leclercq S. Material and environmental parameter effects on the leaching of cement pastes: Experiments and modelling. Cem. Concr. Res. 2008; 38:575–585.

Ma H., Li Z. Realistic pore structure of Portland cement paste: Experimental study and numerical simulation. Comput. Concr. 2013; 11:317–336.

Liu J., Xing F., Dong B., Ma H., Pan D. Study on water sorptivity of the surface layer of concrete. Mater. Struct. 2013 in press.

H.H. Kim, M. Mazumder, S.-J. Lee Micromorphology and rheology of warm binders depending on aging J. Mater. Civil Eng., 29 (2017), p. 04017226

D. Singh, A. Habal, P.K. Ashish, A. Kataware, Evaluating suitability of energy efficient and anti-stripping additives for polymer and Polyphosphoric acid modified asphalt binder using surface free energy approach Constr. Build. Mater., 158 (2018), pp. 949-960

Hager PJ, Schlechte JS, Yorkgitis EM, Jing N. Silica coating for enhanced hydrophilicity. US 2010/0092765, 15 April 2010.

Elisa Ranzoni, Barbara Pigino, Carlo, Pistolesi, Ethyl silicate for surface protection of concrete: Performance in comparison with other inorganic surface treatments, Cement and Concrete Composites, Volume 44, November 2013, Pages 69-76

J.L. Aguiar, A. Camões, P. Moreira, Performance of concrete in aggressive environment, Int. J. Concr. Struct. Mater., 2 (1) (2008), pp. 21-25

C. Christodoulou, C. I. Goodier, S. A. Austin, J. Webb, G. K. Glass, Long-term performance of surface impregnation of reinforced concrete structures with silane, Construction and Building Materials, Volume 48, November 2013, Pages 708-716

V.A. Ganesh, H.K. Raut, A.S. Nair, S. Ramakrishna, A review on self-cleaning coatings, J. Mater. Chem., 21 (2011), p. 16304, 10.1039/c1jm12523k

R. Wang, K. Hashimoto, A. Fujishima, M. Chikuni, E. Kojima, A. Kitamura, et al., Light-induced amphiphilic surfaces, Nature, 388 (1997), pp. 431-432

Fujishima, X. Zhang, Titanium dioxide photocatalysis: present situation and future approaches, Comptes Rendus Chim., 9 (2006), pp. 750-760, 10.1016/j.crc

CHAPTER 5

INVESTIGATION ON AESTHETIC AND WATER PERMEABILITY OF SURFACE

PROTECTIVE MATERIAL UNDER ACCELERATED WEATHERING

5.1 Overview

Based on the above discussion in previous chapters of this thesis, reduced the durability and aesthetic of mortar is an unavoidable phenomenon, which could be caused due to the water evaporation.

So far, there has been a lot of research that focuses on the durability of protective coatings. L. Basheer and P.A.M. Basheer et al. (Basheer et al., 2011; Basheer et al., 1997) demonstrated that the reduction in water absorption due to the application of pore-liners was effectively measured using Autoclam. Moradllo et al. (2012) evaluated the time-dependent performance of concrete surface coatings in tidal zone of marine environment. In that study, surface coatings appropriately decrease chloride diffusion coefficient in first stage of exposure (up to9 months), but the decrease rate of diffusion coefficient of sur-face coatings is less than reference specimen in the exposure times more than 9 months. This was specifically because of gradual deterioration of surface coatings. Further, numerous studies have investigated and con-firmed the benefit of silane-based pore liners on the durability of concrete (Dang et al., 2014; Norvaišienė et al., 2010; Hua et al., 2009; Vries et al., 1997). And Sealing concrete with soluble sodium silicate may improve surface properties such as hardness, permeability, chemical durability, and abrasion resistance (Thompson et al., 1997). In relation to the aging conditions which the specimens treated, surface coatings degrade when exposed to fluctuating conditions of temperature, humidity, and ultraviolet (UV) radiation. At elevated temperatures or UV aging, silanes or siloxanes become less effective in reducing water absorption. From an early age up to a year, some of these coatings can be quite effective in preventing degradation, but after that, their effectiveness may gradually decrease. However, according to other studies, the residual effect of such coatings still results in better service life for treating concrete (Aguiar et al., 2008; Christodoulou et al., 2013). Graziani et al. (2014), who assesses the durability of hydrophilic nature and self-cleaning ability of TiO_2nano coatings applied to a fired clay brick substrate using ultraviolet (UV) lamps and simultaneous UV and wetting/drying cycles. The authors concluded that the remaining TiO_2 nanoparticles, although some surface degradation, kept practically the same efficiency as before the tests.

A preliminary study conducted by Grüllet et al. (2014) showed that the opaque coating systems had not reached the limit state after 60 weeks of artificial weathering. The opaque paints can last up to 10 years of

outdoor exposure as described by Williams et al. (2008). According to Marsich et al. (2017), the effect of artificial weathering on PP coextruded tape and laminate Indiana limestone was heated at 100 °C, 200 °C, 300 °C, 400 °C and 500 °C for 1 h, 4 h and 16 h that evaluation the effect of heating as an artificial weathering method for stone. It is found that a decrease in dynamic elastic modulus linearly proportional to the heating temperature was found for the heated samples. Some authors (Franzoni et al., 2017; Sassoni et al., 2011) studied artificial weathering of stone by heating. The results revealed that in spite of the satisfactory artificial damage induced in calcareous lithotypes by heating at 400 °C, the same weathering condition proved to cause no mechanical damaging in the quarzitic sandstone.

Based on the information provided above, the prior research is solely on the durability of the buildings. Still, there are very few studies of estimating the time to reach a certain state of degradation, considering certain conditions of weathering to various environmental factors, as well as surface treatment which play an important role in protecting against stains of dirt on the building. In particular, the long-term durability of surface protective materials in outdoor service progress (under harsh environmental and pollution conditions, etc.), that needs to verify and evaluated further.

The experimental program has been focused on the analysis of the changes in the aesthetic properties of the surfaces and the water permeability of four types of coatings during xenon-arc light aging and further outlines to get more information on the degradation of the protective properties of the exterior wall protective coatings. Speeding up xenon-arc aging test used for weathering to xenon arc is the most damaging weathering factor with the high energy to break chemical bonds and start the degradation process. Observation of the appearance and water contact angle, color differences, gloss, roughness and water absorption, moisture permeability, evaluation of the aesthetics between coatings and concrete examined in order to monitor age-related changes. To assess the protective performance of coating materials, the resistance to soiling determines. Therefore, the aim of this study is to develop relationships between coating deterioration and protection performance and also to show the influence of surface protection material on its physical and optical deterioration.

5.2 Results and discussion

5.2.1 Visual observation

Fig. 5.1 and Fig. 5.2 shows the visual appearance of the uncoated and coated specimens after 0 hours, 2500 hours and 5000 hours weathering of w/c 0.45 and 0.55

Regarding the differences among the surface coating materials, compared to initial test (0 h data), coating surface became rough appeared on the silane1 A, silane2 B and silicate D surface specimens after 2500 hours and 5000 hours of weathering. That indicates the coating surface is deteriorated. The formation of roughing on surface also has been reported in the literature on the surface of aged silicate and silane coatings, which is the effects of xenon-arc light radiation degradation (Tao et al., 2010; Pigino et al., 2012). However, before and after 5000 hours of weathering, the specimens C that was coated with fluor-resin based were intact condition.

0.45	N	A	B	C	D
0h					
2500 h					
5000 h					
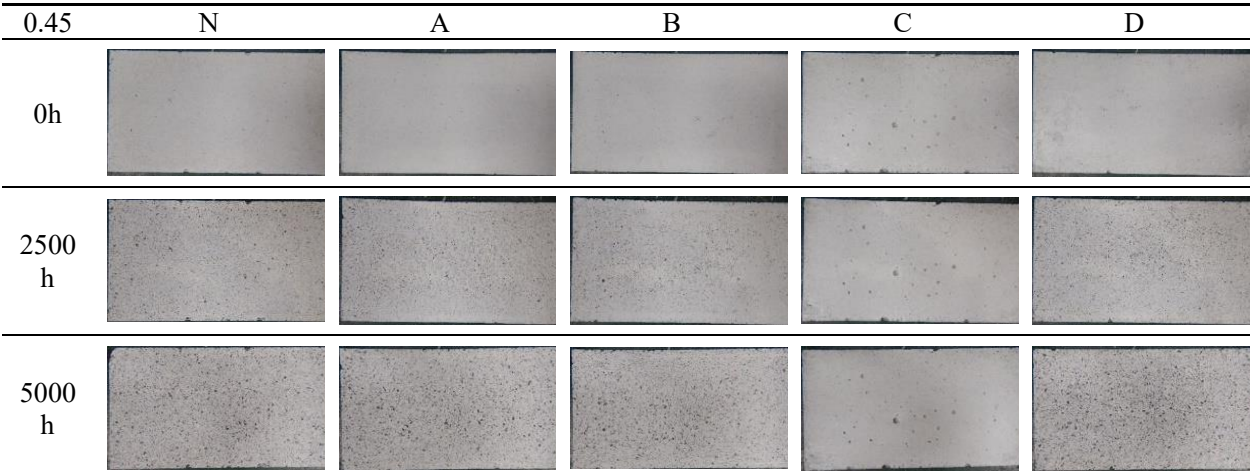
Fig. 5.1 The visual appearance of the uncoated and coated specimens after 0 h, 2500 h and 5000 h weathering of w/c 0.45

0.55	N	A	B	C	D
0h					
2500 h					
5000 h					
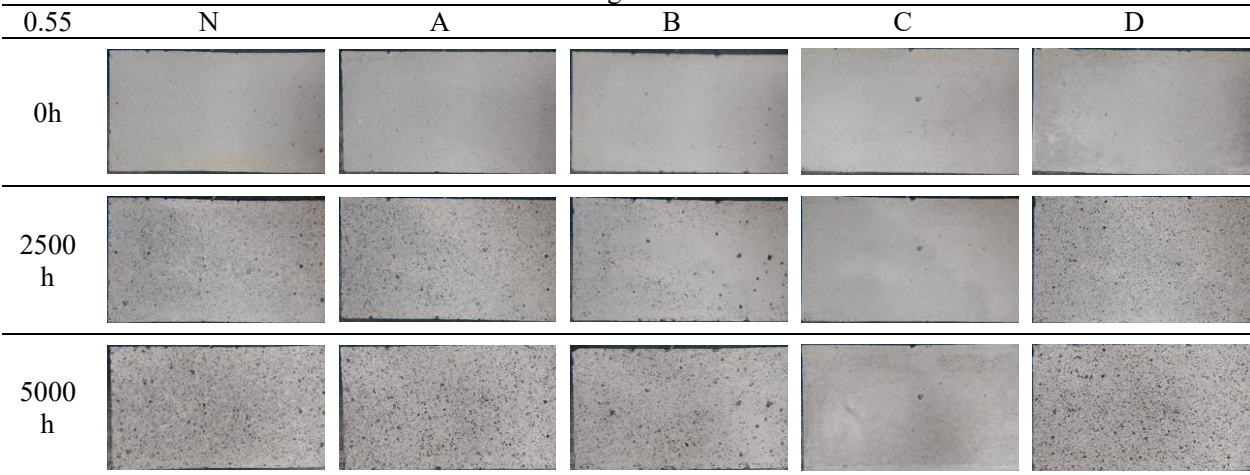
Fig. 5.2 The visual appearance of the uncoated and coated specimens after 0 h, 2500 h and 5000 h weathering of w/c 0.45 and 0.55

5.2.2 Brightness

Additionally, the study of the color differences of the surface coating materials was carried out before and after the xenon-arc light radiation. Fig. 5.3 shows the brightness (L∗).

All surface coating specimens became darkening gradually after 2500 hours and 5000 hours weathering (except C). Regarding the differences among surface coating materials, there are practically no differences among coatings, since L* shows small values. This is agreement with the visual observation result in Fig. 5.2. For both of 0.45 and 0.55 of water cement ratios, the brightness shows identical tendencies but is slightly lower pronounced in case of the w/c 0.55 after 5000 hours weathering.
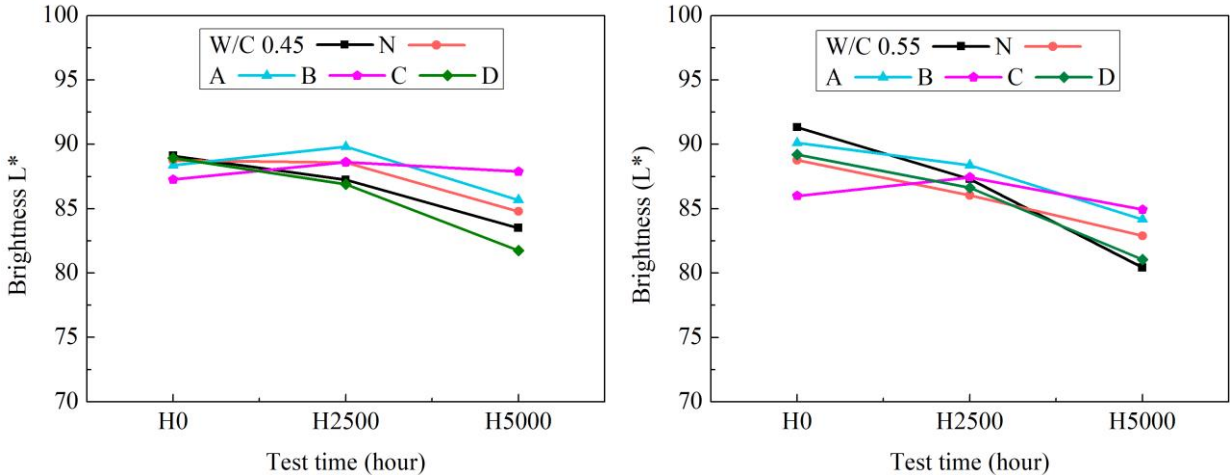
Fig. 5.3 The brightness(L*) of color difference after accelerated aging test after 0 h, 2500 h and 5000 h weathering of w/c ratio 0.45 and 0.55

5.2.3 Gloss

Gloss measurements of uncoated and coated specimens after initial 0 hours, 2500 hours and 5000 hours of accelerated aging test are shown in Fig. 5.4. Regarding sample gloss (measured at 60°), results indicated an increase in gloss loss of all the specimens with increasing periods of xenon-arc light radiation, and after 2500 hours of xenon-arc light radiation, gloss retention remained above 70% (except D). These gloss results are indicative of an increase in surface roughness, later confirmed by Roughness measurements. After 2500 hours of xenon-arc light radiation. Furthermore, over 60% of the initial gloss was lost from the silicate D specimens. The silicate D coating on the surface of the mortar specimens is deteriorated as same as uncoated and un-weathered specimens N. Because D has lower contact angle value (<90°) that indicates that is hydrophilicity of coating. It illustrates that it is not suitable for silicate surface impregnation treatment under high humidity condition. The particular reasons for this question will be explained through the reaction mechanism and morphological of silicate in the future work.
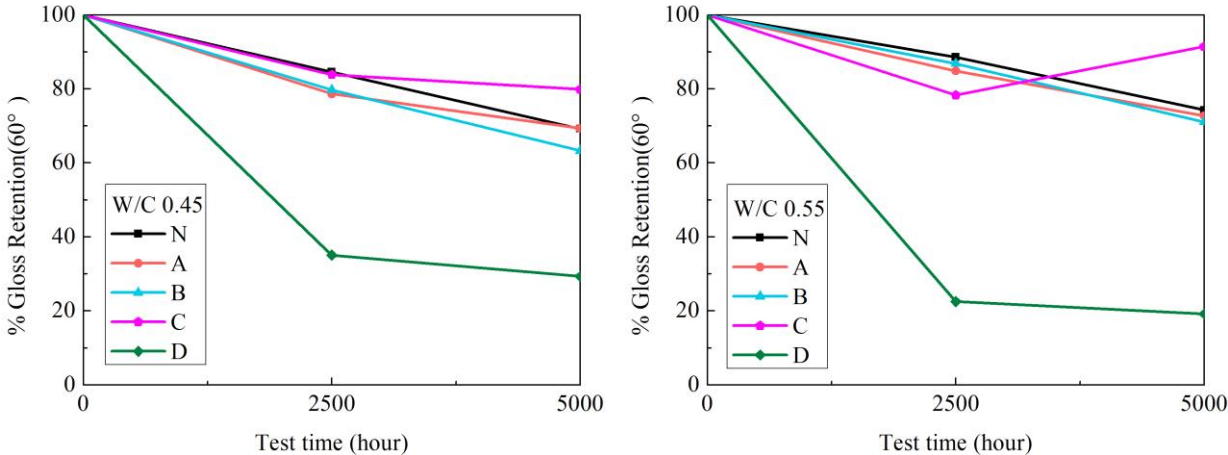
Fig. 5.4 Gloss results of uncoated and coated specimens after 0 h, 2500 h and 5000 h weathering of w/c ratio 0.45 and 0.55

5.2.4 Roughness

Results of roughness is shown in Fig. 5.5. During weathering, the original surface of the mortar samples appeared gradually due to the destruction of the coating. After 2500 hours weathering, the entire original surface of the mortar has appeared clearly (except of C). After weathering 5000 hours (except of C) roughness increased by over a factor of 22 mm ± 2 mm, hence, exposed concrete surface was observed. In case of the C specimen no roughness was observed.
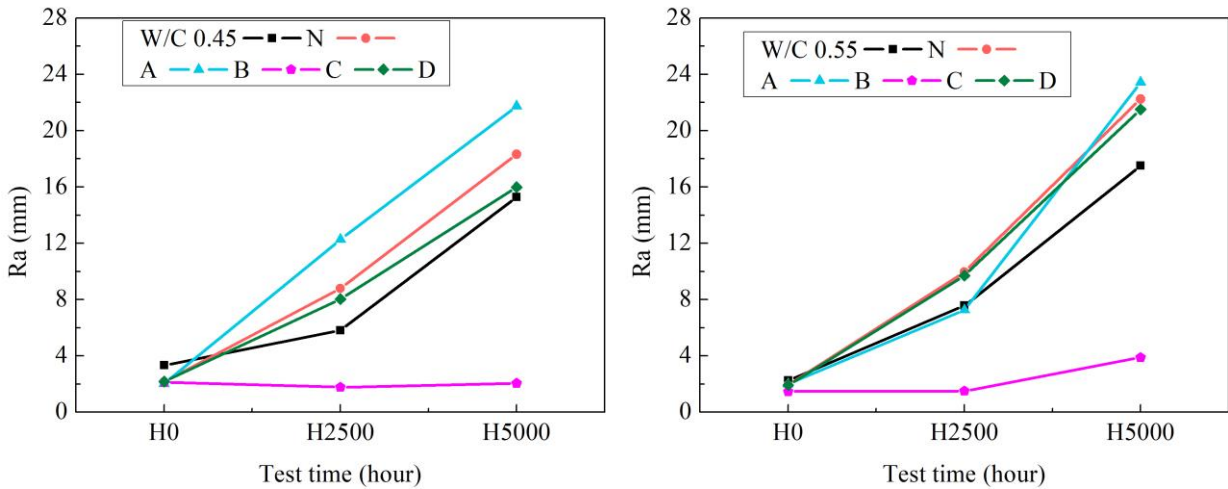
Fig. 5.5 Roughness of surface coating after 0 h, 2500 h and 5000 h weathering of w/c ratio 0.45 and 0.55

5.2.5 Contact angle

The water contact angle is commonly used to characterize a wetting property of surface. The hydrophobic properties of these coatings can be quantified using the value of contact angle which is greater than 90°. The lower contact angle value (<90°) indicates the hydrophilicity of coating. Fig. 6 shows that on average all of the coating specimens different contact angle before xenon-arc light weathering (time zero). It then increased further over time, reaching 42° after 5000 h weathering, the D coating specimen has same tendency with N has lower contact angle value (<90°) indicates the hydrophilicity of coating. The contact angles for A coating and B coating from 78° to 38°, and from 130° to 30°, respectively. After xenon-arc light weathering was able to produce significant contact angle decreased obviously, and approach N the same after 2500 hours. This indicates that the behavior of the coated specimens was decreased the hydrophobic almost the same of the uncoated ones. Regarding the visual inspection angle roughness after 2500 hours and 5000 hours in Fig. 5.3 and Fig. 5.5, coating surface became roughness appeared on all of the specimens because of weathering to xenon-arc light. These surface defects could explain the loss of transmittance and contact angle. The results of contact angle obtained for C coating specimen showed relatively stable behavior. Even though C was some fluctuations during the 5000 hours weathering, the contact angles still remained at around 80°. In conclusion, the most resistant coatings to this accelerated aging test are the coatings C.
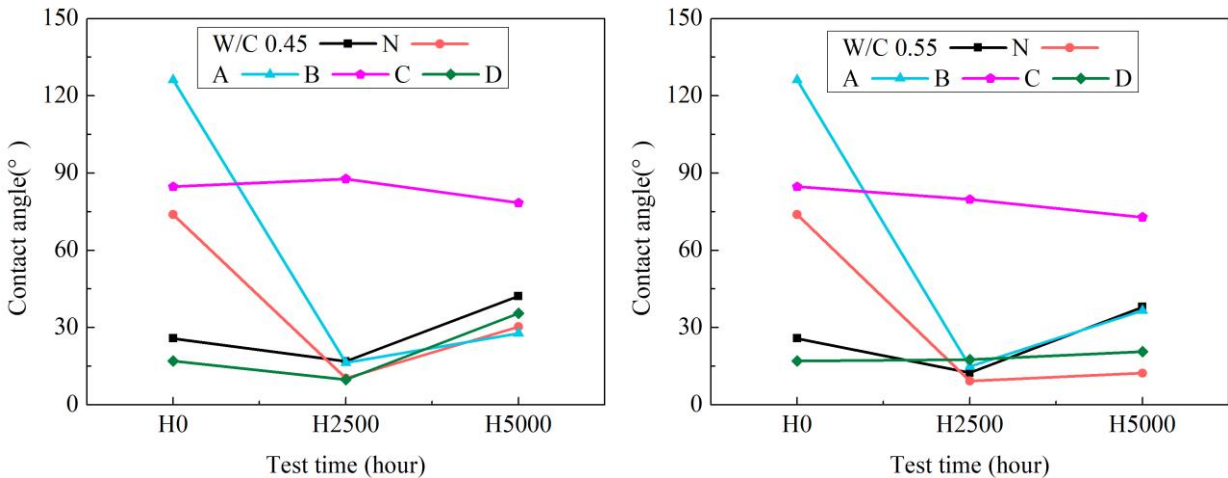
Fig. 5.6 Contact angle test after 0 h, 2500 h and 5000 h weathering of w/c ratio 0.45 and 0.55

5.2.6 Water absorption test

Fig. 5.7 shows the results of the water absorption test for concretes a (left) and b (right). It can be seen that the uncoated sample (N) quickly absorbs water before weathering. After about 2500 hours of weathering, the water uptake decreased; after 5000 hours there is an increased water absorption. Specimens D coated with silicate pore blockers show a similar tendency. This suggests that this is probably due to the hydrophilic nature of the deposited material (Franzoni et al., 2013). Specimens coated with silane A with high penetration and silane B with high water repellency showed exhibited similar water absorption property and hardly any water absorption during the whole weathering period, together with the contact angle results in Fig.5.6, suggesting their hydrophobicity was still kept after aging test because of its deep penetration. Although there was a slight decrease roughness and brightness (L*) after 5000 hours xenon-arc light weathering (Fig.5.2, Fig.5.3 and Fig.5.5). Specimens C even showed a reduced water absorption after 5000 hours weathering. Because the hydrophobic impregnation prevents the penetration of additional external water.
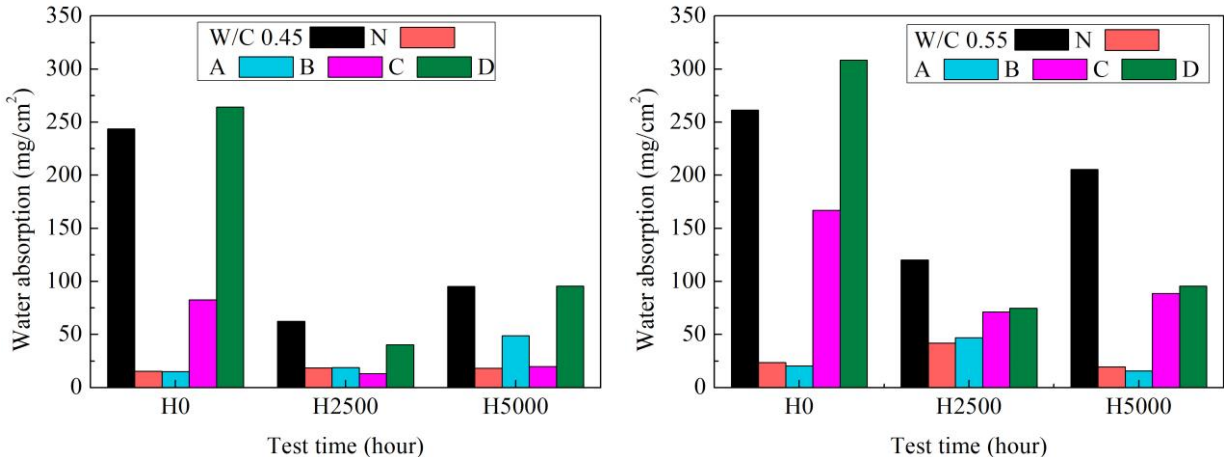
Fig. 5.7 Water absorption test according to Japan standards NSKS-04 on uncoated and coated specimens of concretes for w/c ratio 0.45 and 0.55

5.2.7 Moisture permeability test

The moisture barrier properties of the silane, silicate and fluor resin-based coating with mortar studied using the moisture permeability test. The weight moisture permeability over UV weathering time for mortar with and without coatings are shown in Fig. 5.8.

The mortar specimens with and without coating were fully saturated after immersing water 3 days before the moisture permeability testing in the constant temperature and humidity room. Therefore, their weight moisture permeability represents the specimen moisture release weight at 7 days.

After 2500 hours UV weathering, it is obvious that the presence of silane A and B coatings significantly reduced the moisture permeability of mortar. The penetration depth of silane in the concrete by the coating along with the excellent barrier characteristics of silane were mainly responsible for the reduced moisture permeability. After 5000 hours UV weathering, the amount of moisture released is basically the same. This observation implies that all of the coatings were destroyed.

As expected, a higher penetration was observed at a mortar w/c ratio of 0.55 compared to a mortar w/c ratio of 0.45, which is due to the higher porosity of the former type of mortar.
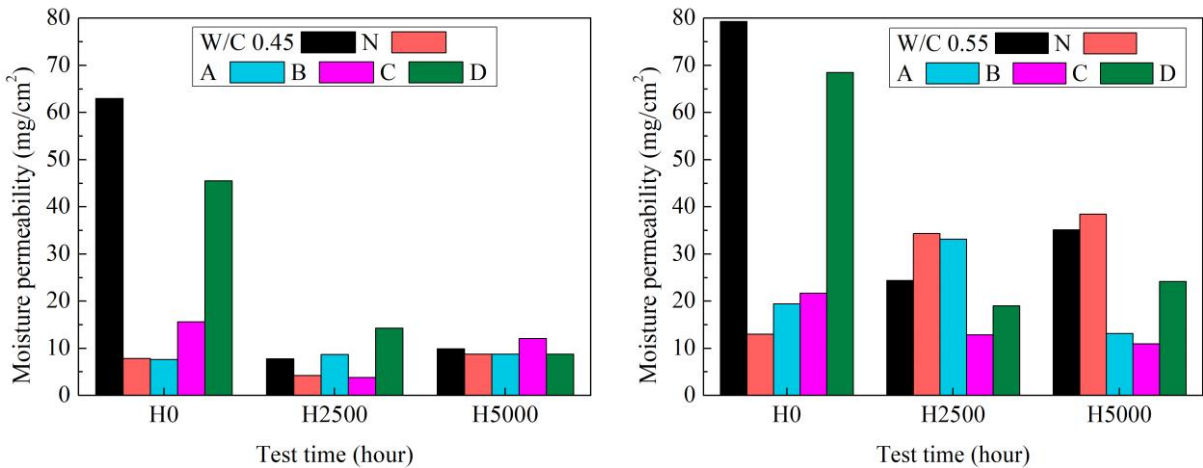
Fig. 5.8 The moisture permeability test after 0 h, 2500 h and 5000 h weathering of w/c ratio 0.45 and 0.55

5.2.8 Anti-soiling test

Anti-fouling is a surface property that prevents dirt from sticking to it. In order to study anti-fouling ability of a coating, antifouling efficiency of aged coatings after 5000 hours accelerated aging test.

5.2.8.1 Visual observation

The pollution resistance capability of the four types coating was checked by visual observation. Carbon black droplets as contaminant were firstly flow-down on the specimens as shown in Fig. 5.9a (1) and Fig. 5.9b (1). Initially, concerning the transmittance results, specimens with the uncoated N and coatings D showed a slight same width of carbon black droplets on surface. The probably due to the hydrophilic nature of the N and D. Specimens with the coatings A, B and C showed the carbon black liquid in a spherical drop ran down the surface along preferential paths and the carbon black vestiges was narrowly than uncoated N on the surface, especially B. Similar observations have been made by Charola et al. (2008), on marble statues. The hydrophobic properties of the treated surface protect rainwater from distributing lead to the formation of spherical drops along the surface.

However, surface coatings tend to degrade over time under weathering to xenon-arc light radiation. In all coating specimens the carbon black droplets became widely the same as uncoated N specimens after 2500 hours and 5000 hours aging, except C. Together with the result of visual observation photograph and roughness, contact angle had same tendency in Fig. 4.1, Fig.4.4 and Fig.4.5 along with the water absorption results in Fig. 4.6, suggesting their hydrophobicity was still kept after aging test because of its deep penetration. Some studies, however, indicate that the residual effect of such coatings still gives better service life for treated concrete (Aguiar et al., 2008; Christodoulou et al., 2013).

Afterwards, to check the cleanability of the surface protection material, spray cleaning and ultrasonic cleaning method two washing methods with different strengths were used on the contaminated surface, respectively (Fig. 5.9 a (2, 3) and Fig. 5.9 b (2, 3). It can be observed that the carbon black vestiges were not easily removed by spray cleaning, as shown in Fig. 5.9 a (2) and Fig. 5.9 b (2). By the away, the carbon black vestiges were easily

removed by ultrasonic cleaning, as shown in Fig. 5.9 a (3) and Fig. 5.9 b (3). It suggests that the four types

coating has self-cleaning ability, but it's need strengths power to washing.

（a）w/c ratio 0.45
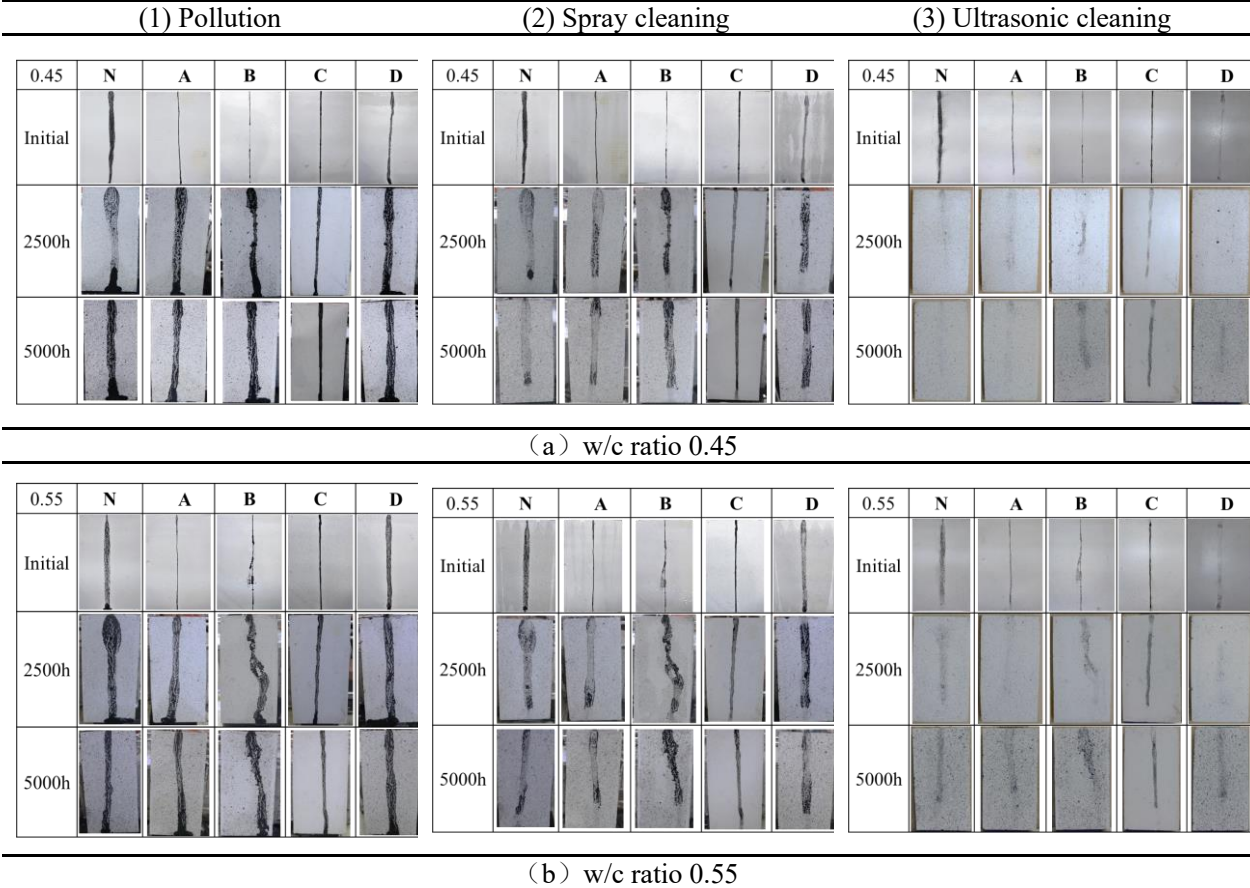
（b）w/c ratio 0.55

Fig. 5.9 The visual appearance of the uncoated and coated specimens after pollution (1), washing (2) and ultrasonic cleaning (3) w/c ratio0.45 (a), 0.55 (b) of accelerated fouling tests

5.2.8.2 Pollution average width

After cleaning, pollution average width was tested to observe possible cleanability of the four types of surface protective material. As can be seen in Fig. 5.10, Fig.5.11, both w/c ratio of 0.45 and 0.55 specimen measurements exhibited changes pollution average width in initial (not weathering) with increased after spray cleaning, and ultrasonic cleaning. Even though the spray cleaning method was lower than ultrasonic cleaning method of all of specimens (except coatings D), a significantly lower value was achieved compared with uncoated specimens N. This means that the four types coating material has cleanability. Meanwhile, the coating specimens A and B exhibited similar anti-fouling features to the C coated specimens, respectively. The most hydrophilicity coated specimen, D was confirmed to be anti-fouling as the pollution average width was bit on its surface. That can be ascribed to the higher hydrophilicity of silicate based, and to the actual onset of self-cleaning based on high hydrophilicity, which allows a better removal by water of the dirt accumulated onto the surface (Ganesh et al., 2011; Wang et al., 1997; Fujishima et al., 2006). However, after washing, it is observed that the pollution average width all of the specimens after weathered at 5000 hours same as nearly, their much smaller than the initial value. These results were consistent with those reported previously (Diamanti et al., 2015). Physical degradation may also induce an apparent self-cleaning behavior when pristine surface is exposed after the detachment of aged portions.

0h   5000h
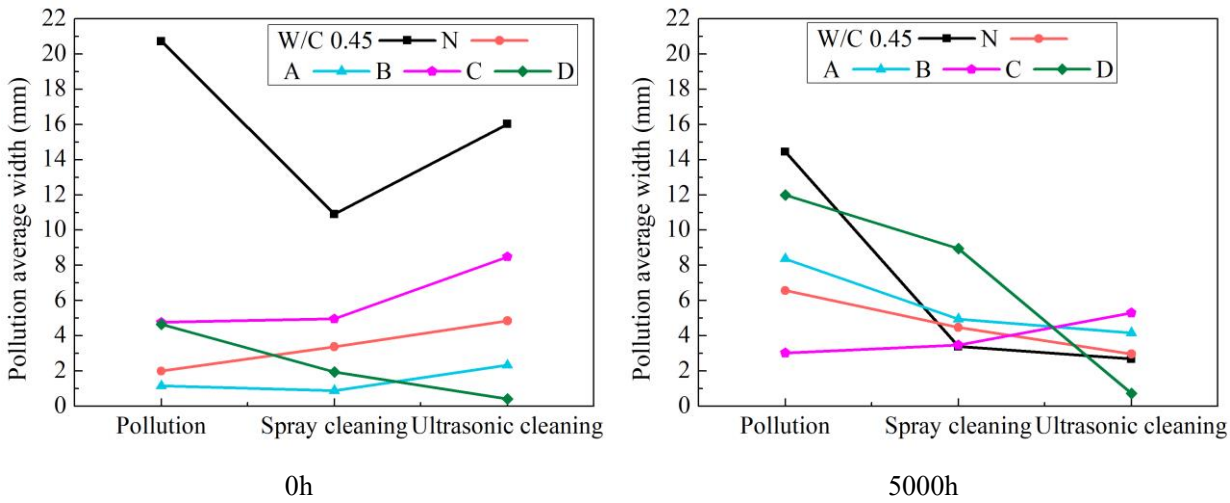
Fig. 5.10 Pollution average width for each type of coating after simulated raindrops method to pollutant, w/c 0.45

| 0h | 5000h |
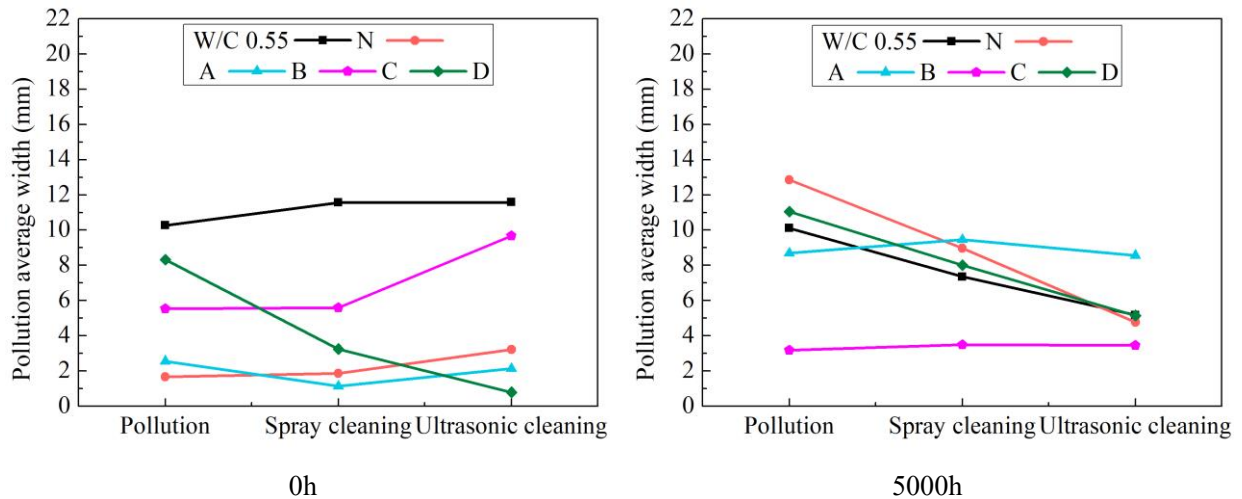
Fig. 5.11 Pollution average width for each type of coating after simulated raindrops method to pollutant, w/c 0.55

5.2.8.3 Brightness difference

As seen in Fig. 5.12, after 5000 hours accelerated aging test all of the specimen measurements exhibited large changes color after weathering, with decreased ΔL*.

Overall, these findings indicated that after 5000 hours of xenon-arc light weathering, accumulated dirt led to the greatest change in color (i.e., appearance) but these effects were easily remedied by sample washing.
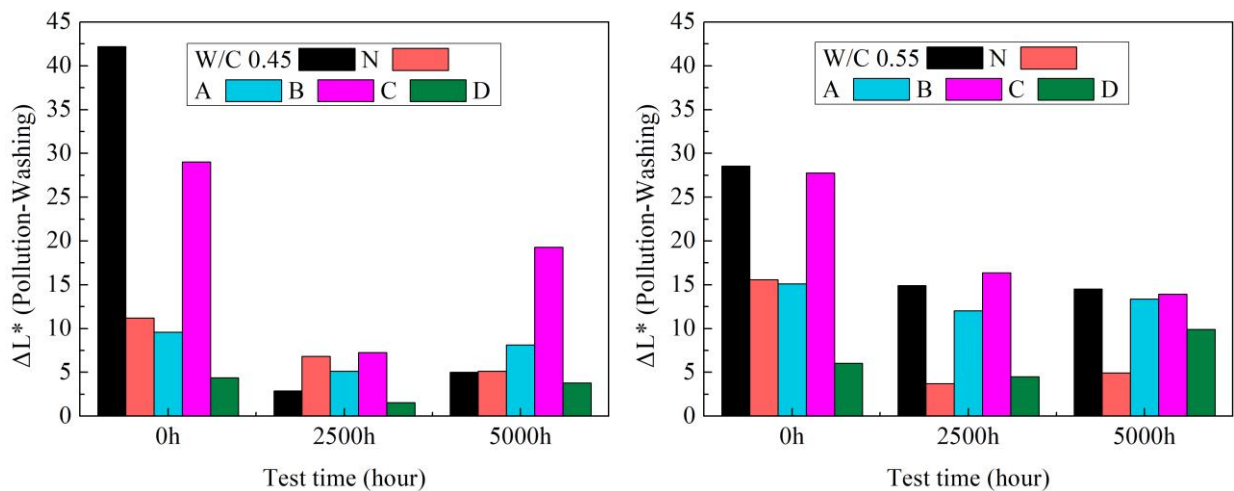
Fig. 5.12 Difference in lightness for each type of coating after simulated raindrops method to pollutant

5. 3 Conclusions

In this chapter, four kinds of external wall protective coatings were used to investigate the effect of artificial accelerating test which was performed to evaluate the aesthetics and material permeability resistance of the surface protective materials of degradation external wall protective coatings to xenon-arc light radiation. Two main conclusions can be drawn.

First, the permeability of the four coats was assessed. Contact angle and surface water absorption analyses were carried out. From the results, a decrease in the contact angle was observed after the aging; in particular, the silicate coating becomes high hydrophilic after 5000 hours of aging. The contact angle of the fluor-resin coating was substantially not influenced after 5000 hours of aging. On the other hand, xenon-arc light irradiation reduces surface water absorption significantly on specimen treated while not affect untreated ones. In this way, silane-based, and the fluor-resin-based coating does not seem to bring greater water absorption, a potential source of damage to concrete surfaces.

Second, the antifouling-cleaning ability of the four coats was then assessed. Specimen measurements exhibited changes in pollution, average width after weathering, increased spray cleaning, and ultrasonic cleaning. However, after washing, it is observed that the pollution, average width of all the specimens after weathered at 5000 hours same as nearly, they are much smaller than the initial value. Initially, the surface could also be observed, for the along paths of carbon black liquid were narrow of the A, B, specimens treated with a water repellent. Initially, the water ran down the surface along preferential paths and spherical drops could be noticed on the surface. For the 2500 hours, however, the surface moistly was increased, with a loss of the water-repellent effects after 2500 hours and 5000 hours tests of silane-based coated with specimens A and B. Specimens C coated with fluor-resin based was kept their water-repellent properties substantially longer.

References:

L. Basheer, D.J. Cleland, Durability and water absorption properties of surface treated concretes. Mater. Struct, 44 (2011), pp. 957-967

P.A.M. Basheer, L. Basheer, D.J. Cleland, A.E. Long, Surface treatments for concrete: assessment methods and reported per-formance. Constr. Build Mater., 11 (7/8) (1997), pp. 413-429

M.K. Moradllo, M. Shekarchi, M. Hoseini, Time-dependent performance of concrete surface coatings in tidal zone of marine environment Constr. Build Mater., 30 (2012), pp. 198-205

Y. Dang, N. Xie, A. Kessel, E. McVey, A. Pace, X. Shi, An accelerated laboratory evaluation of surface treatments for protect-ing concrete bridge decks from salt scaling. Constr. Build. Mater., 55 (2014), pp. 128-135

R. Norvaišienė, A. Burlingis, V. Stankevičius, Durability tests on painted facade rendering by accelerated ageing, Mater. Sci., 16 (2010), pp. 80-85

J.W. Hua, X.G. Li, J. Gao, Q.L. Zhao, UV aging characterization of epoxy varnish coated steel upon weathering to artificial weathering environment, Mater. Des., 30 (2009), pp. 1542-1547

J. de Vries, R.B. Polder, Hydrophobic treatment of concrete. Constr. Build. Mater., 11 (4) (1997), pp. 259-265

J.L. Thompson, M.R. Silsbee, P.M. Gill, B.E. Scheetz, Characterization of silicate sealers on concrete. Cement Concr. Res, 27 (10) (1997), pp. 1561-1567

J.L. Aguiar, A. Camões, P. Moreira, Performance of concrete in aggressive environment, Int. J. Concr. Struct. Mater., 2 (1) (2008), pp. 21-25

C. Christodoulou, C.I. Goodier, S.A. Austin, J. Webb, G.K. Glass, Long-term performance of surface impregnation of rein-forced concrete structures with silane, Constr. Build. Mater., 48 (2013), pp. 708-716

L. Graziani, E. Quagliarini, F. Bondioli, M. D'Orazio, Durability of self-cleaning TiO2 coatings on fired clay brick façades: Effects of UV weathering and wet & dry cycles, Build. Environ., 71 (2014), pp. 193-203

Gerhard Grüll, Florian Tscherne, Irene Spitaler, Boris Forsthuber, Comparison of wood coating durability in natural weathering and artificial weathering using fluorescent UV-lamps and water, European Journal of Wood and Wood Prod-ucts volume 72, pages367–376, 02 April (2014)

Williams RS, Knaebe M, Sotos P (2008), Effect of surface preparation on service life of top coats applied to weathered primer paint. In: Proceedings 6th Woodcoatings Congress, PRA, Hampton

Lucia Marsich, Alessio Ferluga, Luca Cozzarini, Marco Caniato, Orfeo Sbaizero, Chiara Schmid, The effect of artificial weathering on PP coextruded tape and laminate, Composites Part A: Applied Science and Manufacturing, Volume 95, April 2017, Pages 370-376

Elisa Franzoni, Enrico Sassoni, George W. Scherer, Sonia Naidu, Artificial weathering of stone by heating, Journal of Cul-tural Heritage 14S (2013) e85–e93

Sassoni, S. Naidu, G.W. Scherer, The use of hydroxyapatite as a new inorganic consolidant for damaged carbonate stones, Journal of Cultural Heritage 12 (2011) 346–355

H. Tao, Y. Tang, The research progress of silicone compounds in protection of stony historic relics Paint. Coat. Ind., 40 (2010), pp. 74-79

B. Pigino, A. Leeman, E. Franzoni, P. Lura, Ethyl silicate for surface treatment of concrete – Part II: characteristics and per-formance, Cement Concr Compos, 34 (2012), pp. 313-321

E. Franzoni, B. Pigino, C. Pistolesi, Ethyl silicate for surface protection of concrete: Performance in comparison with other inorganic surface treatments, Cement and Concrete Composites, Volume 44, November 2013, Pages 69-76

A.E. Charola, J. Delgado Rodrigues, M. Vale Anjos, An unsatisfactory case of water repellents applied to control biominer-alization, Hydrophobe V: Water Repellent Treatment of Building Materials, Aedificatio, Germany (2008), pp. 117-128

J.L. Aguiar, A. Camões, P. Moreira, Performance of concrete in aggressive environment, Int. J. Concr. Struct. Mater., 2 (1) (2008), pp. 21-25

C. Christodoulou, C.I. Goodier, S.A. Austin, J. Webb, G.K. Glass, Long-term performance of surface impregnation of rein-forced concrete structures with silane, Constr. Build. Mater., 48 (2013), pp. 708-716

V.A. Ganesh, H.K. Raut, A.S. Nair, S. Ramakrishna, A review on self-cleaning coatings, J. Mater. Chem., 21 (2011), p. 16304, 10.1039/c1jm12523k

R. Wang, K. Hashimoto, A. Fujishima, M. Chikuni, E. Kojima, A. Kitamura, et al., Light-induced amphiphilic surfaces, Na-ture, 388 (1997), pp. 431-432

A. Fujishima, X. Zhang, Titanium dioxide photocatalysis: present situation and future approaches, Comptes Rendus Chim., 9 (2006), pp. 750-760, 10.1016/j.crci.2005.02.055

M.V. Diamanti, R. Paolini, M. Rossini, A.B. Aslan, M. Zinzi, T. Poli, M.P. Pedeferri, Long term self-cleaning and photocata-lytic performance of anatase added mortars exposed to the urban environment, Constr. Build. Mater., 96 (2015), pp. 270-278, 10.1016/j.conbuildmat.2015.08.28

CHAPTER 6

EFFECTS OF DIFFERENT ACCELERATED AGING AND SURFACE TREATMENTS ON AESTHETICS AND DURABILITY

6.1 Overview

In Chapter 3, the effects of freeze-thaw cycles on the appearance and water absorption properties of modified materials and anti-soling properties are determined. As a whole, the appearance and water absorption characteristics have almost no effect, and all the surface protective materials after pollution and washing show a cleaner surface with anti-soling ability. However, in Chapter 4, bubbles appear in the appearance of the fluoro-resin-based coating materials, and together with other surface coatings, the surface color becomes darker. The overall pollution resistance is reduced. In Chapter 5, in addition to the fluor-resin surface that remains intact, the surface of other coated materials is significantly roughened, the water absorption is increased, and it has a certain degree of dirt resistance. The previous research has investigated that the effect of concrete coatings to preserve concrete durability and concluded that the application of an impervious surface coating to concrete is a very attractive solution to protect new and existing concrete structures was evaluated (Swamy and Tanikawa, 1990). However, with such a large variety of coatings on the market, selecting the proper type of coating can be tricky, as comparable generic types are known to have significantly distinct qualities. It is necessary to investigate the performance of the available generic types under various service conditions. There is also needed to define the performance criteria for evaluating concrete coatings as well as suggestions for selecting acceptable coatings for different exposure circumstances (Almusallam et al. 2002).

In this thesis, we have discussed the various conditions of concrete wall buildings, the surface coating durability and appearance change and anti-soling test of concrete wall buildings was studied using multi-factor accelerated aging tests composed of warm water immersion, humidity and cool-heat cycling, xenon-arc light radiation, which comparative analysis about the long-term durability of different types of treatments and guidelines for the selection of coatings appropriate for various exposure conditions to facilitates the successful application of the surface treatment method.

Therefore, in this chapter, in order to obtain the applicable environment for surface protective materials were involved in the warm water immersion, humidity and cool-heat cycling and xenon-arc light radiation as environmental factors to conduct a comparative study on the water resistance and aesthetics characterizations of mortar reinforced with four kinds of surface protective materials.

6.2 Comparison of water absorption after three aging environments

Fig. 6.1 show the water absorption of surface coating mortars under different aging environments. It could be seen that the exposure environment has a significant effect on water content for all the specimens while the effect of water-to-cement ratio is not obvious. Compared with the uncoated and non-weathered N specimens of initial, the water absorptions of W28, C20, and H5000 three environments decreased by 80%, 40%, 60% respectively. It can be observed that the water absorption decreased was related to high humidity condition. The water absorption decreased with sample age, because of the continuous hydration of cement and generation of C–S–H gel which could fill the pore space (Taylor, 1997; Ma et al 2013). This is also evidenced by the result of the increased contact angle. Thus, it is obviously observed that the water content of specimens exposed to warm water immersion 28 days (W28) is dramatically lower than the other environments, no matter what the water-to-cement ratio is. For the specimens exposed to the humidity and cool-heat cycling (C20) and xenon-arc light radiation environment (H5000), there is increased water absorption in comparison with the warm water immersion environment (W28).

The water absorption of mortar coated with high penetration (A) and with high water repellency (B) under different environments is shown in Fig. 6.1 (b). It could be seen that the water absorption of the W28, C20, H5000 three environments were little higher than initial. Especially at the water-to-cement ratio of 0.45 specimens B H5000. but the overall water absorption property is similar and hardly any water absorption, it is also concluded that high penetration (A) and with high water repellency (B) have best performance in all three aging environments. It illustrates that the hydrophobic alkyl is driven by the reaction between silane emulsion and cement-based materials to form a protective layer on the coupon surface. The existence of protective layer can not only effectively cover the micro-voids on the concrete surface, but also lower the surface roughness of the concrete, thus reducing the ingress of water because of the decrease in surface area to be exposed to the environment for absorption (Woo et al., 2008). On the other hand, some relevant studies also have reported that the contact angle of water to concrete surface after silane treatment is within the range of 108.3° and 165.5°, which is nearly super-hydrophobicity (contact angle>150°)(Zhang et al.,2019; Geng et al., 2020) together with

the contact angle results in Fig. 7, Most surface coating and hydrophobic impregnation are organic polymers. It was reported that these organic surface treatment agents were very helpful in extending service life of concrete (Tittarelli et al., 2008).

In addition, all the organic surface treatment agents may lose their protective effect under high temperature and weathering. The result was not consistent with previous research (Levi et al., 2002).

The water absorption of mortar coated with fluor-resin (C) under different aging environments is shown in Fig. 6.1 (c). Specimens C showed a reduced water absorption after three aging environments. It is obviously observed that the water absorption of specimens exposed to humidity and cool-heat cycling (C20) dramatically higher than the other environments. The minimum water absorption under xenon-arc light radiation condition (H5000) is found. It illustrates that the fluor-resin coating showed little or no surface degradation. The reason why the fluor-resin coating did not show degradation was thought to be because fluor-resin atoms develop a structure with strong chemical bonding which makes it difficult to produce the free radicals which cause coating decomposition. The presence of fluorine atoms in the commercial products giving their characteristic low surface free energy that makes them water- and oil-repellent could be an explanation. In addition, the C-F bond is very stable towards visible and UV-light that make fluorinated materials more resistant to degradation (Scheerder et al., 2005). The water absorption of silicate (D) under different environments is shown in Fig. 6.1 (e). The result of specimens D show a similar tendency with N. Comparison to initial, the water absorptions of W28, C20, H5000 three environments decreased by 90%, 40%, 60%, respectively. The reason is the later decrease to the refinement of pore structure due to hydration (Liu et al., 2014).
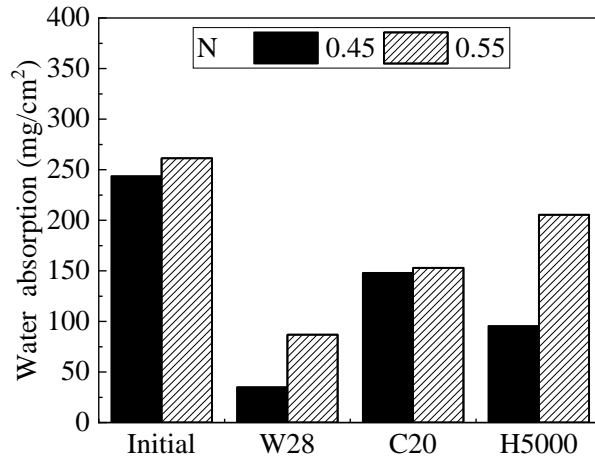
(a) Uncoated
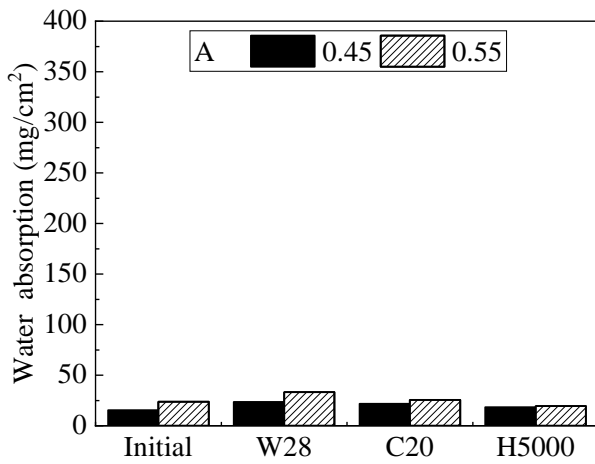
(b) Silane1
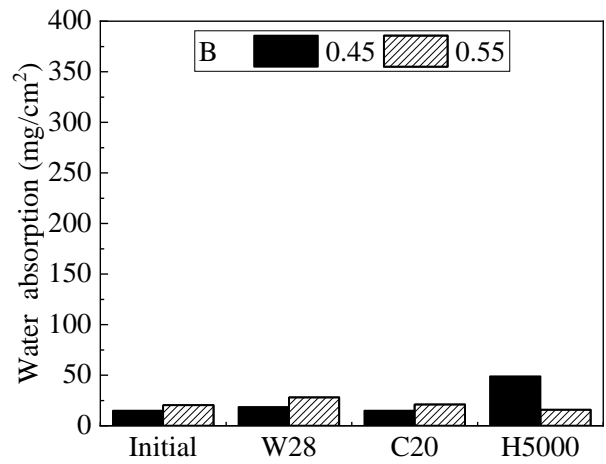
(c) Silane2
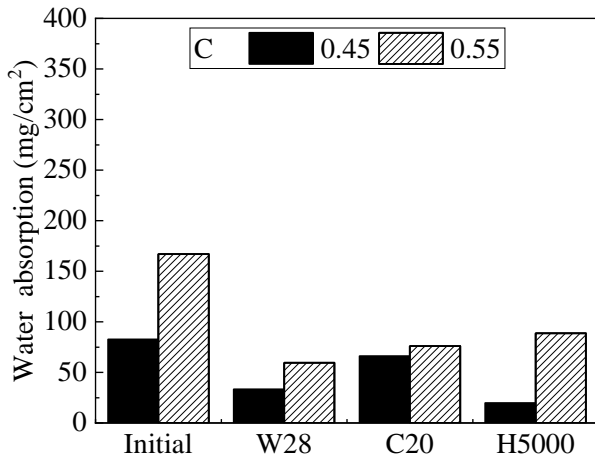
(d) Fluor-resin
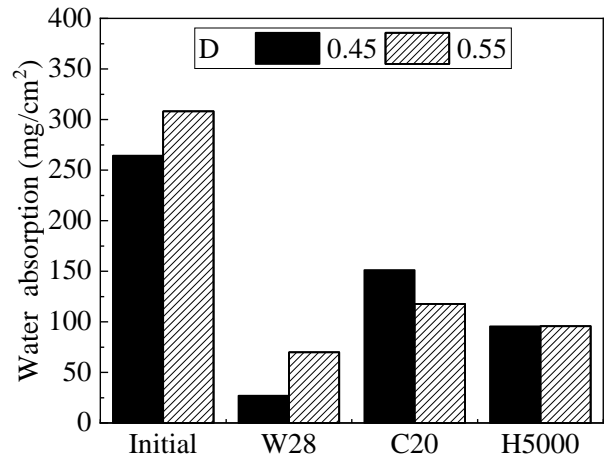
(e) Silicate

Fig. 6.1 Comparison of water absorption under three aging environments

6.3 Comparison of moisture permeability after three aging environments

Fig. 6.2 show the moisture permeability of surface coating mortars under different aging environments. The moisture permeability of uncoated and unweather N specimens, after three different aging environments weathering, it was decreased, respectively.

It is obvious that the presence of silane1 A and silane2 B coatings significantly increased the moisture permeability of mortar after aging the W28, C20 and H5000. The w/c ratio of 0.55 was higher than w/c ratio of 0.45, which is due to the higher porosity of the former type of mortar.

Specimens C obviously observed that the moisture permeability of specimens exposed to humidity and cool-heat cycling (C20) higher than the other environments. The minimum moisture permeability under Xenon-arc light radiation condition (H5000) is found. There was no change after warm water immersion.

Specimens D obviously observed that the moisture permeability of specimens exposed to humidity and cool-heat cycling (C20) higher than the other environments. The lowest moisture permeability under xenon-arc light radiation condition (H5000) and warm water immersion (W28) is found.

(a) Uncoated

(b) Silane1

(c) Silane2

(d) Fluor-resin

(e) Silicate
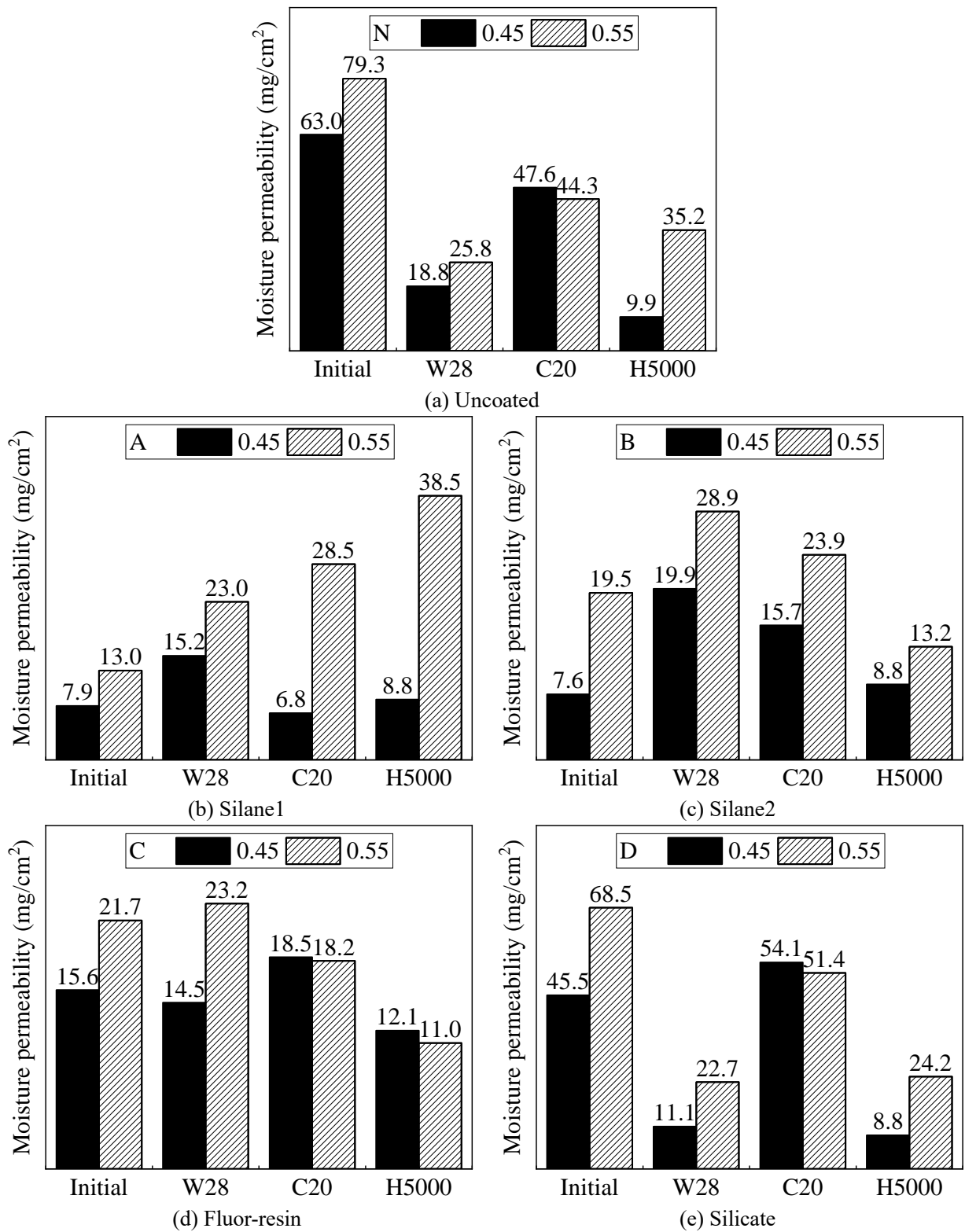
Fig. 6.2 show the moisture permeability in different aging environment of surface protective materials

6.4 Comparison of anti-soiling resistance four type surface protective materials after three aging environments

Visual appearance

The visual appearance for four types coating after different aging environments show in Fig. 6.3. After three aging environments weathering, the visual appearance of uncoated and unweather N, silane1 A and silane2 B and silicate D, which was no change under humidity and cool-heat cycling exposure conditions, these was a slight observed change in warm water immersion 28 days, the coating surface became darkness. After xenon-arc light radiation 5000 hours of accelerated weathering was a clearly observed change, the surface gradually roughens due to the surface of the coating being lost appeared on the specimens.

It is also obviously observed that fluor-resin C coatings was slight observed the darkness of change under humidity and cool-heat cycling aging. The surface became darkness and covering a small swelling was substantial change observed after warm water immersion28 days. And it no change in xenon-arc light radiation 5000 hours.

	0.45				0.55			
	Initial	C20	W28	H5000	Initial	C20	W28	H5000
N								
A								
B								
C								
D								
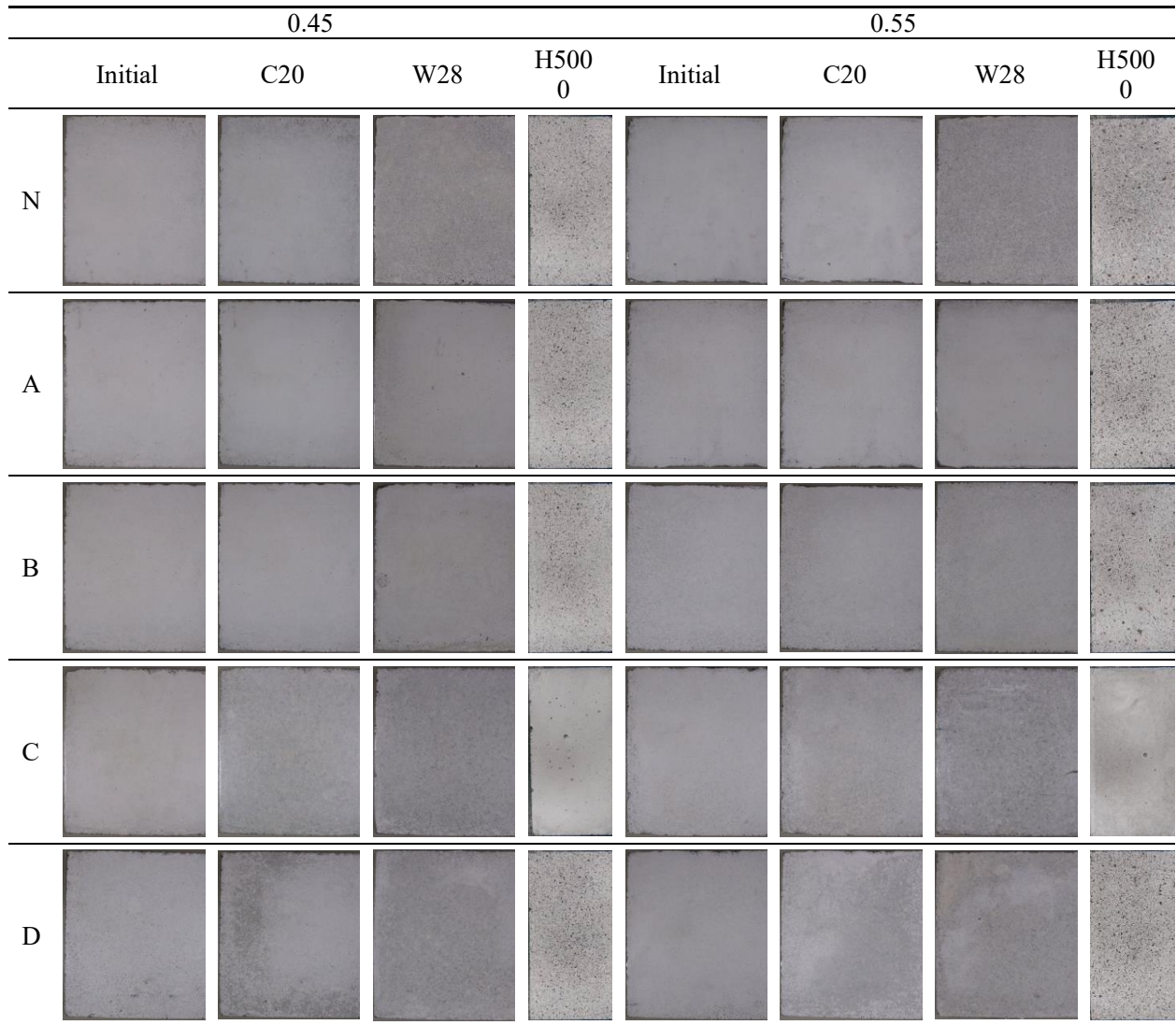
Fig. 6.3 The visual appearance for four types coating after different aging environments

Brightness

Comparison of brightness of the four types coating specimens in three aging environments is reported in Fig. 6.4. We observed for all the aging tests, there are practically no differences among coatings, since the L* parameter of all the coating specimens were kept over 80 and this stands for a good resistance in term of discoloration.

In the case of the silane1 A and silane 2 B coating (Fig. 6.4b, c), there are practically no differences among aging environments coatings.

As can be observed, after humidity and cool-heat cycling 20 cycles and warm water immersion 28 days aging, fluor-resin C decreased the values of L* parameter (Fig. 6.4d), as found in other studies. Moreover, there are no change of parameter L* after xenon-arc light radiation 5000 hours.

Brightness of silicate D (Fig. 6.4e), it was better under humidity and cool-heat cycling 20 cycles aging conditions, it not good in warm water immersion 28 days and xenon-arc light radiation 5000 hours of accelerated weathering was a slightly deteriorated. While the effect of water cement ratio is not obvious.

(a) Uncoated

(b) Silane1

(c) Silane2

(d) Fluor-resin

(e) Silicate
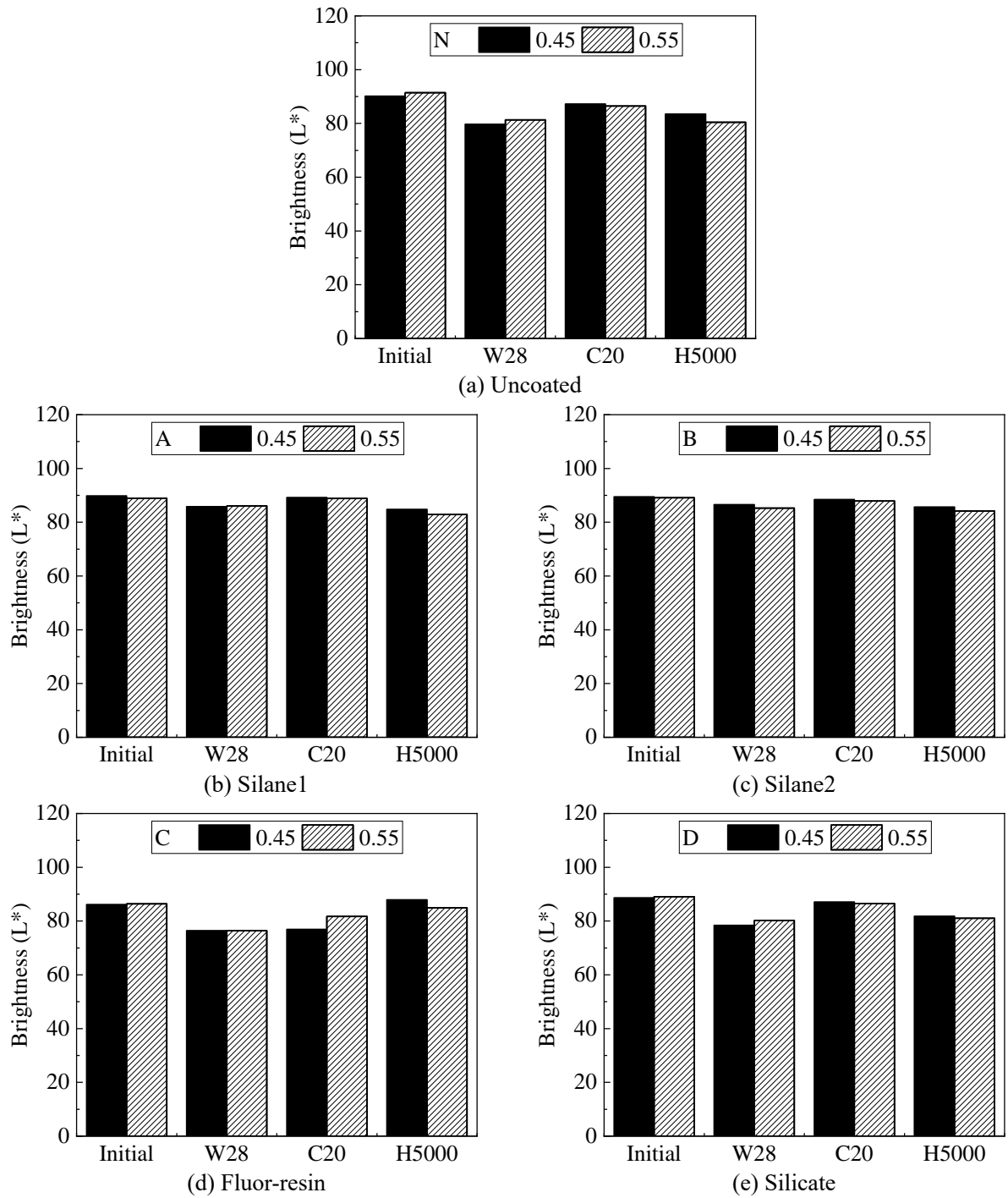
Fig. 6.4 Comparison of brightness of the four types coating specimens in three aging environments

Gloss

Fig. 6.5 Comparison of gloss of the specimens in three aging environments. From Fig. 6.5 (a), it is observed that N was slightly reduced in all three aging environments, the xenon-arc light radiation environment is the most decreased of gloss for N specimens.

From Fig. 6.5 (b), it is obviously observed that the gloss of specimens exposed to three aging environments is lower than initial specimens, no matter what the water-to- cement ratio. Besides, the same variation tendency of gloss in three aging environments can be observed.

From Fig. 6.5 (c), it can be found that the exposure xenon-arc light radiation environments (H5000) of surface coated silane have an apparent influence on the amount of gloss, no matter what is the water-to- cement ratio.

Fig. 6.5 (d) show that the fluor-resin C almost no loss of gloss, indicating that these coatings had an excellent gloss retention, even under the xenon-arc light radiation and the humidity and cool-heat cycling. The reason why the fluor-resin coating did not show degradation was thought to be because fluorine atoms could form a continuous uniform coating film develop a structure with strong chemical bonding which makes it difficult to produce the free radicals which cause coating decomposition (Wood et al., 2000; Song et al., 2004; Yuan et al., 2020). However, the loss of gloss of warm water immersion indicates that some kind of degradation of these coatings is nevertheless occurring. The reason is the gloss loss must be attributed either to non-chemical changes (e.g., small swelling), or to chemical changes localized in the top fraction of a micron of the coating.

From Fig. 6.5 (e), comparison to initial, the gloss of W28, C20, H5000 three environments decreased by 70%, respectively. It could be seen that the exposure environment has a significant effect on gloss while the effect of water-to-cement ratio is not obvious. It illustrates that it is not suitable for silicate surface impregnation treatment under high humidity and long-time xenon-arc light radiation condition.

(a) Uncoated

(b) Silane1

(c) Silane2

(d) Fluor-resin

(e) Silicate
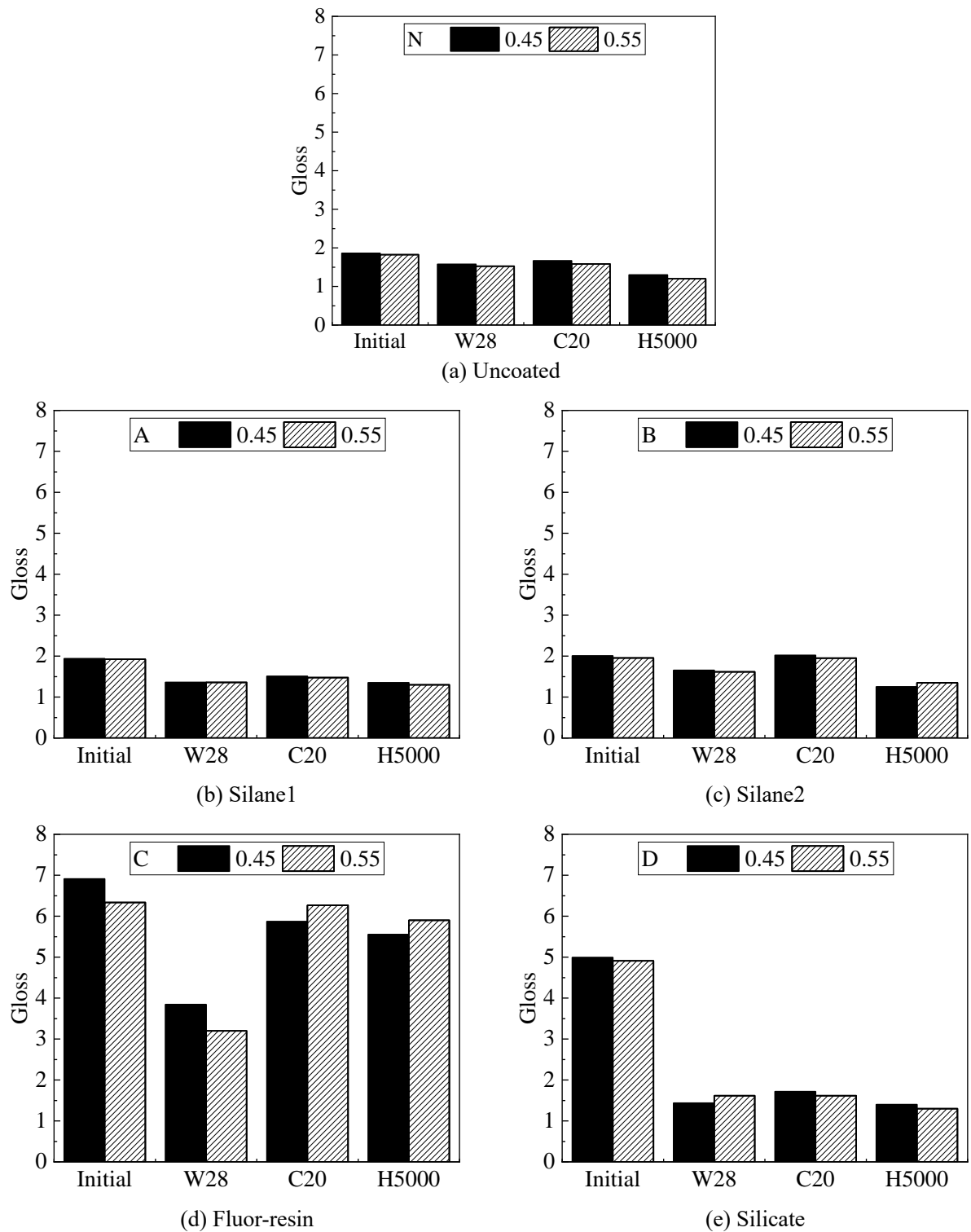
Fig. 6.5 Comparison of gloss of the specimens in three aging environments

Roughness

The roughness for four types coating after different aging environments show in Fig. 6.6. After three aging environments weathering, the roughness of uncoated and unweather N, silane1 A and silane2 B and silicate D, there were large increased roughness after xenon-arc light radiation 5000 hours of accelerated weathering. It a slight increased roughness after warm water immersion 28 days. Fluor-resin C coatings, for the three aging environments, the roughness is quite similar, but perhaps slightly higher for humidity and cool-heat cycling.
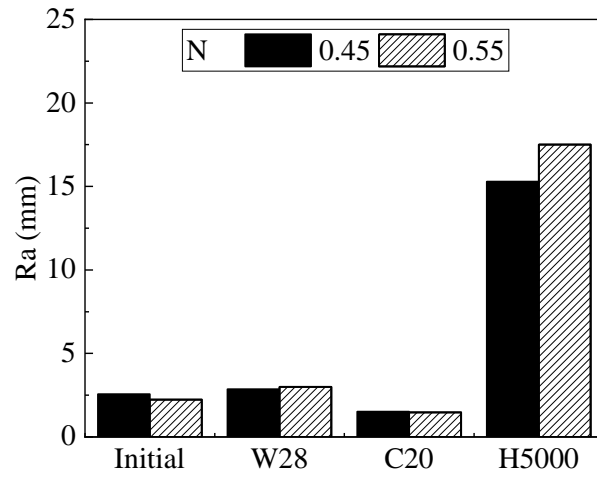
(a) Uncoated
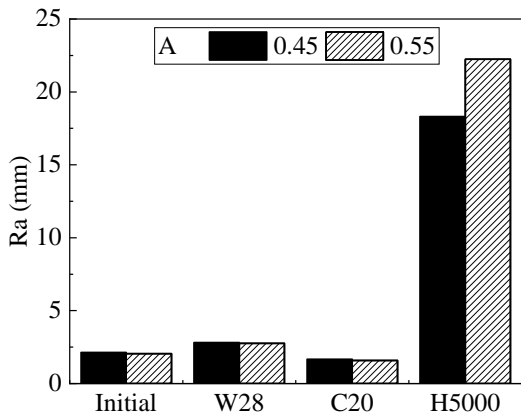
(b) Silane1
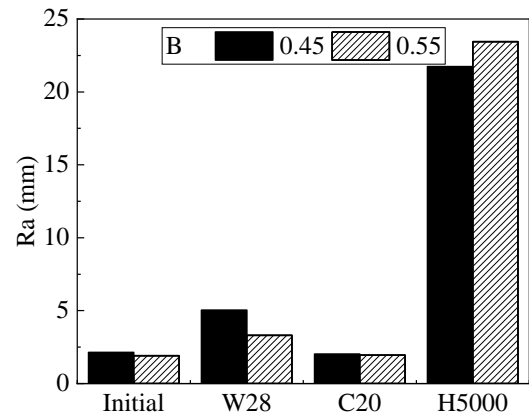
(c) Silane2
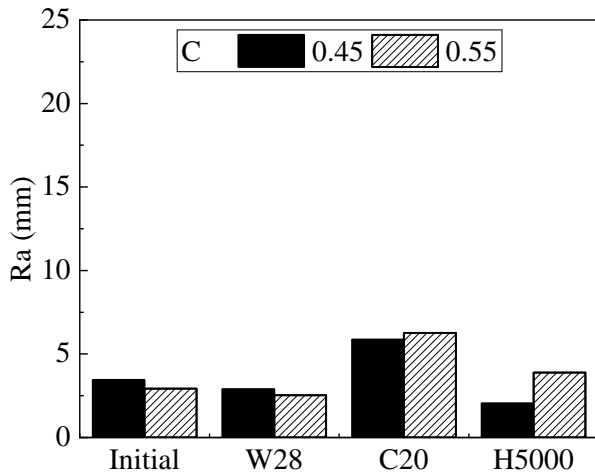
(d) Fluor-resin
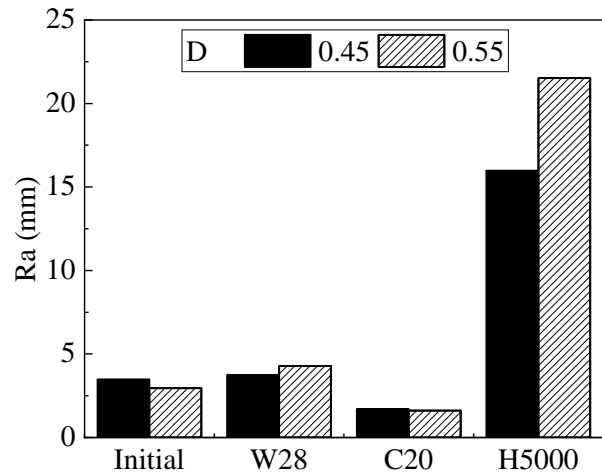
(e) Silicate

Fig. 6.6 Comparison of roughness of the specimens in three aging environments

Contact angle

A higher value of the contact angle (θ) indicates the good hydrophobic nature of the surface, while low values indicate the non-hydrophobic surface. The solid surface is perfectly wetted for $\theta=0$ and it is hydrophilic for $\theta<90°$ while it is hydrophobic for $\theta\geq90°$ (Zielecka, 2004). The sufficient hydrophilization is achieved at contact angle greater than 90° (Alvarez et al., 2001).

The contact angle values for the uncoated and unweather N specimens were increased after three aging environments weathering, respectively. It is indicated that the CA $\theta<90°$was hydrophilic. In other words, the untreated concrete surface is inherently hydrophilic.

Xenon-arc light radiation weathering has considerably reduced contact angle in silane1 A and silane 2 B, show a hydrophilic surface (a CA between approximately 20° and 30°), which suggests a decrease in the protective abilities of the silane coatings. The results obtained proving the occurrence of hydrolysis and photodegradation reactions during xenon exposure in silane coatings, so this decrease in all CA can be easily understood. After aging environment in warm water immersion and under humidity and cool-heat cycling silane1 A exhibited water contact angles similar to those of the initial (a CA 80°), it is indicated the non-hydrophobic surface. It can be noticed from Fig. 6.7(c) that mortar coated with silane2 B has the highest hydrophobicity. The contact angle of silane2 B is 126° at the initial test and decreased gradually to 117° after in warm water immersion weathering and increased to 130° after humidity and cool-heat cycling weathering, respectively.

As shown in Fig. 6.7 (d), Fluor-resin C coatings turned the concrete surface somewhat hydrophobic. After aging environment in warm water immersion and under humidity and cool-heat cycling demonstrated significant increases in the water contact angle, while after xenon-arc light radiation weathering exhibited water contact angles sightly decreased to those of the non-weathered initial.

Comparison to non-weathered initial (a CA under 20°), silicate D coatings was increased after three aging environment, especially warm water immersion 28 days (a CA between approximately 40° and 60°). However, it has shown the least hydrophobic properties that exhibited water contact angles similar to those of the uncoated and unweather N specimens. Despite the low contact angle of silicate D coatings, its hydrophobicity was two

times higher than non-weathered initial mortar. This also indicates that silicate D coating material has penetrated through the surface and have created a lining rather than blocking the pores, allowing concrete to breathe.

(a) Uncoated

(b) Silane1

(c) Silane2

(d) Fluor-resin

(e) Silicate
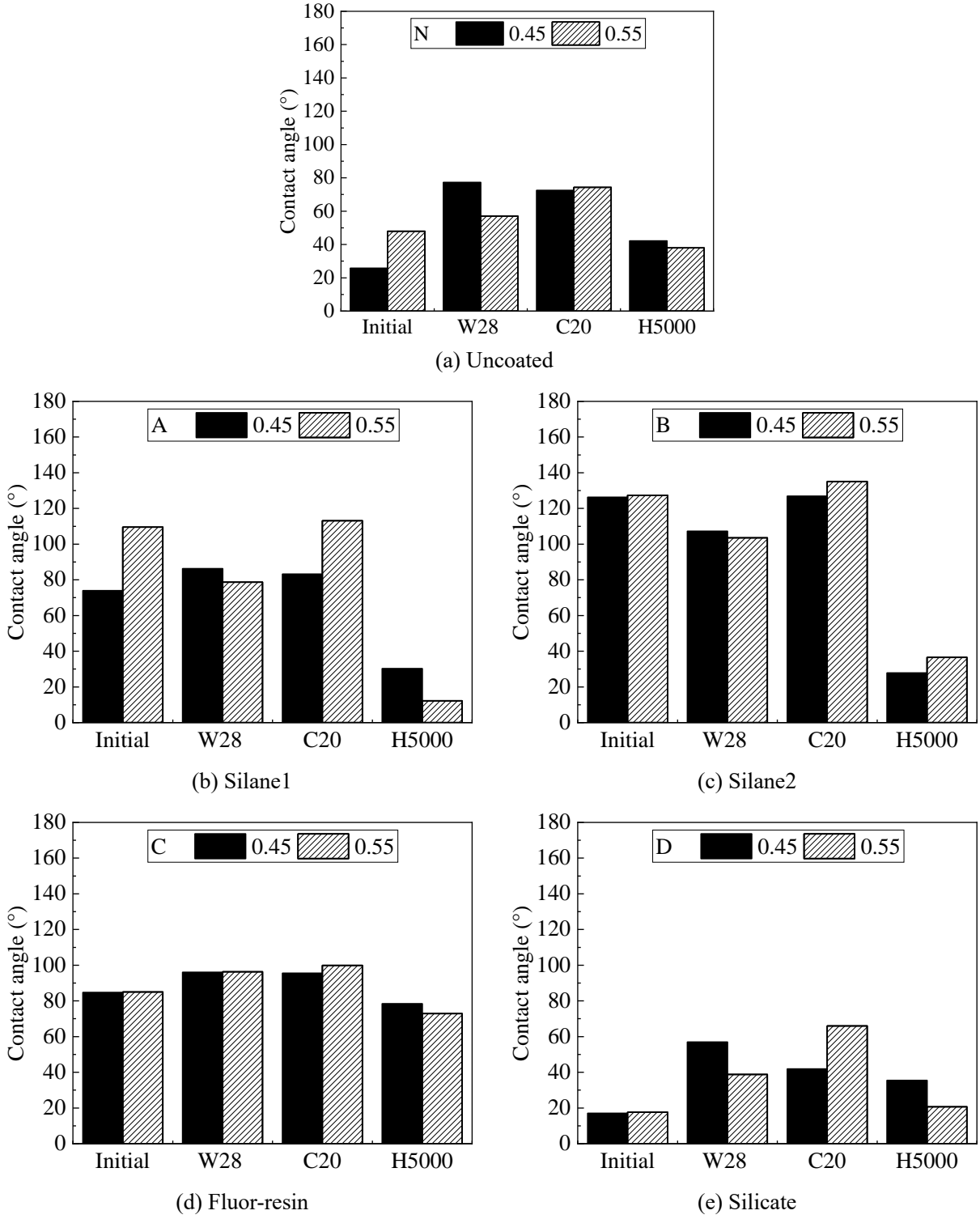
Fig. 6.7 Comparison of contact angle of the specimens in three aging environments

Coating method to pollutant

The effect of different accelerated aging methods on the different methods for measuring anti-soiling test on mortar with surface protective materials.

Visual observation results of uncoating N are shown in Fig.6.8. The result of brightness and pollution area fraction are shown in Fig. 6.9, Fig.6.10.

After pollution, the initial, C20 and W28 surfaces is similar, where soiling presents of uniformly soiled. Compared with the initial samples, the W28 is soiled most seriously, and its surface is almost covered by contaminants after ultrasonic cleaning. The result of brightness and pollution area fraction are similar. After ultrasonic cleaning w/c 0.55 samples are difficult to clean the contaminants than w/c 0.45.

N	0.45			0.55		
	Initial	C20	W28	Initial	C20	W28
Pollution						
Ultrasonic cleaning						

Fig. 6.8 Visual observation for uncaoted N after coating method to pollutant
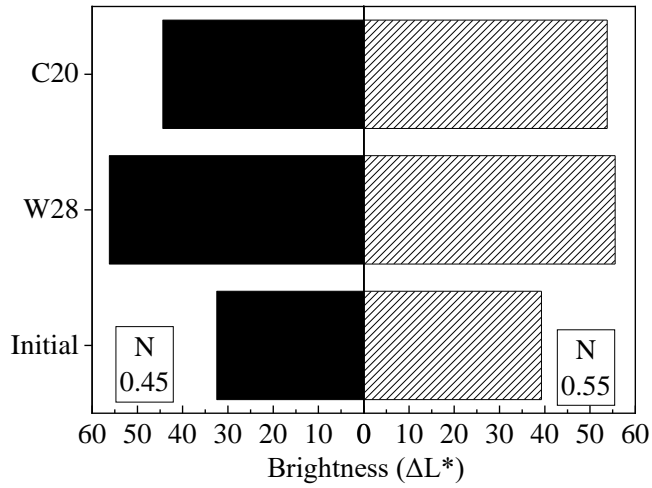
Fig. 6.9 Shows the brightness in different aging environment of uncoated N
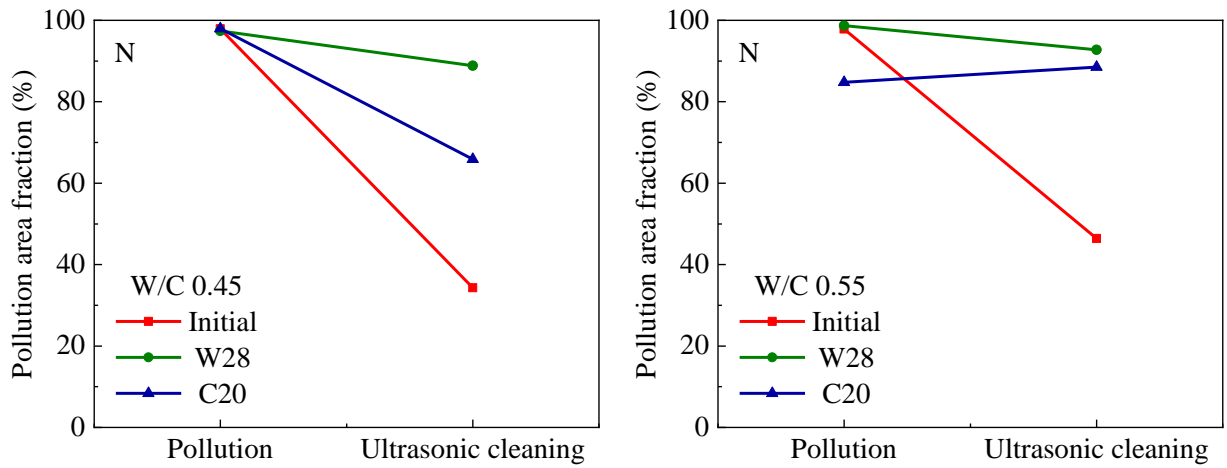
Fig. 6.10 Shows the pollution area fraction in different aging environment of uncaoted N

Visual observation results of silane1A are shown in Fig. 6.11. The result of brightness and pollution area fraction are shown in Fig. 6.12, Fig. 6.13.

The After pollution on the initial, C20 and W28 surfaces is similar, where soiling presents of uniformly soiled. Compared with the initial samples, the W28 is soiled most seriously, and its surface is almost covered by contaminants after ultrasonic cleaning. The results of brightness and pollution area fraction consistent with visual observation. The reason is after 28 days in warm water immersion, the surface became a large surface roughness than C20, so that W28 is difficult to clearer.

	0.45			0.55		
A	Initial	C20	W28	Initial	C20	W28
Pollution						
Ultrasonic cleaning						
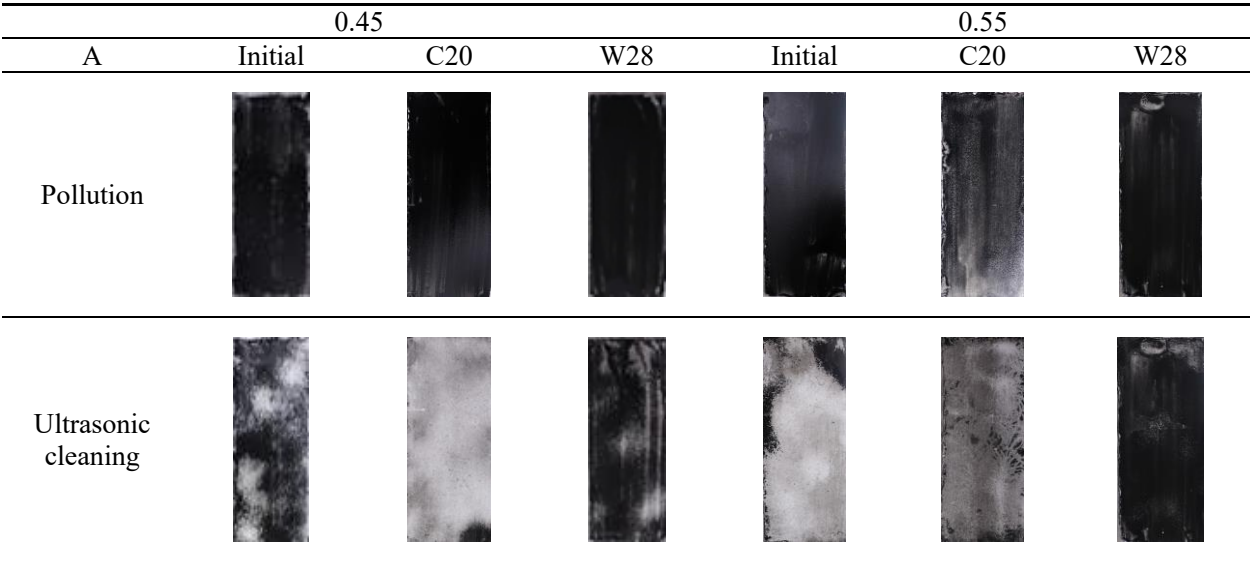
Fig. 6.11 Visual observation for coating A after coating method to pollutant
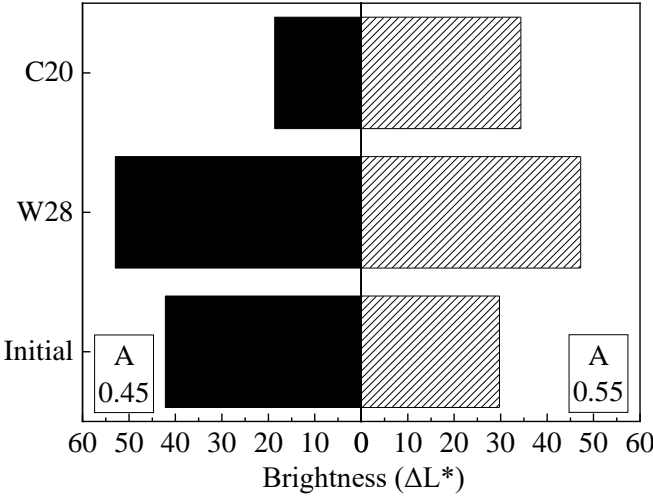
Fig. 6.12 Shows the brightness in different aging environment of coating A
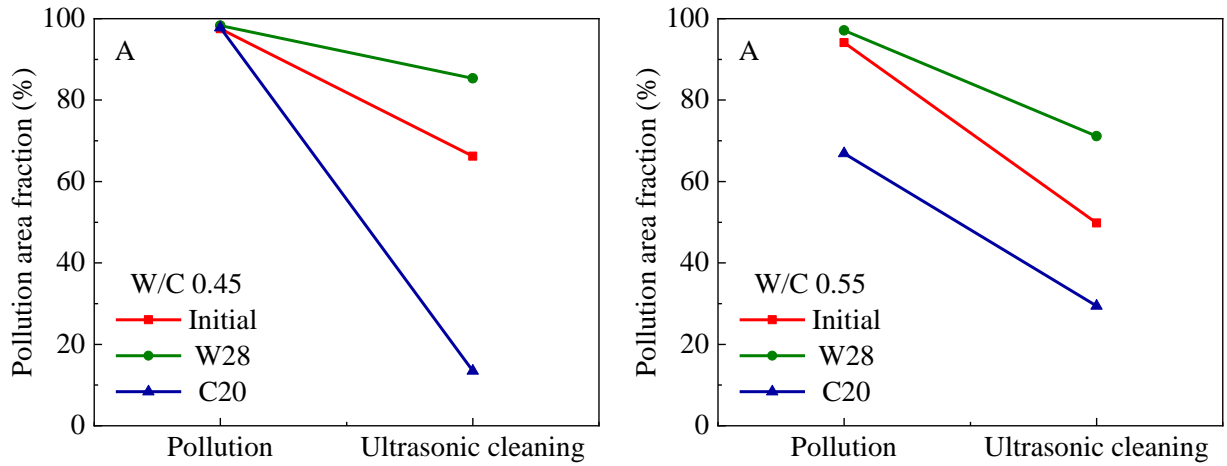
Fig. 6.13 Shows the pollution area fraction after different aging environment of coating A

Visual observation results of silane2 B is shown in Fig. 6.14. The result of brightness and pollution area fraction are shown in Fig. 6.15, Fig. 6.16. After pollution, the hydrophobicity of the initial conditions has little carbon black liquid in the form of drops on the surface. after C20 ageing, the hydrophobicity becomes weaker and the dirty water spreads on the surface. after W28, the hydrophobicity is almost lost, and the carbon black liquid covered the surface. After ultrasonic cleaning, the majority of the contaminants are removed by ultrasonic cleaning, except w28. The results of brightness and pollution area fraction consistent with visual observation. All of the results have not much effect of the difference water cement ratio.
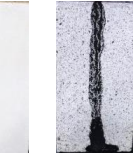
	0.45			0.55		
B	Initial	C20	W28	Initial	C20	W28
Pollution						
Ultrasonic cleaning						
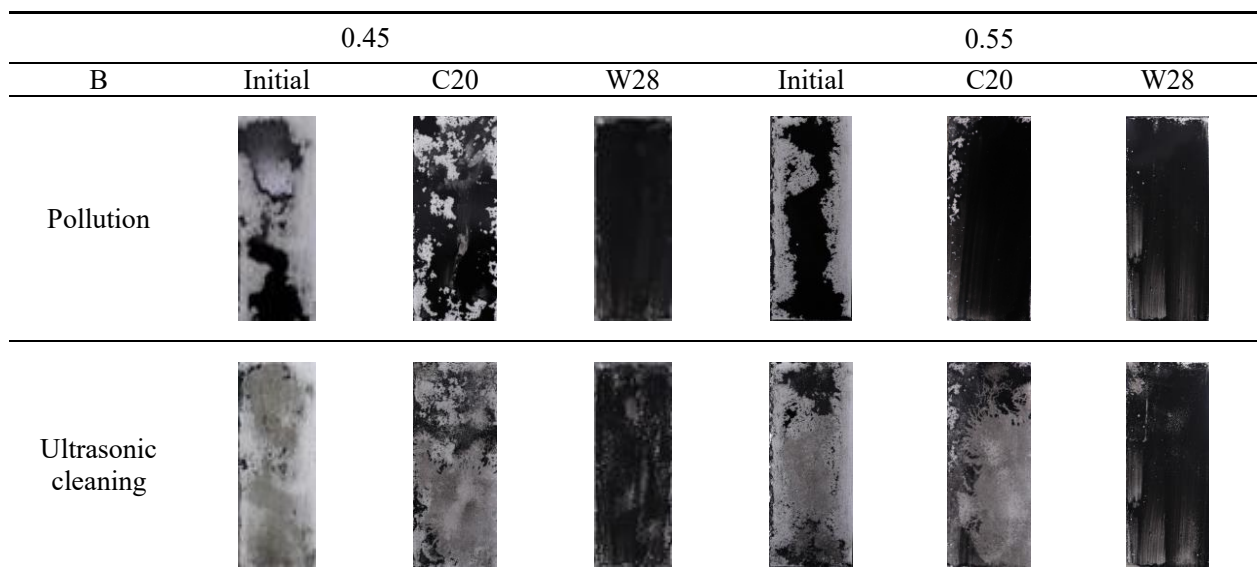
Fig. 6.14 Visual observation for coating B after coating method to pollutant
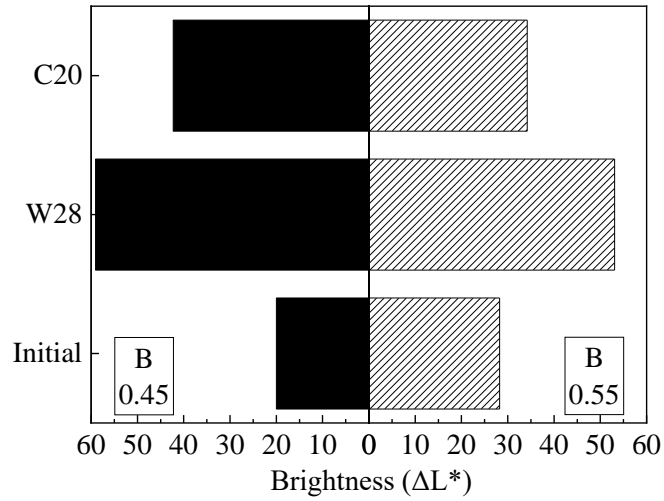
Fig. 6.15 Brightness difference for coating B after coating method to pollutant
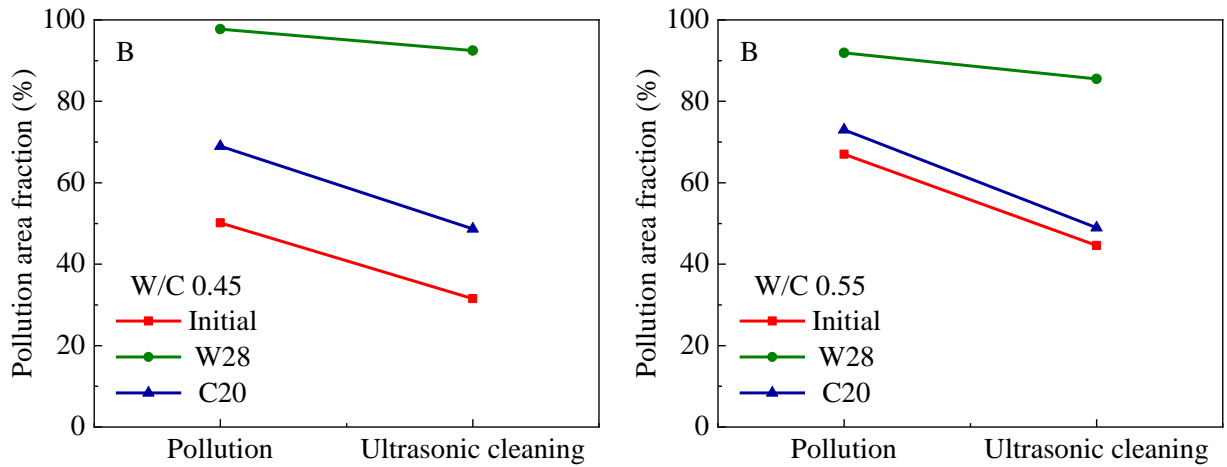
Fig. 6.16 Pollution area fraction for coating B after coating method to pollutant

Visual observation results of fluor-resin C coating are shown in Fig.6.17. The result of brightness and pollution area fraction are shown in Fig.6.18 and Fig,6.19.

After pollution, initial, C20 and W28 is similar, where carbon black liquid is spreading evenly on the surface. After cleaning, the C20 and W28 have majority of the contaminants are removed by ultrasonic cleaning. Initial has soiled most seriously, and its surface is almost covered by contaminants, it is difficult to clean the contaminants. The results of brightness and pollution area fraction consistent with visual observation. All of the results have not much effect of the difference water-cement ratio.
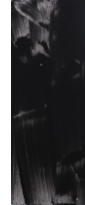
	0.45			0.55		
C	Initial	C20	W28	Initial	C20	W28
Pollution						
Ultrasonic cleaning						

Fig. 6.17 Visual observation for coating C after coating method to pollutant
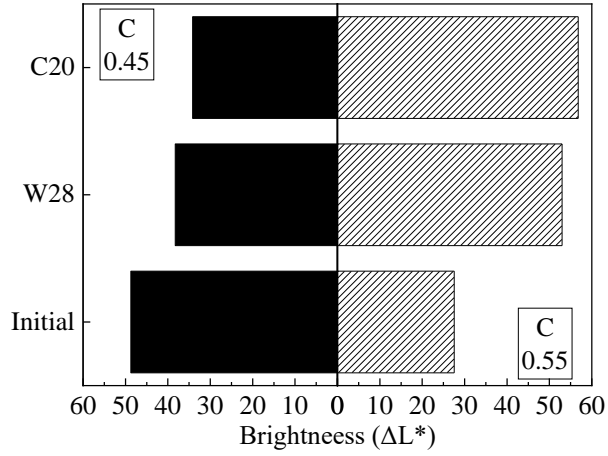
Fig. 6.18 Brightness difference for coating C after coating method to pollutant
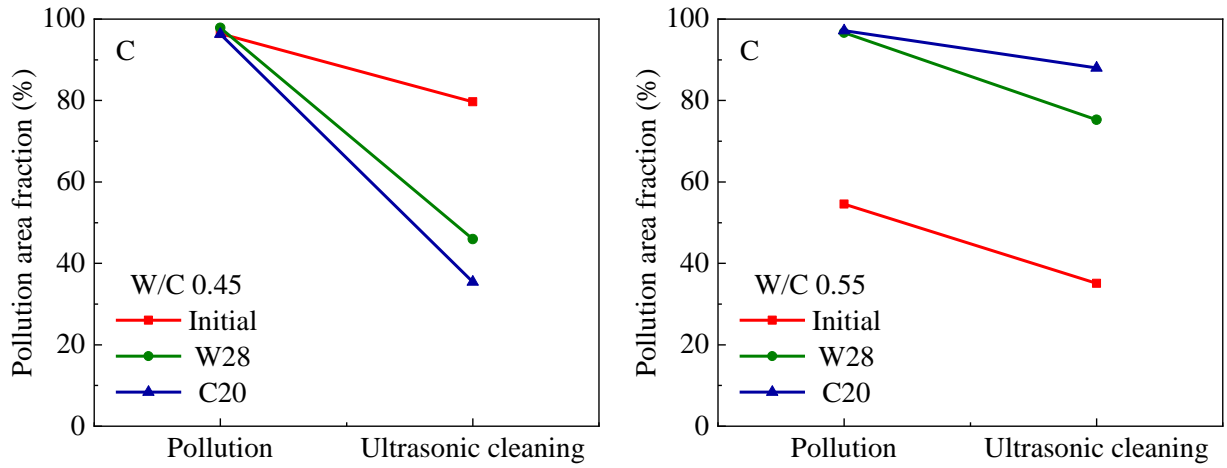
Fig. 6.19 Pollution area fraction for coating C after coating method to pollutant

Visual observation results of silicate D coating are shown in Fig. 6.20 The result of brightness and pollution area fraction are shown in Fig. 6.21and Fig. 6.22

After pollution, initial, C20 and W28 is similar, where carbon black liquid is spreading evenly on the surface.

After cleaning, the C20 and W28 have becomes difficult to remove by ultrasonic cleaning. W28 environment ageing is the most difficult to remove.

D	0.45			0.55		
	Initial	C20	W28	Initial	C20	W28
Pollution						
Ultrasonic cleaning						
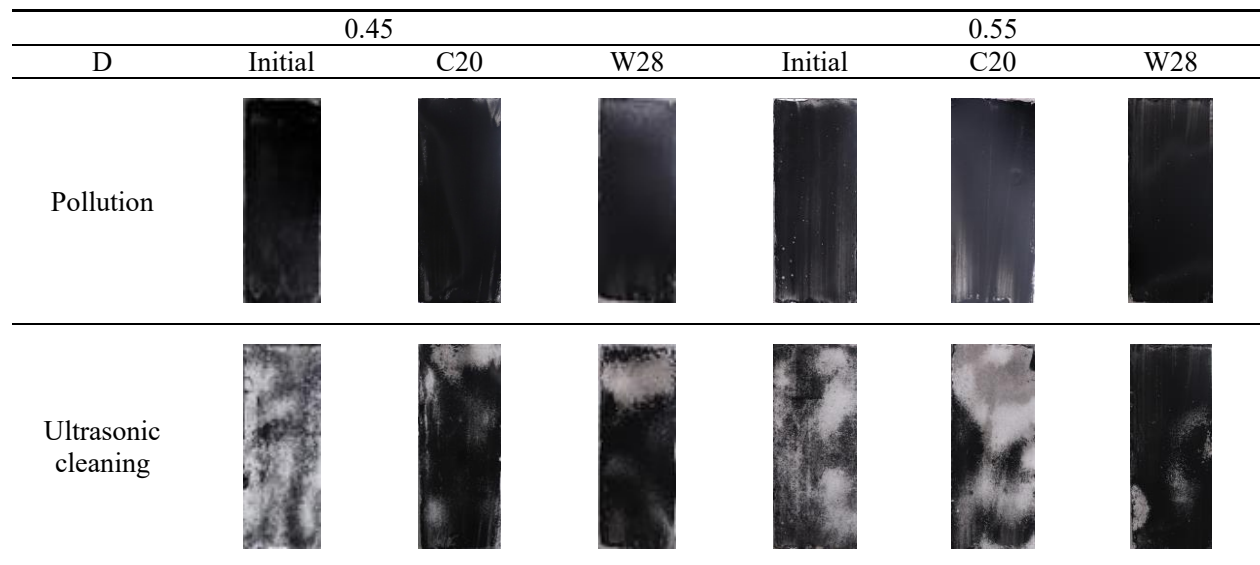
Fig. 6.20 Visual observation for coating D after coating method to pollutant
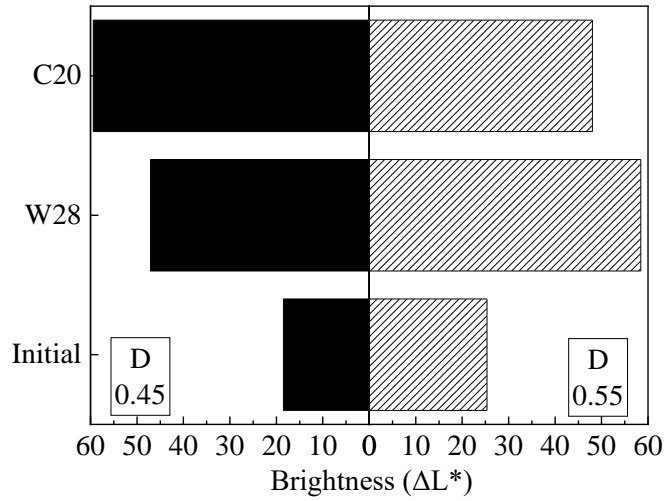
Fig. 6.21 Brightness difference for coating D after coating method to pollutant
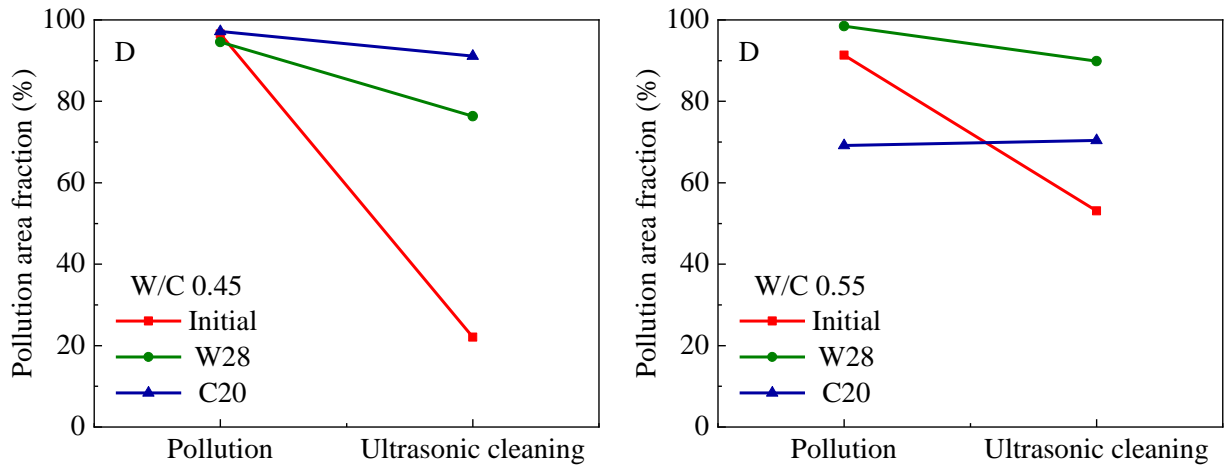
Fig. 6.22 Pollution area fraction for coating D after coating method to pollutant

Simulated raindrops method to pollutan

Visual observation results of uncoating N are shown in Fig. 6.23. The result of brightness and pollution area fraction are shown in Fig. 6.24 and Fig. 6.25.

The contaminants cannot be washed off with spray cleaning, and it can be removed by ultrasonic cleaning.

Especially after H5000 hours weathering, the surface becomes cleaning. It means that the surface of N has become hydrophilic, the contaminants are easily removed, as can be obtained from the results in Chapter 5. The result of brightness and pollution area fraction keep it consistent to visual observation result.
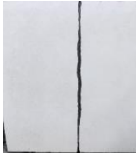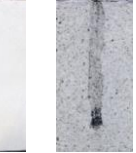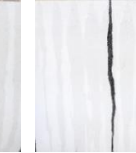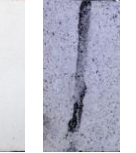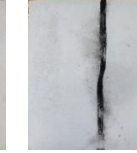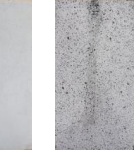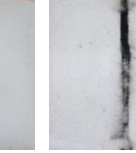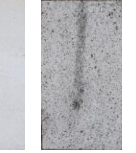
N	0.45				0.55			
	Initial	C20	W28	H5000	Initial	C20	W28	H5000
P								
SP								
UL								

Fig. 6.23 Visual observation for uncoated N after simulated raindrops method to pollutant
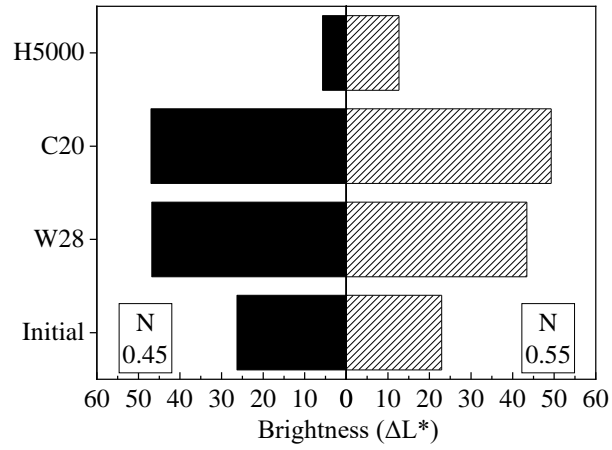
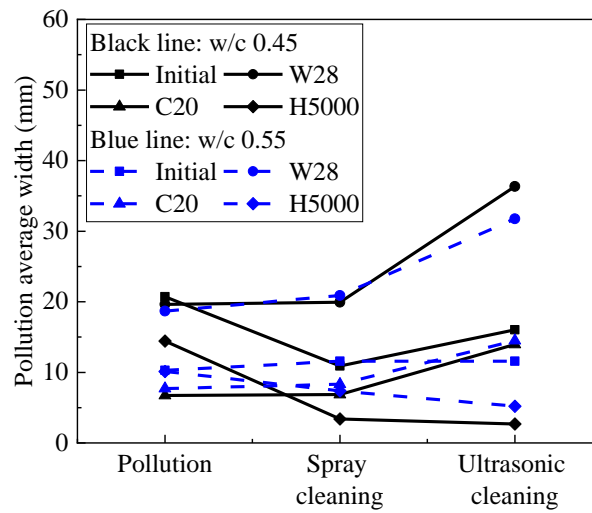Fig. 6.24 Brightness after different aging environment of N

Fig. 6.25 Pollution area fraction after different aging environment of N

Fig. 6.26 shows the results of visual observation. Brightness difference (ΔL*) and pollution average width results was shown in Fig. 6.27, Fig. 6.28.

From the pollutant raindrop line of the Fig. 6.26, it becomes thicker and thicker follow the order C20, w28, H5000, therefore, the greatest influence is H5000 weathering resistance, the smallest is the humidity and cool-heat cycling. And it showed that the contaminants are easily removed after H5000 hours aging. he results of brightness and pollution area fraction consistent with visual observation. All of the results have not much effect of the difference water-cement ratio.
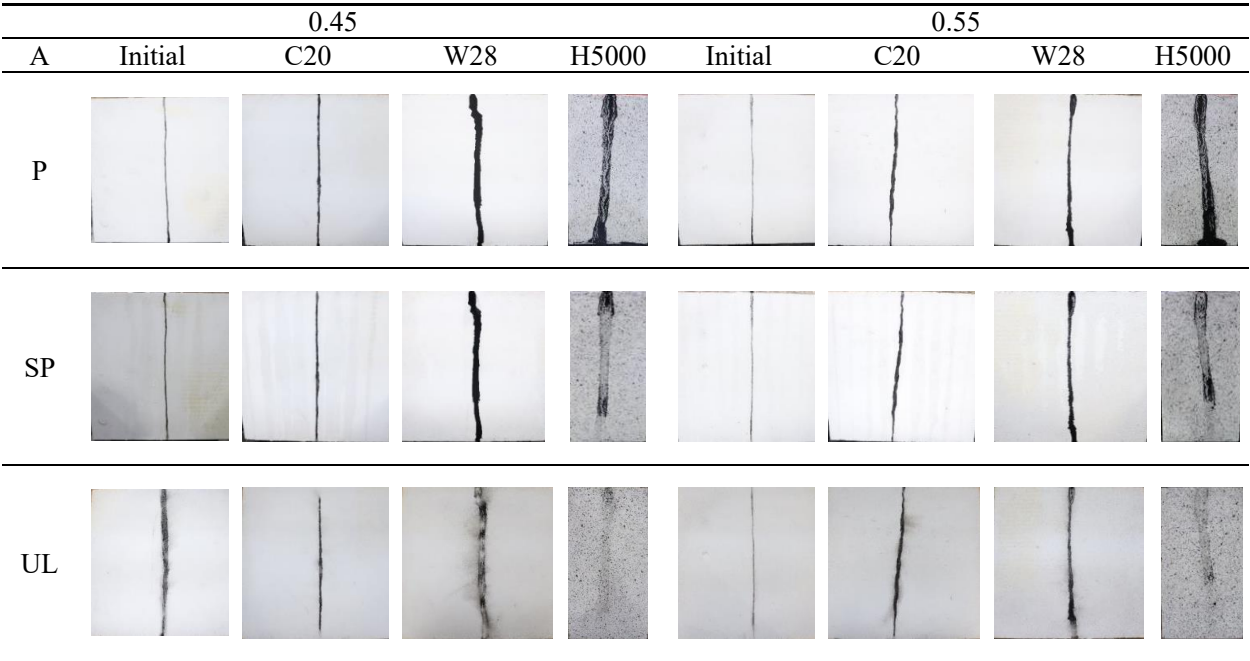

Fig. 6.26 Visual observation for coating A after simulated raindrops method to pollutant
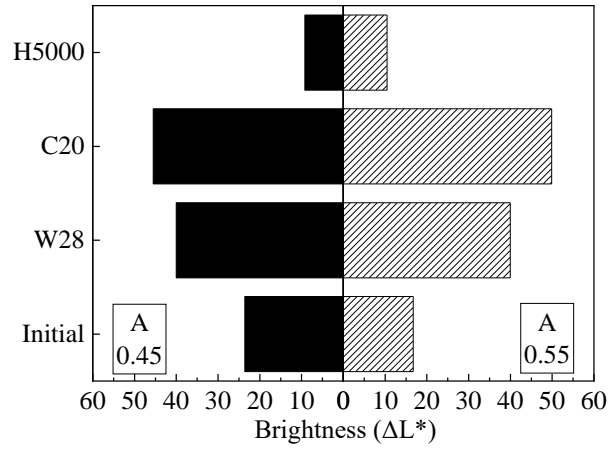
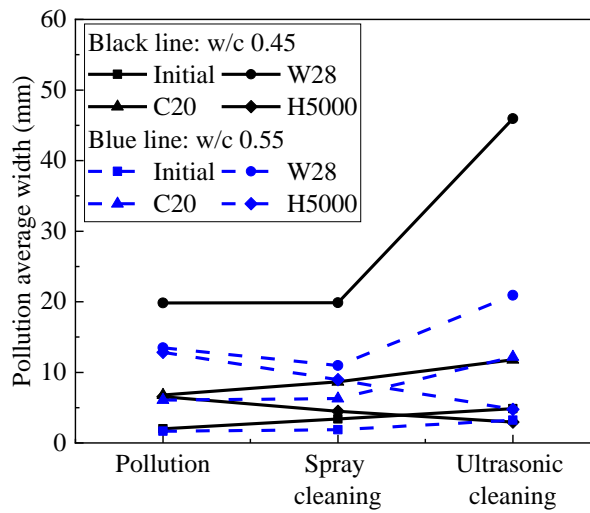Fig. 6.27 Brightness after different aging environment of coating A

Fig. 6.28 Pollution area fraction after different aging environment of coating A

After pollution, after H5000 hours aging, others aging environment has not significant effects. After cleaning, just only H5000 was easy removed the contaminants by ultrasonic cleaning, the results of brightness and pollution area fraction consistent with visual observation (Fig. 30, Fig. 31). All of the results have not much effect of the difference water-cement ratio.

B	0.45				0.55			
	Initial	C20	W28	H5000	Initial	C20	W28	H5000

Fig. 6.29 Visual observation for coating B after simulated raindrops method to pollutant

Fig. 6.30 Brightness after different aging environment of coating B

Fig. 31 Pollution area fraction after different aging environment of coating B

Fig. 6.32. Fig. 6.33, Fig. 6.34 showed the results of the visual observation, brightness and pollution area fraction. Regardless of the water-cement ratio and degradation status, there appeared to be no change in the width and colour of the poullution before and after washing. Flurorein C show the same level of pollution for all aging environments.

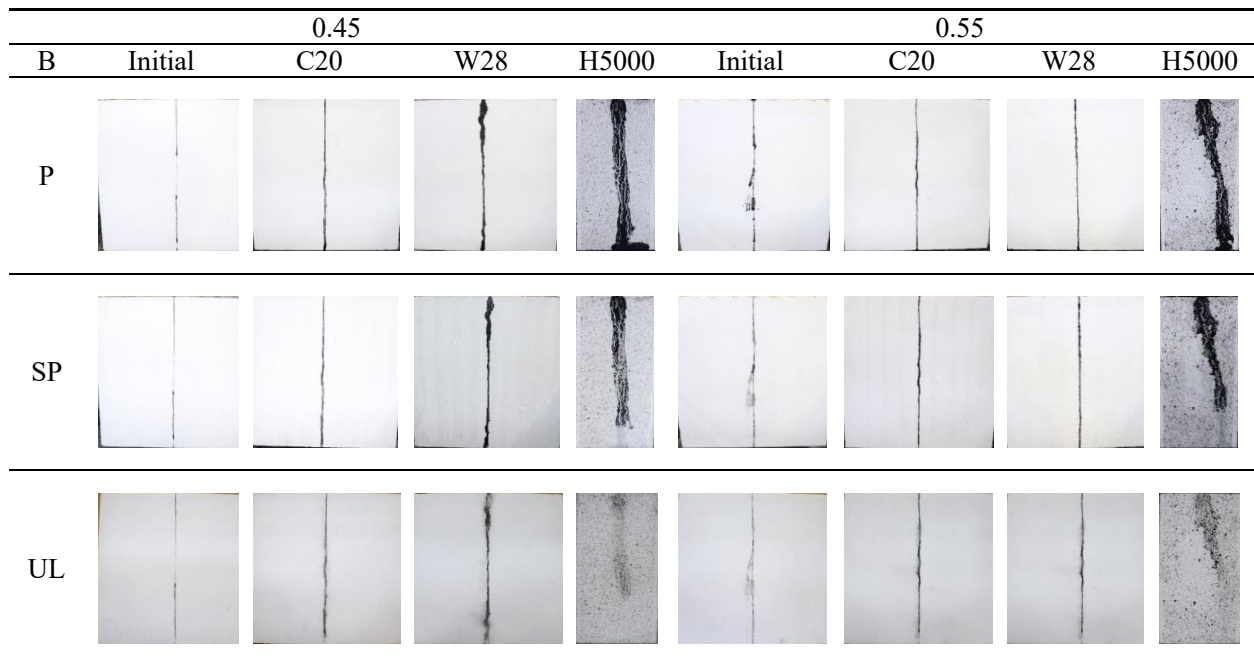| C	0.45				0.55			
	Initial	C20	W28	H5000	Initial	C20	W28	H5000
P								
SP								
UL								

Fig. 6.32 Visual observation for coating C after simulated raindrops method to pollutant
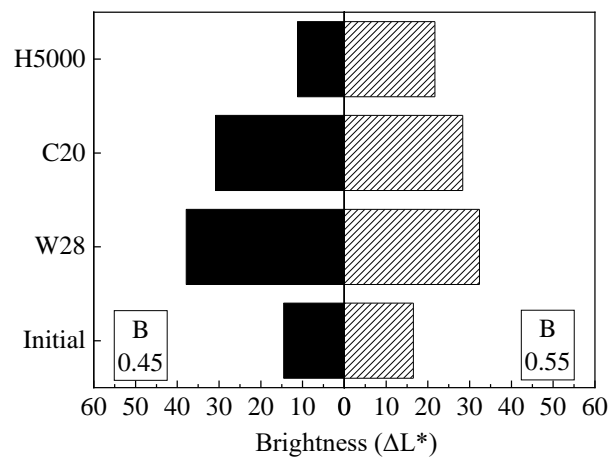

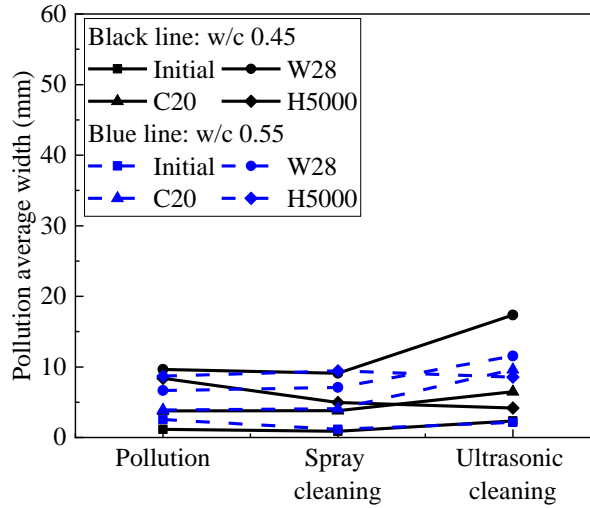Fig. 6.33 Brightness after different aging environment of coating C

Fig. 6.34 Pollution area fraction after different aging environment of coating C

Fig. 6.35, Fig. 6.36 and Fig. 6.37 showed the results of the visual observation, brightness and pollution area fraction.

Silicate D show the same level of pollution for all degraded environmen is easily contaminated.
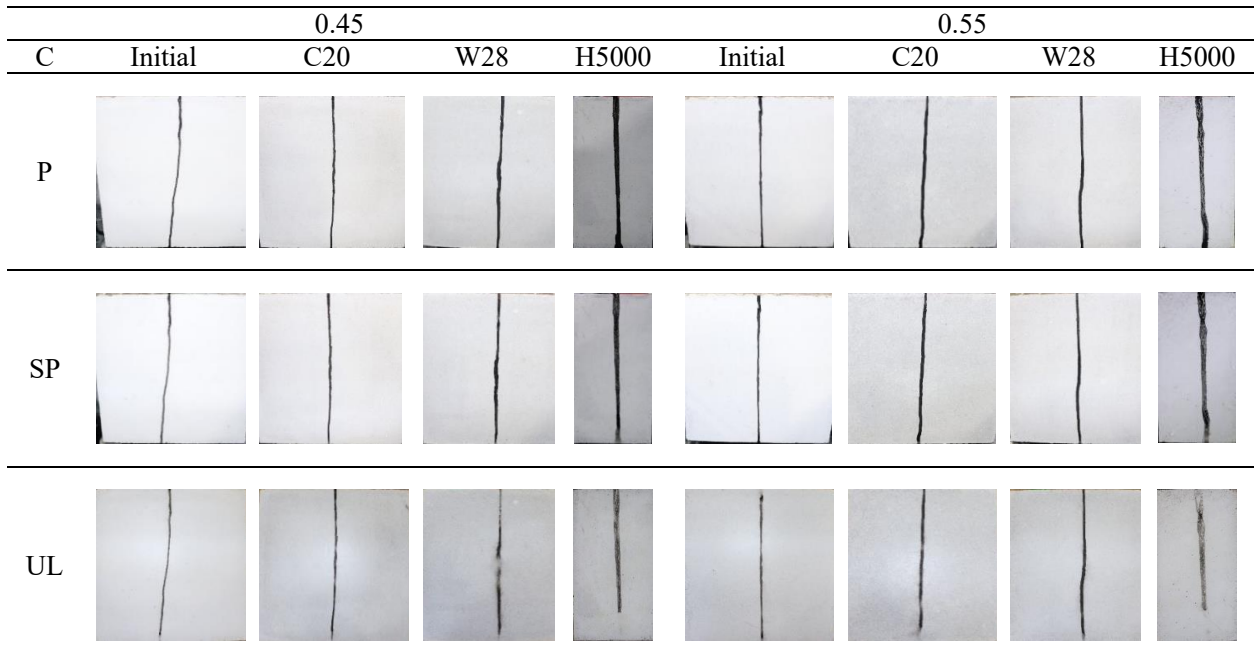

Fig. 6.35 Visual observation for coating D after simulated raindrops method to pollutant
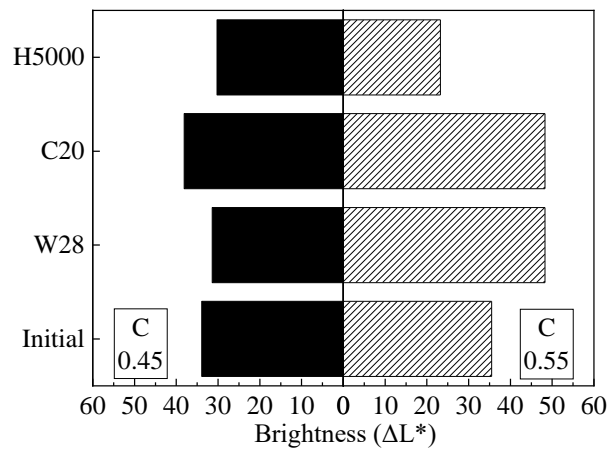
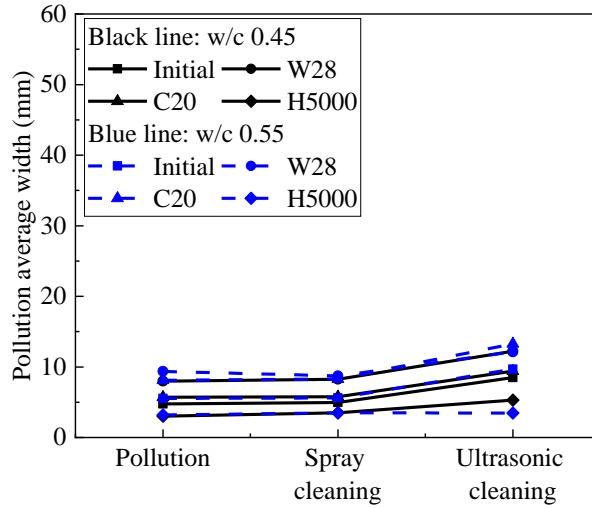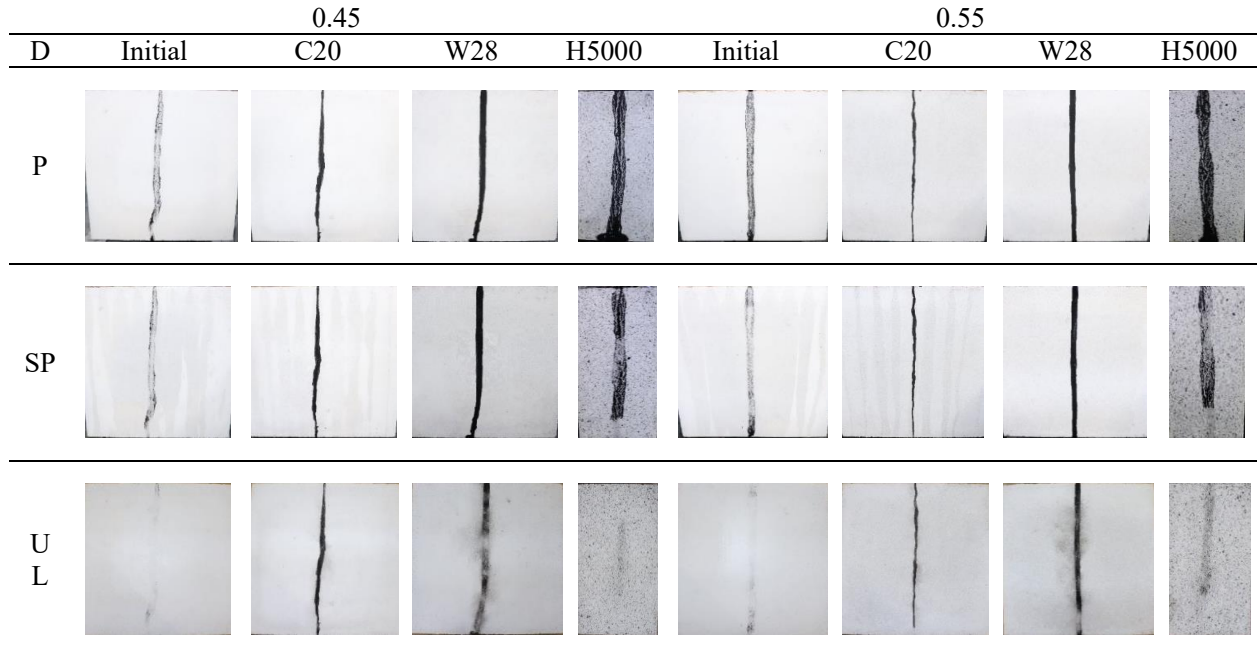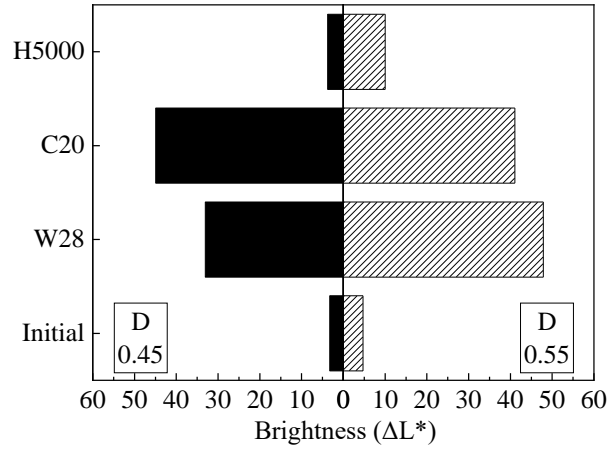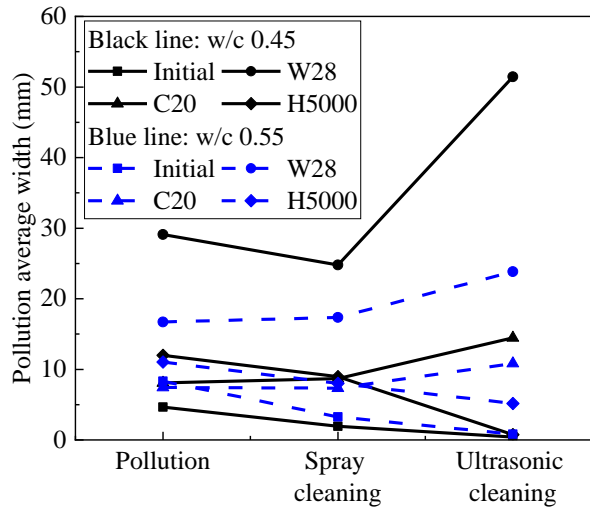Fig. 6.36 Brightness after different aging environment of coating D

Fig. 6.37 Pollution area fraction after different aging environment of coating D

6.5 Conclusion

In this chapter, in order to obtain the applicable environment for surface protective materials were involved in the warm water immersion, humidity and cool-heat cycling and xenon-arc light radiation as environmental factors to conduct a comparative study on the water resistance and aesthetics characterizations of mortar reinforced with four kinds of surface protective materials.

In this study have indicated that the performance of surface coating varies depending on exposure conditions, i.e., aging by warm water immersion, humidity and cool-heat cycling and xenon-arc light radiation. While the performance of a certain product was better under certain exposure conditions, it may not perform better than the other product in another environment. The main findings of this chapter were shown as following:

(1) The warm water immersion exposure environment has significant influences on the color, gloss, and roughness for mortar coated by surface silane1 A and silane2 B and silicate D. The coating surface became darkness, which gloss were slightly reduced and It a slight increased roughness. there were no change under humidity and cool-heat cycling exposure environment. The humidity and cool-heat cycling and warm water immersion exposure environment have a remarkable influence on the Fluor-resin C coatings color, gloss and roughness of mortar. The surface covering a small swelling after 28 day. And it no change under xenon-arc light radiation exposure environment .

(2) The xenon-arc light radiation exposure environment e has significant influences on the contact angle for mortar coated four types of surface protective materials. The contact angle obviously was averagely reduced by approximately 20° and 30°after 5000 hours ageing. After humidity and cool-heat cycling and warm water immersion exposure environment ageing, The contact angle obviously reduced of uncoated N, A coatings, B coatings and C coatings were increased.

(3) The silane1 A and silane2 B coatings were the most effective in reducing water absorption in the coated specimens exposed to humidity and cool-heat cycling and warm water immersion and xenon-arc light radiation ageing. Fluor-resin C coatings performed better than the silicate D coatings in humidity and cool-heat cycling and xenon-arc light radiation ageing. Silicate D showed a similar tendency with N.

Comparison to initial, the water absorptions of W28, C20, H5000 three environments decreased by 90%, 40%, 60%, respectively. The reason is the later decrease to the refinement of pore structure due to hydration.

(4) The H5000 hours exposure environment has a significant effect moisture permeability for all the specimens. The lowest moisture permeability than other exposure environment.

(5) The humidity and cool-heat cycling and warm water immersion exposure environment ageing has significant influences on the capacity of anti-soiling for mortar treated by four types of surface protective materials. After exposure environment ageing, the resist soiling was reduced. However, the four types of surface protective materials exhibited the highest resist soiling to xenon-arc light radiation exposure environment.

References:

Adolphs, J., Excess Surface Work – A Modelless Way of Getting Surface Energies and Specific Surface Areas Directly from Sorption Isotherms, Applied Surface Science, Vol. 253, 2007, pp. 5645-5649

Swamy, R. N. and Tanikawa, S. "Surface coatings to preserve concrete durability." Proceedings of International Conference on Protection of Concrete, edited by R.K. Dhir and J. W. Green, E & FN Spon, London, 149-165, (1990).

Almusallam, A., Khan, F. M. and Maslehuddin, M. "Performance of concrete coatings under varying exposure conditions." Materials and Structures, 35, 487-494. (2002).

Kurt A.Wood, Christopher Cypcar, otfi Hedhli, Predicting the exterior durability of new fluoropolymer coatings, Journal of Fluorine Chemistry Volume 104, Issue 1, June 2000, Pages 63-71

Li-Piin Song, Silvia Vicini, Derek L.Ho,Lotfi Hedhli, Christyn Olmstead, Kurt A.Wood, Effect of microstructure of fluorinated acrylic coatings on UV degradation testing, Volume 45, Issue 19, 3 September 2004, Pages 6639-6646

Yuan Jianga, GangLiua, Fabrication and structural characterization of poly (vinylidene fluoride)/polyacrylate composite waterborne coatings with excellent weather resistance and room-temperature curing, Colloids and Surfaces A: Physicochemical and Engineering Aspects, Volume 598, 5 August 2020, 124851

Zielecka M, Methods of contact angle measurement as a tool for characterization of wettability of polymers. Polymers 49:327–332, 2004

Alvarez de B, Ballester M, Fort Gonzales R, Basic methodology for the assessment and selection of water-repellent treatments applied on carbonatic materials. Prog Org Coat 43:258–266, 2001

H.F. Taylor, Cement Chemistry, Thomas Telford (1997)

Ma H., Li Z. Realistic pore structure of Portland cement paste: Experimental study and numerical simulation. Comput. Concr. 2013; 11:317–336.

R.S.C. Woo, H. Zhu, M.M.K. Chow, C.K.Y. Leung, J. Kim, Barrier performance of silane–clay nanocomposite coatings on concrete structure, Compos Sci Technol, 68 (2008), pp. 2828-2836

S. Li, W. Zhang, J. Liu, D. Hou, Y. Geng, X. Chen, et al., Protective mechanism of silane on concrete upon marine exposure, Coatings, 9 (9) (2019), p. 558

Y. Geng, S. Li, D. Hou, W. Zhang, Z. Jin, Q. Li, et al., Fabrication of superhydrophobicity on foamed concrete surface by GO/silane coating, Mater Lett, 265 (2020), Article 127423

F. Tittarelli, G. Moriconi, The effect of silane-based hydrophobic admixture on corrosion of reinforcing steel in concrete, Cem. Concr. Res., 38 (11) (2008), pp. 1354-1357

M. Levi, C. Ferro, D. Regazzoli, G. Dotelli, Comparative evaluation method of polymer surface treatments applied on high performance concrete, J. Mater. Sci., 37 (22) (2002), pp. 4881-4888

Scheerder J, Visscher N, Nabuurs T, Overbeek A (2005) Novel, water-based fluorinated polymers with excellent antigraffiti properties. J Coat Tech Res 2:617–625

Jun Liu, Feng Xing, Biqin Dong, Hongyan Ma,and Dong Pan ,Study on Surface Permeability of Concrete under Immersion, Materials (Basel). 2014 Feb; 7(2): 876–886.

CHAPTER 7

CONCLUSION

7.1 Introduction

Considering the actual working conditions of external walls of concrete buildings, the water absorption durability of mortar was studied using multi-factor accelerated aging tests composed of xenon-arc light radiation, warm water immersion, and freeze-thaw cycling. The aesthetic properties of concrete specimens are evaluated. After the accelerated aging tests, observation of the appearance and water contact angle, color differences, gloss, roughness and water absorption, moisture permeability, evaluation of the aesthetics between coatings and concrete examined in order to monitor age-related changes. To assess the protective performance of coating materials, the resistance to soiling determines. which facilitates the successful application of the surface treatment method.

7.2 Influence of surface protective material on appearance change and moisture properties after immersion in warm water (Chapter 3)

This chapter presents an experimental study to characterize the product effectiveness, the surface coated mortar was subjected to 20 wet/freeze/thaw(50℃ dry) cycles of mortar samples made with w/c = 0.45 and 0.55, coated with different types of surface protective materials has been investigated in this study. To help interpret the difference in product performance, the surface-coated mortar specimens were tested for their water absorption, moisture permeability. To characterize the product surface change under deterioration, the appearance characteristics and dirt resistance effectiveness of mortar coated by each product was tested. On the other hand, use the coating method and simulated raindrops method to pollutant of anti-soiling test of comparative experiments were performed by humidity and cool-heat cycling for 20 cycles to systematically study the effects of anti-soiling performance of surface protective materials

For mortar specimens, the water absorption was decreased coated four types of surface protective materials. A and B showed the least water absorption among all other coatings. Regarding concrete surface protective materials, silane A and B coatings would be the most suitable and compatible treatment to reducing water permeability of concrete. In the silicate D it was about the same as in N. This may be due to the hydrophilic

material dissolving into water in D.

Regarding aesthetic properties, the color, gloss and roughness have acceptable variations after exposure. For the coated samples A, B and D after 20 cycles of aging test, was still keep the brightness of 98% and this stands for a good resistance in term of discoloration. Also, for the C we had observed, after 20 cycles of aging, the brightness has a small decreased than other types.

To assess the protective performance of coating materials, the resistance to soiling determines. The coating method to pollutant, after the aging tests, expect N, C coating, A, B, D coatings practically maintained the same efficiency as at time zero. Among the four types of surface protective materials, hydrophobic C encountered the most serious soiling problems in both before and after aging tests, which was ascribed to it having the largest adhesion force between contaminants and the surface. However, the simulated raindrops method to pollutant, the either hydrophilic or hydrophobic N, D and A, B, C were compared. In terms of surface chemistry, the A and B with a hydrophilic surface showed a better soiling resistance than the hydrophobic ones.

7.3 Evaluation of surface characterizations and water resistance of surface coatings after humidity and cool-heat (Chapter 4)

This chapter presents an experimental study to water resistance of coating film, the surface coated mortar was subjected to warm water immersion for 14 days and 28 days of mortar samples made with water cement ratio 0.45 and 0.55, coated with different types of surface protective materials has been investigated in this study.

The aesthetic properties could be changed by warm water immersion. After 28 days in warm water immersion, the color, gloss and roughness have changed on the surface of coated A, B, C, D. The small swelling occurred on the fluorine resin-based C surface. The least influence on aesthetics is the silane A and B.

The water resistance of the four coats was assessed, it was found that for mortar samples coated silane A and B and fluor resin C coating showed relatively higher effect of restrain water absorption compared to uncoated N and silicate D coating. Moreover, the longer of immersion in warm water, the moisture permeability becomes higher of silane A and B and fluor resin C.

After water immersion, the surface coating material silane B and fluor-resin C has the good anti-soiling resistant.

7.4 Investigation on aesthetic and water permeability of surface protective material under accelerated weathering (Chapter 5)

This chapter presents an experimental study to four kinds of surface protective materials conducted on the effects of the weather resistance, which was proven by examining the aesthetic properties and the water permeability of the building materials and the pollutant resistance of the surface protection material coating to artificial stain was assessed using xenon-arc light. The result shows that the appearance of the silane types did not change significantly, and the water permeability could be improved. In addition, the silicate types did not improve water permeability and the surface color was changed. The fluorocarbon resin could effectively improve the water permeability, but the surface color becomes dark. Sample measurements showed changes in the average width of the contamination after weathering, with an increase after spray cleaning and ultrasonic cleaning, that the resist soiling was increased.

The permeability of the four coats was assessed. Contact angle and surface water absorption analyses were carried out. From the results, a decrease in the contact angle was observed after the aging; in particular, the silicate coating becomes high hydrophilic after 5000 hours of aging. The contact angle of the fluor-resin-based coating was substantially not influenced after 5000 hours of aging. On the other hand, xenon-arc light irradiation reduces surface water absorption significantly on specimen treated while not affect untreated ones. In this way, silane-based, and the fluor-resin-based coating does not seem to bring greater water absorption, a potential source of damage to concrete surfaces.

The antifouling-cleaning ability of the four coats was then assessed. Specimen measurements exhibited changes in pollution, average width after weathering, increased spray cleaning, and ultrasonic cleaning. However, after washing, it is observed that the pollution, average width of all the specimens after weathered at 5000 hours same as nearly, they are much smaller than the initial value. Initially, the surface could also be observed, for the along paths of carbon black liquid were narrow of the A, B, specimens treated with a water repellent. Initially,

the water ran down the surface along preferential paths and spherical drops could be noticed on the surface. For the 2500 hours, however, the surface moistly was increased, with a loss of the water-repellent effects after 2500 hours and 5000 hours tests of silane-based coated with specimens A and B. Specimens C coated with fluor-resin based was kept their water-repellent properties substantially longer.

7.5 Effects of different accelerated aging and surface treatments on aesthetics and durability (Chapter 6)

In this chapter, in order to obtain the applicable environment for surface protective materials were involved in the warm water immersion, humidity and cool-heat cycling and xenon-arc light radiation as environmental factors to conduct a comparative study on the water resistance and aesthetics characterizations of mortar reinforced with four kinds of surface protective materials.

The warm water immersion exposure environment has significant influences on the color, gloss, and roughness for mortar coated by surface silane1 A and silane2 B and silicate D. The coating surface became darkness, which gloss were slightly reduced and it a slight increased roughness. there was no change under humidity and cool-heat cycling exposure environment. The humidity and cool-heat cycling, and warm water immersion exposure environment have a remarkable influence on the Fluor-resin C coatings color, gloss and roughness of mortar. The surface covering a small swelling after 28 days. And it no change under xenon-arc light radiation exposure environment.

The xenon-arc light radiation exposure environment e has significant influences on the contact angle for mortar coated four types of surface protective materials. The contact angle obviously was averagely reduced by approximately 20° and 30° after 5000 hours ageing. After humidity and cool-heat cycling and warm water immersion exposure environment ageing, the contact angle obviously reduced of uncoated N, A coatings, B coatings and C coatings were increased.

The silane1 A and silane2 B coatings were the most effective in reducing water absorption in the coated specimens exposed to humidity and cool-heat cycling and warm water immersion and xenon-arc light radiation

ageing. Fluor-resin C coatings performed better than the silicate D coatings in humidity and cool-heat cycling and xenon-arc light radiation ageing. Silicate D showed a similar tendency with N. Comparison to initial, the water absorptions of W28, C20, H5000 three environments decreased by 90%, 40%, 60%, respectively. The reason is the later decrease to the refinement of pore structure due to hydration. However, the H5000 hours exposure environment has a significant effect moisture permeability for all the specimens. The lowest moisture permeability than other exposure environment.

The humidity and cool-heat cycling and warm water immersion exposure environment ageing has significant influences on the capacity of anti-soiling for mortar treated by four types of surface protective materials. After exposure environment ageing, the resist soiling was reduced. However, the four types of surface protective materials exhibited the highest resist soiling to xenon-arc light radiation exposure environment.

The data developed in this study have indicated that the performance of coatings varies with the exposure conditions.

7.6 Summary and future work

Considering the actual working conditions of external walls of concrete buildings, the water absorption durability of mortar was studied using multi-factor accelerated aging tests composed of xenon-arc light radiation, warm water immersion, and freeze-thaw cycling. The aesthetic properties of mortar samples are evaluated.

Accordingly, this study is believed to be beneficial to both the scientific understanding of the interaction between silane based, silicate based, fluorine based and mortar, and the practical environment application of three types of surface protective materials coating to concrete to avoid misapplication requiring expensive and time-consuming maintenance work.

It has been investigated that the silicate D coating on the surface of the mortar specimens is deteriorated as same as uncoated and un-weathered specimens N in this research. Because D has lower contact angle value (<90°) that indicates that is hydrophilicity of coating. It illustrates that it is not suitable for silicate surface impregnation treatment under high humidity condition. It illustrates that it is not suitable for silicate surface

impregnation treatment under high humidity condition. The particular reasons for this question, a series of studies need to be conducted.

In addition, fluor-resin C showed a reduced water absorption after 5000 hours xenon-arc light radiation aging. These results indicate that because the fluorine atoms could form a continuous uniform coating film to develop a structure with strong chemical bonding and makes it difficult to produce the free radicals which cause coating decomposition. The particular reasons for this question would be explored by transmission infrared spectroscopy (FT-IR) and nuclear magnetic resonance spectroscopy (Si NMR), and the surface of the fluor-resin coating is analyzed using reflection infrared spectroscopy (RA-IR) and X-ray spectrometer (EDS) in the future work.

ACKNOWLEDGEMENTS

I would like to take this opportunity to express sincerest thanks and gratitude to all people who gave their time to help me in the production of this dissertation, for their expertise and supports.

First and foremost, I would like to show my deepest gratitude to my advisor, Professor Hama Yukio. I was honored to join the Hama laboratory during the course of the graduate studying. He patiently provided the guidance, encouragement and advice and the lively atmosphere of the Hama laboratory, which helped me decide to come back again for the doctoral journey. During my doctoral study, Professor Hama has provided me with valuable guidance in every stage of the research and writing of this thesis. Without his enlightening instruction, impressive kindness and patience, I could not have completed my thesis. His keen and vigorous academic observation enlightens me not only in this thesis but also in my future study and career.

I am sincerely grateful to the vice supervisors, Professor Mizoguchi and Associate Professor Takase, who provided me important opinions for the revision of my doctoral dissertation and the doctoral dissertation presentation.

Further, I also wished to express my appreciation to Assistant Professor Kim. He always provides encouragement and kind advice for my research, which is very important to the completion of a major part of my dissertation.

Grateful acknowledgements are also extended to the Joint Research Project Participants: Naoto Ueda of Takenaka Corporation and Hiroo Hoshi of Pozoris Solutions Co., Ltd. and Kouichi Takahashi of Local Independent Administrative Agency Hokkaido Research Organization, who gives me the project support provided and creative comments and suggestions.

In additional, I would like to thank to the post-doctor Quy from Vietnam, who gives me some important advice for my study and improved my academic writing skills. Sincere help and valuable suggestions for my journal papers by him are highly appreciated. Also, sincere appreciations are also extended to Dr. Noguchi for his comments and suggestions and help. We started our doctoral journey together in Hama laboratory, and he meticulously carried out the help for my trouble despite his busy study schedule.